# Isolation and characterisation of *Arabidopsis* mutants altered in the regulation of flavonoid biosynthetic genes by UV-B and blue light

A thesis submitted to the University of Glasgow for the degree of Doctor of Philosophy

George R. Littlejohn

September, 2005

Plant Molecular Science Group,
Division of Biochemistry and Molecular Biology,
Institute of Biomedical and Life Sciences,
University of Glasgow.

# Acknowledgements

This volume describes the most emotionally difficult, testing and frustrating thing I have ever had to do and I owe a great debt of thanks to a great many people. It has also been exciting and rewarding at times. And that's what makes it worthwhile.

My great thanks to Prof. Gareth Jenkins who enthusiastically took me into his lab. in the first place and has shown me unwavering support and encouragement throughout the course of my research.

I must also thank the University of Glasgow and BBSRC for financial support before (BBSRC), during (BBSRC) and after (UofG) the disruption caused by the Bower fire. Thanks too to Prof. Richard Cogdell for arranging attendance at an international conference and extra financial help after the Bower fire. Thanks also to the Graduate School for allowing extensions for me at the time of the fire and the birth of my daughter.

Thanks to IBLS computer services for all their help in rescuing my data from the Bower fire and to the magician Brendan Kirk and to Alan McIlroy for their assistance.

I thank all members of the Hooker lab., past and present, for their hard work, friendliness and support, but I owe warm and particular thanks to Drs. Matt Shenton, Helena Wade and Bobby Brown. Matt not only guided me into the lab., and performed the transformations which were crucial for the success of my mutant screen, but was always on hand with coffee and appropriate words of encouragement. Helena has always been ready with an understanding ear, coffee and day old cakes and I thank her for her advice on everything from RT-PCR to nappy changing. Bobby is the rock on which the Hooker lab. stands and as such I owe him a great debt in terms of advice, plant watering, friendly encouragement and arranging the Research Club lunch every Friday.

Thanks also to Prof. Gareth Jenkins, Dr. A. John Clutterbuck, Dr. Mike Hansell, Mrs. Sheila Barr and the pupils of Port Glasgow High School, Drs. Maureen Griffiths and Geoffrey Moores of the Undergraduate School and fellow demonstrators for enriching the greatly rewarding experience of teaching still further.

My incalculable thanks to my father, George Littlejohn, who taught me how to think and to gaze in awe at the universe. Thanks also to my schoolteachers Drs. William Jaap and John May and to Drs. Susan Stuart, Adrienne Jessop, John Clutterbuck, and Richard Wilson of the University of Glasgow, each of whom helped me appreciate and wonder a little more.

Finally, I have to thank my family. My parents and sister, Suzanne, have always been and continue to be very supportive and I owe them so much. I could not have produced this thesis without the love and support of my wife Marian and daughter Genevieve and Marian's artistic skills.

# Index

# Abstract

This thesis presents the application of a genetic approach to study aspects of the regulation of flavonoid biosynthesis. The gene encoding the first committed step in flavonoid biosynthesis is chalcone synthase (*CHS*). *CHS* is induced by a range of biotic and abiotic stimuli in *Arabidopsis thaliana*. Among these stimuli are various light qualities, including UV-B (280-320 nm) and blue light (390-500 nm). These light qualities each have the capacity to stimulate chalcone synthase gene expression, but when UV-B and blue light are used together to illuminate *Arabidopsis*, *CHS* expression is induced synergistically (i.e. to a greater than additive degree). As no genetic elements of the synergistic mechanism had been identified, a screen for mutants in UV-B and blue light synergistic induction of *CHS* in *Arabidopsis thaliana* was developed and carried out. A forward genetic approach was employed to identify mutants, using a transgenic line in which firefly luciferase (*Luc*) was expressed under the control of the *CHS* promoter. Luciferase can easily be visualised in plants, allowing mutants in the regulation of *CHS* to be selected. The screen resulted in the identification of a number of mutants. Among them was probably a novel *uvr8* (*ultra-violet resistant locus 8*) allele.

A second approach to study the genetic basis of flavonoid gene regulation was to further characterise a previously isolated mutant, *icx2* (increased chalcone synthase expression 2). *icx2* was originally identified as a mutant over-expressing *CHS* in the presence of UV-B. Previous characterisation had shown *icx2* to over-express not only *CHS*, but also other genes of the flavonoid biosynthetic pathway in response to a range of light qualities. In addition, *icx2* individuals had been shown to have reduced stature and deep purple leaves. The purple leaf phenotype resulted from hyper-accumulation of anthocyanins. The work detailed here further characterised the pleiotropic phenotype of *icx2*, identifying a new short-root phenotype. The plant hormone auxin has an effect

on root architecture and has its own function disrupted by flavonoids.

Experiments were undertaken to assess the effect of flavonoid accumulation in *icx2*. The root phenotype was seen in individuals grown on medium containing sucrose and was shown to be independent of *CHS* over-expression or flavonoid accumulation. A screen for suppressor mutants of the *icx2* mutation was carried out, which suggested the pleiotropic phenotypes of *icx2* are monogenic. Map-based cloning of icx2 had been attempted before, but had been hindered by an unreliable phenotype. Efforts were made in this study to overcome the problems with the phenotype. In addition, mapping resources and data were produced.

# Table of Contents

# Table of figures

# Nomenclature

Standard nomenclature for mutant and wild type genes and proteins in Arabidopsis thaliana is used throughout. Genes and proteins are usually given a 3-letter name (e.g. CHS) and an identifying number (e.g. ICX2), although some exceptions are used (e.g. PHOT1). Multiple mutant alleles of a given gene are distinguished by use of a number separated from the gene name by a hyphen (e.g. phot1-5). Where multiple names for genes are used in the literature, the more common name is used here and use of alternative names explained where necessary.

Italicised and non-italicised letters are used to refer to genes and proteins, respectively. Uppercase and lowercase letters were used to refer to wildtype and mutant alleles or proteins, respectively. Chalcone synthase (CHS) is used as an illustrative example below. Mutant plants are referred to by the mutant allele nomenclature. Mutant phenotype is represented by the gene name italicised and with capitalisation of the first letter (e.g. *Icx2*) but is rarely used.

Where the promoter region of one gene is fused to the coding region of another, such fusions are represented by the use of a colon (:) between each element and are italicised. The use of :Ω: represents fusions where full length sequence of the first gene is also used.

# Abbreviations

| | |
|---|---|
| 4L13BC2 | *icx2* double backcrossed line |
| ACT | Actin |
| *At* | *Arabidopsis thaliana* (prefix used to distinguish from genes of other species) |
| cDNA | Complementary DNA |
| CHS | Chalcone synthase (protein) |
| chs | Chalcone synthase (mutant protein) |
| *CHS* | Chalcone synthase (wild type allele) |
| *chs* | Chalcone synthase (mutant allele) |
| *CHS:Luc* | *CHS* promoter fused to *Luc* coding sequence |
| *cop* | Constitutively photomorphogenic mutants |
| CRY | Cryptochrome |
| *det* | De-etiolated mutants |
| DFR | Dihydroflavonol reductase |
| DNA | Deoxyribonucleic acid |
| EMS | Ethylmethane sulphonate |
| F1 | First filial generation |
| *fus* | Fusca mutants |
| GUS | β-glucuronidase |
| HWL | High white light (150 μmol $m^{-2}$ $s^{-1}$) |
| *hy* | Long hypocotyl mutants |

| | |
|---|---|
| HYG | Hygromycin |
| ICX2 | Increased chalcone synthase expression 2 |
| LOV | Light, oxygen, voltage domains (of PHOT) |
| *Luc* | Luciferase (*Photinis pyralis*) |
| LWL | Low white light (20 μmol $m^{-2}$ $s^{-1}$) |
| M1 | First generation of mutagenised plants (i.e. from seeds mutagenised) |
| NM4 | Non-mutant 4 (*CHS:GUS* reporter line) |
| *nph* | Non-phototropic hypocotyl mutants |
| *PAP1* | MYB75 over-expressing line |
| PCR | Polymerase chain reaction |
| PHOT | Phototropin |
| PHY | Phytochrome |
| RNA | Ribonucleic acid |
| RT-PCR | Reverse transcribed PCR |
| $T_1$ | Primary transformants |
| *tt* | Transparent testa mutants |
| *tt4* | Transparent testa 4 (*chs* mutant) |
| ULI3 | UV-B light insensitive mutant 3. |
| UV-B | Ultraviolet-B radiation (λ= 280 – 320 nm) |
| UV-A | Ultraviolet-A radiation (λ= 320 – 390 nm) |
| UVR8 | UV resistance locus 8 |
| wt | wild type |

# 1. Chapter 1. Introduction

## 1.1. Introduction

### 1.1.1. Plants are at the mercy of their environment

It cannot be stated too strongly the degree to which plants are dependent on and influenced by their immediate environment. Every aspect of their lives, from the timing of germination, rate and direction of growth, and response to pathogens, nutrients and light, through to flowering, setting seed and senescence is intimately influenced by their environment, acting within the constraints set by their genes.

Most higher plants are rooted to the spot, so must have coping strategies to allow them to adapt and survive in a range of likely environments. For this reason they have evolved a great plasticity of developmental, physiological and biochemical responses, allowing them to deal with a wide range of environmental stresses.

Diverse environmental signals are sensed by plants and appropriate intracellular adjustments, including changes in gene expression, made. The emphasis given to particular signals is crucial as individuals must respond dynamically and economically to changing conditions. Economy with resources drives plants to hierarchically weigh up diverse environmental signals with resources available (which may be pulling in opposite directions) and respond. Plants do much to achieve the required economy by maintaining comparatively few, degenerate signalling structures and components that are utilised by multiple input signals. This allows the transduction of some stimuli, when received together, to effect less or greater than additive responses, meaning that plants can avoid needless expense and can predict likely environmental change.

### 1.1.2. The light environment

The science of optics, which describes the nature and properties of light, has developed from the fascination our visual species has with the world around us and from the drive with which thinkers from Plato through to Isaac Newton, James Clerk Maxwell and Richard Feynman have pursued it.

Quantum electrodynamics was developed over the first half of the twentieth century and served to unite the wave and particle theories of light. Throughout this thesis, light will be largely understood by reference to wavelength but it is important to bear in mind that energy varies inversely with wavelength, and that observed physical and biological effects are best understood with reference to photons (or quanta, the bundles of energy which belie its particulate nature).

Plants, just like curious philosophers and scientists, also find themselves bathed in light of varying wavelengths and energies and have made their own sense of their surroundings. Figure 1.1 represents the electromagnetic spectrum. Some features of the spectrum with bearing on the lives of plants, such as absorption peaks of Pfr and Pr forms of phytochrome and those regions defined as PAR (photosynthetically active radiation), visible (including blue) light, and UV-A, B and C radiation are indicated.

The work presented in this volume relates to the response of the model plant *Arabidopsis thaliana* to ultraviolet B (UV-B, 280 – 320 nm) and blue (390 – 500 nm) light.

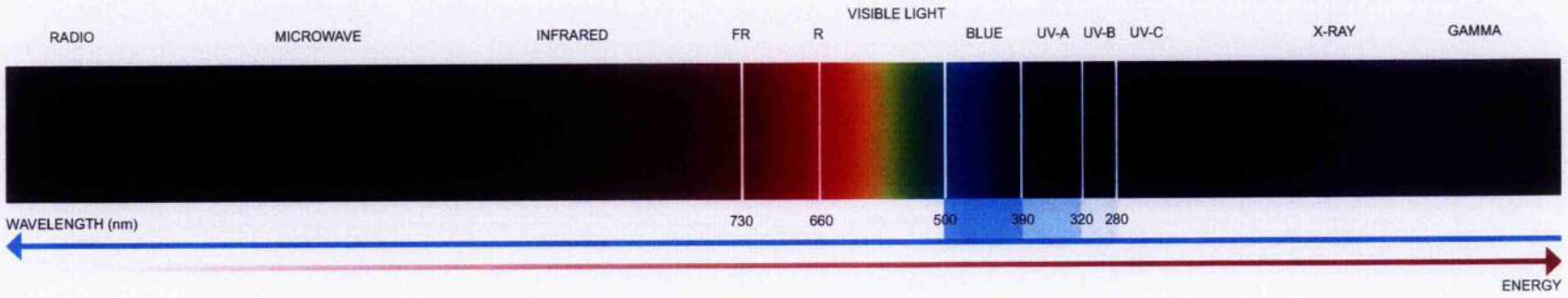


**Figure 1.1 Electromagnetic spectrum**

Plants require and respond to solar radiation of wavelengths from far-red to ultraviolet. Note that as wavelength decreases, energy increases in inverse proportion. Absorption maxima for phytochromes are found at 730 and 660 nm, blue light UV-A and UV-B are defined as 500-390 nm, 390 - 320 nm and 320 - 280 nm respectively. Photosynthetically active radiation (PAR) is defined as the region 400 - 700nm, which roughly corresponds to visible light.

### 1.1.3. Light can be a signal, stress or source of energy

The ability of plants to harness light energy from the sun, via photosynthesis, supports (directly and indirectly) the vast majority of life on earth. Various light qualities also provide a wide range of cues affecting development, growth, metabolism and physiology by the differential induction of gene expression and modulation of protein conformation, interactions and intracellular location.

Plants use specific incident wavelengths (e.g. cryptochrome 1 mediation of blue light initiation of flowering (Bagnall et al. 1996), light intensity (e.g. the high and low fluence rate responses of the phototropins (Konjevic et al. 1989), and ratios of wavelengths (e.g. phytochrome-mediated shade avoidance (Schepens et al. 2004); (Schmitt et al. 2003) to inform their responses. The effects that given light qualities have on plants differ developmentally, temporally and spatially and include initiation of germination, photomorphogenesis, co-ordinated gene expression for primary and secondary metabolism, and physiological effects such as circadian rhythmicity, solar tracking, stomatal opening and chloroplast alignment.

Light is vital but also potentially damaging to plants. Although plants rely so heavily on solar radiation, it can also cause major damage to photosynthetic machinery, other cellular components and particularly to DNA.

Almost all low wavelength (< 300 nm) solar radiation is absorbed (mainly by oxygen in the Earth's upper atmosphere and the stratospheric ozone layer) or scattered and reflected by the troposphere (Frederick and Lubin 1988; Frederick, Snell et al. 1989). Despite this, enough damaging ultra-violet B (UV-B, 280 – 320 nm) reaches the

biosphere to cause significant damage to macromolecules such as DNA, proteins and lipid membranes. As with other wavelengths of light, high energy UV-B radiation induces expression of various subsets of genes in plants (Casati and Wolbot, 2003; Ulm et al. 2004; Tamaoki et al. 2004; Brown 2005). Much of this response is involved in protection from environmental insult.

### 1.1.4. Protection from light

As plants are under attack from the source of their energy, they have evolved physiological and biochemical methods of protection which minimally compromise energy production. The main defence in their arsenal of response to the damaging effects of solar radiation is the production of photoprotective phenolic compounds, particularly flavonoids and hydroxycinnamic acid esters, which are deposited in vacuoles of epidermal cells and absorb UV radiation, thereby acting like a sun-screen and providing some protection from cellular damage.

## 1.2. Flavonoids and function

Flavonoids are a class of diphenolic secondary metabolites produced ubiquitously in and exclusively by plants. Chemically, they can be characterised by their basic three-ringed structure seen in Figure 1.2. Flavonoids are formed from a branch of the general phenylpropanoid biosynthetic pathway (Figure 1.2) and include molecules such as anthocyanins, chalcones, flavanones and flavonols.

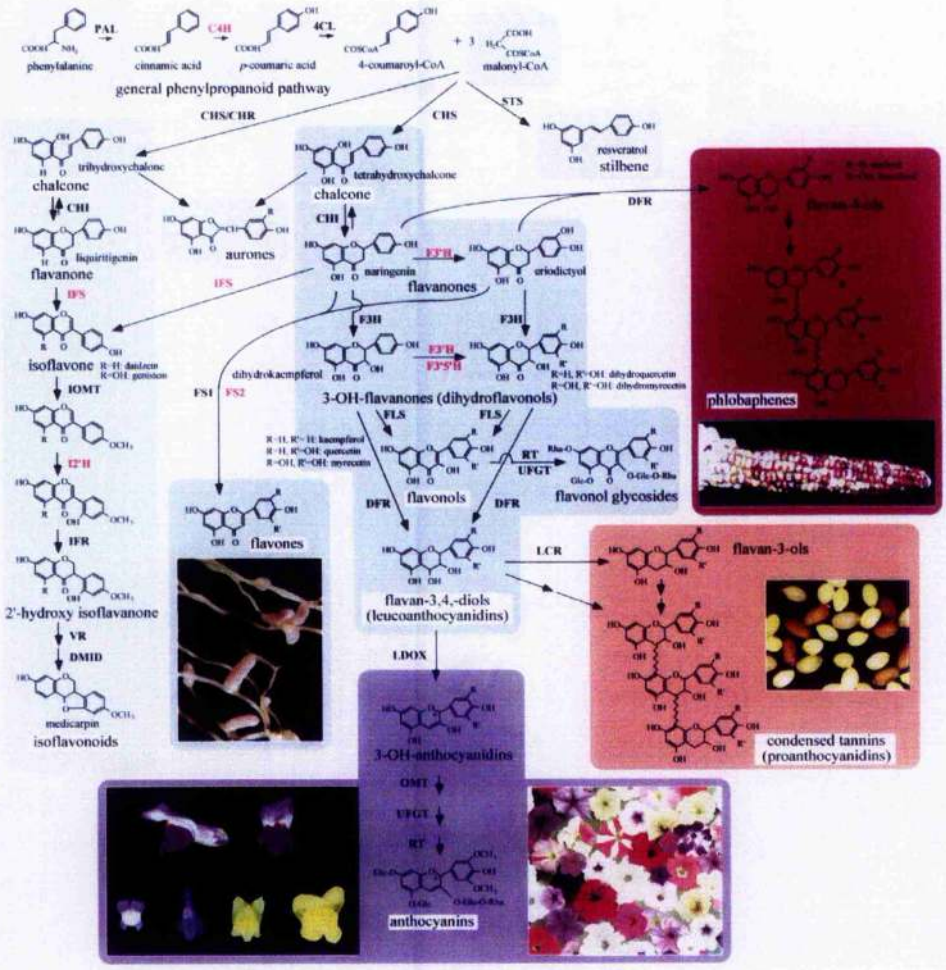


**Figure 1.2 Summary of Phenylpropanoid Biosynthesis (Taken from Winkel-Shirley, 2001).**

Schematic of the major branch pathways of flavonoid biosynthesis, starting with general phenylpropanoid metabolism and leading to the nine major subgroups: the colourless chalcones, aurones, isoflavonoids, flavones, flavonols, and flavandiols (gray boxes), and the anthocyanins, condensed tannins, and phlobaphene pigments (colored boxes). Enzyme names are abbreviated as follows: cinnamate-4-hydroxylase (C4H), chalcone isomerase (CHI), chalcone reductase (CHR), chalcone synthase (CHS), 4-coumaroyl:CoA-ligase (4CL), dihydroflavonol 4-reductase (DFR), 7,2'-dihydroxy, 4'-methoxyisoflavanol dehydratase (DMID), flavanone 3-hydroxylase (F3H), flavone synthase (FSI and FSII), flavonoid 3' hydroxylase (F3'H) or flavonoid 3'5' hydroxylase (F3'5'H), isoflavone *O*-methyltransferase (IOMT), isoflavone reductase (IFR), isoflavone 2'-hydroxylase (I2'H), isoflavone synthase (IFS), leucoanthocyanidin dioxygenase (LDOX), leucoanthocyanidin reductase (LCR), *O*-methyltransferase (OMT), Phe ammonia-lyase (PAL), rhamnosyl transferase (RT), stilbene synthase (STS), UDPG-flavonoid glucosyl transferase (UFGT), and vestitone reductase (VR). Photographs are courtesy of Cathie Martin (John Innes Centre, Norwich, UK; *Antirrhinum*), Francesca Quattrocchio (Free University, Amsterdam; petunia), Erich Grotewold (Ohio State University, Columbus; maize), and Yimei Lin and Ann Hirsch (University of California, Los Angeles; sweet clover).

Many conjugated forms of flavonoids exist. The most abundant of these include glycosyl and methyl substituted groups. The great diversity this produces within the flavonoid family is such that many flavonoids are unique to a given species or have a very limited distribution, perhaps only within one genus. These distributions have been used as a basis of chemotaxonomic profiling (Iwashina et al, 2000) and the enzymes of the flavonoid biosynthetic pathway have been used as phylogenetic markers themselves. The complexity and variety of flavonoid structure is mirrored by the multitude of different functions which have been ascribed to them.

### 1.2.1. Flavonoid function *in planta*

It is widely thought that the original function of flavonoid accumulation in plant cells was to serve as a UV-A (320-390nm) and UV-B (280-320nm) filter which strengthened the mutualistic dependency of the green algae and fungus-like endosymbiont and anticipated early land plants (Jorgensen, 1993) although it has also been suggested that flavonoids originally acted as "internal regulatory agents" (Stafford, 1991).

Exposure to UV-B radiation induces the expression of genes of the phenylpropanoid biosynthetic pathway which lead to the accumulation of flavonoids and which may be expected if flavonoids are active in limiting UV damage. Evidence for the protection of DNA by flavonoids comes from the *Arabidopsis* transparent testa (*tt4,* and *tt5*) mutants, which have reduced levels of (or no) flavonoids and are more susceptible than the wild-type to the harmful effects of UV-B radiation (Li et al, 1993). In addition, *in vitro* studies show the protective effects of flavonoids on naked DNA (Kootstra et al.1994).

Certain classes of flavonoids, notably the anthocyanins, play an important role in the pigmentation of plants. Red and blue pigmentation of certain flowers, are attributable to anthocyanins deposited in the vacuole where pH (an observation made by Robert Boyle in 1664 (Winkel-Shirley 2001)) determines the colour. A recent communication in Nature (Shiono et al, 2005) has shown the same anthocyanin molecule which colours both red roses and blue cornflowers owes its different hues to its being found in a complex with flavone molecules and iron, magnesium and calcium ions only in cornflowers. Anthocyanins are also thought to protect deciduous species in senescence during the process of reabsorbing nutrients from their leaves (Hoch et al. 2003). Flavonols, another important class of flavonoids have a role in pigmentation and are responsible for some yellow and cream colourations.

Flavonols have also been shown to have significant effects on flower fertility. Pollen development, germination and tube growth have all been shown to be flavonol dependent (Ylstra et al. 1992), but later evidence which noted that the *chs* mutant *tt4* was fully fertile despite its inability to produce flavonols (Ylstra et al. 1996) has confused this assertion. Van der Meer et al. (1992) provided evidence for male fertility in petunia being dependent on anther-derived flavonoids. In this study, transformants which produced an antisense *CHS* transcript (thereby knocking out CHS activity, which in turn affected the flavonoid levels) were found to be male-sterile.

Other evidence suggests that flavonoids provide plants with some protection from insect predators (Hedin PA, et al. 1992; Rousseaux et al 2004 ), and in the case of the phytoalexins, against microbial attack (Dakora FD, et al. 1996). Transgenic tobacco with antisense suppressed levels of *PAL* (*Phenylalanine Ammonia Lyase*, an enzyme found

early in the production of phenylpropanoids) has shown decreased resistance to fungal attack (Maher et al. 1994).

### 1.2.2. Dietary Flavonoids

As well as being important molecules for plants, it is worth noting that flavonoids may also have a significant effect on human health. Common foods such as onions, broccoli and apples are high in flavonoid content (Herrmann, 1976; Hertog et al, 1992; Crozier et al, 1997) and as such, flavonoids are molecules normally present in our diet.

Epidemiological data indicate that regular intake of flavonoids in the diet will help lower the risk of coronary heart disease (Hertog et al, 1993) and cancer (Kato et al. 1983, Wattenberg et al. 1985 and more recent studies reviewed in (Kanadaswami et al. 2005). It is believed that dietary flavonoids may work *in vivo* by directly stabilising cellular free radicals which cause oxidative damage (Yamasaki et al. 1997). This may in turn prevent the oxidation of other proven antioxidants like vitamins A and C. Oxidative damage to DNA, proteins and cellular lipids can lead to these diseases, so antioxidant effects flavonoids have shown *in vivo* and *in vitro* (Rice-Evans et al, 1997; Negre-Salvayre et al, 1992) provide some weight to the claims of the epidemiological data.

More recent evidence has suggested that consumption of polyphenolics in red grape juice (Bub et al. 2003) stimulates immune cell functions and reduces oxidative damage to DNA. Other proposed modes of action (reviewed by Hoensch and Kirch, 2005) include the ability of flavonoids to disrupt oestrogen reception, which may in turn limit cancer growth. In particular, the flavonol quercetin and its glycosides have been the focus of proposed beneficial effects of flavonoids.

Over-expression of the flavonoid biosynthetic gene *CHI* (*chalcone isomerase*)in tomato in order to produce a "healthier" tomato has led to 78-fold increased levels of flavonols (Verhoeyen, Bovy et al. 2002). This approach may be misguided though, as there is public mistrust of transgenic foods and other vegetables have naturally higher levels of flavonols.

### 1.3. Chalcone synthase

Chalcone synthase (CHS) catalyses the first enzymatic step in the commitment to channel carbon into the production of flavonoids (Figure 1.2) and is a homodimeric protein which probably forms part of a complex with other flavonoid biosynthetic enzymes (Burbulis and Winkel-Shirley 1999), (Winkel-Shirley 1999). *CHS* gene expression is stimulated by a variety of environmental stimuli relating to stress, including low temperature, high sucrose concentration, herbivory, pathogenic attack and drought. Not unexpectedly for a gene involved in the production of metabolites acting as sun-screens, exposure to various light qualities also give rise to *CHS* gene expression. Importantly for the work presented in this volume, both UV-B and blue light induce *CHS* gene expression in *Arabidopsis* (Kubasek et al 1992; Christie and Jenkins 1996).

#### 1.3.1. Mutants in *CHS* induction

In addition to mutant alleles of the *CHS* gene (*tt4*) (*transparent testa 4*), several mutants in *CHS* induction have been described in *Arabidopsis*. These include regulatory mutants like *hy5* (Oyama et al. 1997), *pap1* and *pap2* (Borevitz et al. 2000) and two conditional negatively regulating mutants, *icx1* (Jackson et al. 1995), (Wade et al. 2003) and *icx2*.

*icx2* was isolated as a conditional over-expressor of *CHS* gene expression in UV-B light in a screen using a *CHS:GUS* reporter line. Gene expression studies have shown *icx2* to negatively regulate the expression of CHS and other flavonoid biosynthetic enzymes (unpublished data, section 4.1). Aspects of the *icx2* phenotype are studied and discussed in Chapter 4.

### 1.3.2. *CHS* as a model of gene regulation

CHS lies at a control point of the general phenylpropanoid pathway, one of the best understood and most studied biochemical pathways in plants, channelling carbon flux into the production of flavonoids (Figure 1.2).

*CHS* exists as a single copy gene in *Arabidopsis,* which is advantageous for studying gene regulation, as there are no functional homologues. Deletion analysis of the *CHS* promoter (Hartmann et al. 1998) identified a 1972 bp region, with a 164 bp core promoter sequence (of reduced sensitivity) both of which were capable of specifying *CHS* response to UV-B and UV-A/blue light. Mutation of either a MYB recognition motif or ACGT element abolished the induction of *CHS* by these light qualities. Furthermore, this study was not able to separate elements required for UV-A/blue and UV-B induction thus indicating that the signal transduction pathways involved must merge between photoreception and contact with the *CHS* promoter. The simplicity of the *CHS* promoter might be expected when it is considered that a number of disparate signals are able to stimulate it and so a one-fits-all promoter with higher order interactions occurring before the point of interaction with the promoter would seem economical.

### 1.3.2.1. Co-ordinated *CHS* expression requires HY5 and a MYB transcription factor

The transcription factor HY5 (long hypocotyl 5) (Oyama et al. 1997) is a bZIP (basic leucine zipper) motif-containing transcription factor which binds the G box LRE (light responsive element) of light responsive promoters (Chattopadhyay et al. 1998; Gao et al. 2004), including that of *CHS*. HY5 has been shown to be essential for the expression of *CHS* (for which it is necessary but not sufficient).

As well as HY5, *CHS* induction requires the presence of a MYB (myeloblastoma) co-factor. MYB transcription factors are the largest single family of transcription factors in *Arabidopsis*, with well over 100 members (Romeroet al. 1998). The size of this family of transcription factors goes someway to explaining the plasticity of development and gene regulation seen in plants as individual MYBs are likely to have overlapping but not redundant functions (Jin et al. 1999).

MYBs are characterised by the presence of a conserved N-terminal DNA-binding MYB domain, which binds to MYB-box (G-box-like) consensus sequences in the 5' region of target genes. The DNA binding domain consists of a tandemly repeated region of ~50 amino acids and may be imperfectly repeated 1-3 times but is usually found repeated twice in plant *MYB* genes (R2R3) and three times in animal homologues (Martin et al, 1997). The repeating units form a helix-turn-helix (HTH) DNA-binding domain reminiscent of that found in homeobox binding proteins, which allow it to bind to DNA's major groove. It is a result of this binding and with the possible help of other trans-acting proteins and cis-acting elements associated with the target gene that transcriptional activation occurs.

#### 1.3.2.1.1. HY5

HY5 has been shown to be involved in blue, red and far-red responses and represents convergence between these pathways. *hy5* mutants lack hypocotyl inhibition in response to light (Jackson et al. 1995; Oyama et al. 1997) as well as UV-B and CRY1-mediated blue light *CHS* induction (*hy5* seedlings also lack far-red *CHS* induction) (Wade, 1999).

The light responsiveness of HY5 may be explained by its interaction with COP1 (constitutively photomorphogenic 1) (Andersson and Kay 1998, Ang et al. 1998). COP1 binds HY5 in the dark and targets it for degradation (Osterlund et al. 2000). On exposure to red or blue / UV-A light, COP1 is excluded from the nucleus and releases HY5 allowing it to function as a transcription factor. Phosphorylation also plays a part in the regulation of HY5 function (Hardtke et al. 2000). COP1 shows a stronger interaction with unphosphorylated HY5, which also seems to be the biologically active form as it has higher binding affinity for the *CHS* promoter. It has been suggested that the reason for maintaining a pool of phosphorylated HY5 in the cell is to facilitate a rapid response to light. HY5 is regulated, then both by the presence of COP1 and by its phosphorylation state.

In addition to the central role HY5 plays in initiation of *CHS* transcription, *hy5* mutants have been shown to exhibit a range of altered light and gravitropic responses in *Arabidopsis* (Oyama et al. 1997; Oyama et al. 2002), including reduced formation and elongation of lateral roots (Okada et al. 1998). The *hy5* root phenotype may be explained by the apparent induction of negative regulators of auxin signalling by HY5 (Cluis et al. 2004). This is an exciting observation as it links light and auxin / IAA (indole acetic acid)

pathways in *Arabidopsis*. Previous evidence from the moss *Physcomitrella patens* had shown a link between the blue light photoreceptor cryptochrome and auxin signalling (Imaizumi et al. 2003) and phosphorylation of *Arabidopsis* and pea Aux/IAA proteins by oat phytochrome A has been demonstrated in vitro (Colon-Carmona et al. 2000).

#### 1.3.2.1.2. MYB transcription factors in phenylpropanoid biosynthesis

The role of MYB transcription factors in phenylpropanoid biosynthesis has been noted in maize, petunia and snapdragon as well as *Arabidopsis*. An interesting example is provided by Moyano et al (1996) who showed that two snapdragon *(Antirrhinum majus)* transcription factors, AmMYB340 and AmMYB305 (isolated by Jackson et al, (1991)), are expressed solely in mature snapdragon flowers and bind specifically to the promoters of genes involved in flavonoid biosynthesis.

Specifically, both these transcription factors were shown by electromobility shift assay (EMSA) to bind the promoters of phenylalanine ammonia lyase (*PAL*), chalcone synthase (*CHS*), chalcone isomerase (*CHI*), flavonol-3-hydroxylase (*F3H*), dihydroflavonol reductase (*DFR*), and Anthocyanin Synthase (*AS*) in yeast. Both MYB proteins were demonstrated to enhance the expression of the structural genes *PAL*, *CHI*, and *F3H*, with AmMYB340 having a greater effect on all these genes than AmMYB305. The expression of *CHS*, *DFR*, and *AS* was not upregulated. AmMYB305 bound these target sequences with greater affinity than AmMYB340. The differential between AmMYB340 and AmMYB305, both in binding affinity and capacity for transcriptional enhancement, whilst maintaining degeneracy of function, is proposed to constitute a gearing mechanism for the regulation of the biosynthetic genes influenced by them

(Moyano et al, 1996). It is also suggested that the binding of the two MYB proteins to the regulatory sequences of *DFR* and *AS* may inhibit their transcription through competition with proteins which enhance *DFR* and *AS*. This neatly suggests that these transcription factors preferentially activate the expression of the genes involved in flavonol biosynthesis, and prevent the expression of the genes responsible for converting the possible flavonol precursors to anthocyanins. In addition, over-expression of these two factors in *Nicotiana* (Littlejohn, unpublished) produced individuals exhibiting stunted growth and various floral abnormalities suggesting that the use of MYB transcription factors is tissue and species-specifically tuned.

In *Arabidopsis*, Borevitz et al (2000) found by activation tagging, a purple mutant designated *PAP 1* (production of anthocyanin pigment 1). *PAP1* and was shown to over-express the transcription factor AtMYB75 along with genes of the phenylpropanoid biosynthetic enzymes including *CHS*. A second activation-tagged line, *PAP2*, corresponds to an insertion locus *AtMYB90*. Whereas AtMYB75 and AtMYB90 have a role in transcriptional activation, AtMYB4 has been shown to have a role in the production of sinapate esters (which have a photoprotective role in plants) by derepression of cinnamate 4-hydroxylase (*C4H*) (Jin et al. 2000; Hemm, 2001). Exposure to UV-B light results in reduced expression of *AtMYB4*. Recently, *Arabidopsis* MYB12 has been shown to specifically activate genes of flavonol biosynthesis (*CHS*, chalcone flavanone isomerase, flavanones 3-hydroxylase and flavonol synthase), showing it to have functional as well as structural similarity to the P factor of maize (Mehrtens et al. 2005).

### 1.3.2.2. *CHS*, light and development

Light is crucial for the transition of plants from skotomorphogenesis to photomorphogenesis and as plants develop and age, their responsiveness to individual light qualities changes. For example, expression of the flavonoid biosynthetic gene *CHS* (chalcone synthase) is induced by red light via phytochrome in young seedlings but not in 3 week old plants, where blue / UV-A light sensing cryptochrome 1 is mainly responsible (Jackson et al 1995).

## 1.4. Photoreceptors

Photoreceptors are apoproteins which, along with a chromophore (a light absorbing / transmitting ligand), comprise a light sensing holoprotein. Photoreceptors also typically have a biochemical activity (e.g. the serine / threonine kinase autophosphorylation of the phototropins (Christie et al. 1998)), which is activated on exposure to light of the relevant wavelength by a conformational change and allows the signal to be perpetuated. The specific wavelengths of light to which photoreceptors react depends very much on the absorption spectra of the bound chromophores. Absorption spectra of the relevant bound chromophores also underlie measurable physiological or biochemical responses exhibiting corresponding characteristic action spectra.

In the model plant *Arabidopsis thaliana*, there are nine currently well-described photoreceptors. These are phy (phytochrome) A-E, cry (cryptochrome) 1 and 2 and phot (phototropin) 1 and 2. In addition to these photoreceptors are FKF1 (a flavin-binding protein that has been named as a putative photoreceptor for photoperiodism (Imaizumi et

al. 2003)) as well as a further cryptochrome (cry3, (Kleine et al 2003)). Other species have varying numbers of members of each family of photoreceptors. In addition, one superchrome (phy3) has been described in fern *Adiantum capillus-veneris* (Nozue et al 1998; Briggs, 2001).

Specific responses are linked to specific photoreceptors, but as well as individual photoreceptors having control over multiple observable phenomena, there is also functional overlap between photoreceptors. In addition, where multiple photoreceptors are involved in a common response, functional interactions, or cross-talk are often seen.

### 1.4.1. Phytochromes

In the 45 years since their discovery, phytochromes have become the most characterised photoreceptors in higher plants, as any relevant textbook reflects. There are five phytochromes in *Arabidopsis thaliana* (PHYA-E) which fall into two sub-classes reflecting their evolutionary origins, the light labile type I (PHYA) and light stable type II (PHYB-E). All phytochromes absorb primarily red and far-red radiation (absorption maxima at 660 and 730 nm, respectively) but also blue / UV light (Lin et al 2000) and act as the major photoreceptors responsible for photomorphogenesis (e.g. germination, de-etiolation, shade avoidance, flowering). On exposure to red light, phytochromes undergo a conformational change of their chromophore from the $P_R$ (maximally red light absorbing) *cis* isomer to the $P_{FR}$ (maximally far-red light absorbing) *trans* isomer, a reaction which is reversible with subsequent far-red light exposure. Phytochromes A and B show associated movement from cytoplasm to the nucleus under exposure to red light.

There is much functional redundancy between the phytochromes, making mutant studies difficult, but PHYA and PHYB do exhibit different response times and light stability.

### 1.4.2. Cryptochromes

In 1980, Marten Koornneef et al (1980) published the results of probably the single most important mutant screen in photoreceptor biology. This screen identified the *hy* (long hypocotyl) mutants as individuals compromised in the transition from skotomorphogenesis to photomorphogenesis. These mutants were shown to include many important mutant alleles including *hy4, hy3* (*phyB* mutant (Somers et al. 1991)) which, along with *hy1, 2* and *6* are all phytochrome or associated chromophore mutants), and *hy5* (an important transcription factor for light regulated gene expression). *hy4* was eventually characterised as a blue / UV-A light photoreceptor, cloned and called cry1 (Ahmad and Cashmore 1993). *cry2* (originally called *AtPHH1*) was later found by sequence homology to *Sa-PHR1*, a photolyase like gene from *Sinapis alba* (Hoffman et al. 1996; Lin et al.1996).

Cryptochromes are flavoproteins (i.e. use a flavin chromophore), which function as blue / UV-A photoreceptors. Although they share homology with photolyases they lack photolyase activity. The often notable difference between cryptochromes and photolyases is in a C-terminal extension found only in the cryptochromes, which allows them to bind their signalling partner, COP1 (constitutively photomorphogenic 1) (Yang et al. 2001; Wang et al. 2001). The interaction with COP1 also gives an insight into their function. In addition to its interaction with CRY1, COP1 also binds the transcription factor HY5 ( as discussed in section 1.2.3.1.1) in the dark, targeting it for degradation. It has been

suggested that the cryptochromes may exist in a complex with COP1 and HY5 in the dark, releasing HY5 on exposure to blue / UV-A light.

Both cryptochromes function in blue light dependent responses (e.g. inhibition of hypocotyl elongation, cotyledon expansion and control of flowering timing) with some degeneracy in function. Broadly though, CRY1 functions in flavonoid biosynthesis and inhibition of hypocotyl growth. Specific functions of CRY2 include initiation of flowering. Cryptochromes are found in plants and animals, and are implicated in circadian rhythmicity in both.

A third cryptochrome, identified in the cyanobacterium *Synechocystis*, has an *Arabidopsis* homologue (CRY3, At5g24850) which binds both a flavin chromophore and DNA but has no photolyase activity (Kleine et al. 2003).

### 1.4.3. Phototropins

There are two phototropins described, PHOT1 (*nph1*) and PHOT2 (*npl1*), both of which are flavoproteins and sense blue / UV-A light. As their names suggest, these photoreceptors are involved in the phototropic response, which describes the tendency for plants to move (usually) toward a light source. PHOT1 is involved in what is termed the first positive curvature and PHOT2 in the second positive curvature (Briggs, 2002). As well as the central role the phototropins play in phototropism, they also have functions in stomatal opening, and chloroplast alignment (Kagawa et al. 2002; Kagawa et al. 2003).

*phot1* came from a forward genetic screen for mutants exhibiting non-phototropic hypocotyls, and was originally designated *nph1* (non-phototropic hypocotyl 1) (Liscum et al 1995; Christie et al. 1998). *phot2* was originally called *npl1* (nph-like 1) and was

shown to be a second functional phototropin (Kagawa et al 2001). Both phototropins have two LOV (light, oxygen, voltage) domains each of which bind a flavin (FMN) chromophore (Christie et al. 1999; Christie et al. 2002).

Phototropism is effected in growing hypocotyls by the directed redistribution of the plant hormone auxin. Recently, Leyser et al (2005) have described the discovery of an auxin receptor.

### 1.4.4. DNA photolyases

Although not strictly photoreceptors, it is probable that cryptochromes evolved from photolyases, and their function depends on electron transfer from two chromophores to DNA (Heelis et al 1993). DNA photolyases fall into two classes: the first class being type I and II, which repair CPDs (cyclobutane pyrimidine dimers), and the second class being (6,4) photolyases, which repair (6,4) photoproducts (Kim et al. 1993). Both CPDs and (6,4) photoproducts are DNA lesions caused by UV-B radiation. There has been some speculation over the role of DNA photolyases, and more widely DNA damage in UV-B perception and signalling.

### 1.4.5. Photoreceptors involved in CHS expression

Figure 1.3 is adapted from Wade (2001) and shows interactions between the various photoreceptors responsible for light induction of *CHS*. The main photoreceptor mediating *CHS* induction in mature (3 week old) *Arabidopsis* leaves is cry1. phy A and B both have a role in red light potentiation of cry1 mediated *CHS* induction with phy B also showing co-action with cry1 without the presence of red light. This work also showed that phyB

negatively regulates UV-B induction of *CHS*, which leads to the suggestion that phyB acts to balance flux through the main UV-A / blue and UV-B inductive pathways.

### 1.4.6. The existence of other photoreceptors is implied

There are several responses to UV-B light in plants which are not attributable to any described photoreceptor (e.g. hypocotyl growth inhibition, or UV-B induction of *CHS*) which suggests that there must be at least one mechanism of photoreception, responsive to UV-B radiation. Further evidence for the existence of a UV-B photoreceptor comes from studies of UV-B induced gene expression (Ulm et al. 2004). UV-B has been shown in this microarray study to rely on none of the known photoreceptors and to induce HY5.

The synergistic (sections 1.7 and 1.8) induction of *CHS* by UV-B and either blue or UV-A light is not disturbed by the loss of any known blue / UV-A photoreceptors or PHYA or PHYB (Wade 1999). A clear implication of these observations is that further, undescribed photoreceptors, including (putatively) at least one UV-B photoreceptor, must exist. As the entire *Arabidopsis* genome has been sequenced, it is possible to search for further putative photoreceptors by sequence homology to existing photoreceptor classes.

## 1.5. The biological relevance of UV-B

It is important to learn how plants respond to UV-B radiation, as depletion of atmospheric ozone seen in recent years may have a deleterious effect on crop plants. Recent work has shown that field-grown wheat (Ambasht and Agrawal 2003) and sorghum (Ambasht and Agrawal 1998) given supplemental UV-B (corresponding to a 20% reduction in stratospheric ozone) exhibit reduced biomass, yield and photosynthetic

rate. Similar effects were not seen in tomato (Bacci, Grifoni et al. 1999). Studies have also suggested that although the mechanism of photosynthesis is damaged by high fluence rate UV-B, it is not threatened by likely increases in solar UV-B as acclimation occurs (Caldwell et al. 1998; Rousseaux et al. 1999).

Ozone layer depletion has highlighted the dangers of UV-B radiation, but there is a biological relevance beyond this. Kim et al (1998) have shown that UV-B mediated photomorphogenesis (hypocotyl growth inhibition and cotyledon expansion) is not dependent on any one of the phytochrome or cryptochrome photoreceptors (the photoreceptors mainly responsible for these photomorphogenic changes). They present evidence that photomorphogenic effects of UV-B are ameliorated in the *phyA / phyB* double mutant and draw the conclusion that either PHYA or PHYB is required for UV-B photomorphogenesis. Based on mutant studies with *cop* (*constitutively photomorphogenic*) and *det* (*de-etiolated*) mutants, this paper also suggests that *COP1* and *DET1* act downstream of UV-B photoreception, as they do in other photoreception mechanisms. Importantly, this paper also suggests that the effect UV-B radiation has on *Arabidopsis* depends very much on its intensity. Low fluence rate (<1 μmol $m^{-2}$ $s^{-1}$) UV-B may trigger photomorphogenic responses, where higher fluence rates (>1 μmol $m^{-2}$ $s^{-1}$) have their biological function via damage. Very little exposure to UV-B is required in order to stimulate *CHS* gene expression. Five minutes in *Arabidopsis* (Jenkins et al. 2001), short (millisecond) pulses in parsley cell culture (Frohnmeyer et al 1999) and low fluence rates are sufficient (Brown, 2005). These observations further argue against the involvement of DNA damage in induction of *CHS* gene expression.

*CHS* is induced by UV-B in a manner which suggests the presence of a specific photoreceptor (Jenkins, 1995; Jenkins, 2001). The function of *CHS* in the production of flavonoids sets it in such a biochemical role where it might be used to anticipate damage caused by UV-B.

In addition to the photomorphogenic responses described by Kim et al (1998), evidence exists that in addition to blue light (working through the phototropins), UV-B may also be able to mediate a phototropic response in etiolated (dark-grown) seedlings (Shinkle et al. 1999; Brown, 2005). The developmental switch from skotomorphogenesis to photomorphogenesis is important to the growing plant. This is highlighted by the ability of multiple wavelengths, received by multiple photoreceptors, and using multiple photoreception pathways to interact in a complex manner (but presumably using the many of the same signal transduction elements along the way) to elicit the same crucial outcomes.

### 1.5.1. UV-B photoreception and signalling

#### 1.5.1.1. A UV-B photoreceptor?

Naturally occurring levels of UV-B (around 3 μmol $m^{-2}$ $s^{-1}$) cause (directly and indirectly) chemical changes in DNA and other macromolecules that other lower energy wavelengths of light do not. In addition, UV-B promotes the formation of ROS (reactive oxygen species). Intriguingly, and uniquely, this raises the possibility that chemical damage might be the mediator, or primary receptor of UV-B in plants. This is in marked contrast to all described photoreceptors, which work by sensing a conformational change in a chromophore on exposure to light.

It is likely that there are several UV-B pathways and DNA damage undoubtedly leads to oxidative stress which in turn excites responses via jasmonic acid, but compelling evidence argues for the existence of at least one UV-B photoreception mechanism which does not rely on damage. The work of Kim et al (1998), as discussed above, clearly suggests that at fluence rates of UV-B which are not sufficient to damage DNA, photomorphogenesis occurs and Boccalandro et al (2001) asserts that a photoreception mechanism exists for low doses of UV-B which enhances PHYB mediated de-etiolation and which does not require phytochromes, cryptochromes or DNA damage. The observation that PHYB mediated de-etiolation is enhanced by UV-B when viewed alongside evidence of the antagonistic effect PHYB has on UV-B induced expression of *CHS* (Wade et al, 2001) again may suggest different UV-B photoreception pathways for photomorphogenesis and the anticipatory induction of *CHS*.

With respect to the induction of *CHS* expression, it has been argued that synergism between UV-B and blue or UV-A light (discussed in section 1.7) indicates the likely existence of a photoreception mechanism that does not require DNA damage (Jenkins et al. 2001; Brosche and Strid, 2003).

There is the suggestion that a UV-B photoreceptor may, based on action spectra for UV-B responses (which differs from spectral peaks of DNA damage), contain a flavin or pterin chromophore (Brosche and Strid, 2003).

### 1.5.1.2. UV-B signalling

Pharmacological studies using *Arabidopsis* cell suspensions (Christie and Jenkins, 1996) provided evidence that UV-B and UV-A / blue photoreception utilised (at least partially)

different signalling mechanisms. This study included evidence that calcium, calmodulin, reversible protein phosphorylation and protein synthesis were required for UV-B induction of *CHS*. Further work (Long and Jenkins, 1998) with inhibitors led to the observation that calcium increases required for *CHS* expression were achieved by release of calcium from intracellular stores via plasma membrane redox activity coupled to photoreception.

Mackerness et al., (2001) suggested that nitric oxide has a role in UV-B induction of *CHS*, but also showed reactive oxygen species (ROS), despite having a role in UV-B signalling, are not involved in the induction of *CHS*. The production of ROS complicate UV-B signalling, as it establishes a link with general defence pathways and particularly with jasmonic acid, salicylic acid and ethylene signalling (Mackerness et al, 1999; Jenkins et al, 2001) and leads to the up-regulation of key defence genes (Surplus et al. 1998).

Pharmacological studies have given insights into the nature of UV-B photoreception and signal transduction, but it is in recent years that two concrete mutants have been described which add to the discussion. These are *uli3* (UV-B light insensitive 3) (Suesslin et al., 2003) and *uvr8* (UV resistant mutant 8) (Kliebenstein et al., 2002). *uli3* was proposed to be a specific component of UV-B signal transduction. The light source used in these experiments included UV-A light, however, meaning that the conditions used were akin to the synergistic conditions used in other studies (e.g. Fuglevand et al, 1996). The uncertainty this produces in characterisation of this mutant means that it is prudent to reserve opinion on its importance until further studies are published. The discovery of *uvr8* is all together more tantalising.

### 1.5.2. *UVR8*

*UVR8* was originally identified as a having increased sensitivity (assessed via leaf damage) to white light with supplemental UV-B radiation (Kliebenstein et al, 2002). *uvr8* exhibits reduced flavonoid accumulation and expression of *CHS,* as well as reduced expression of *PR-1* and *PR-5* genes (both UV-B inducible). UV-B specificity of the *CHS* response has been demonstrated (Brown, 2005). Brown has shown that in addition to the abolition of *CHS* transcription, microarray data which identifies many genes known to be UV-B induced, have altered transcript levels in *uvr8*. The clear implication of Brown's work is that expression of a significant subset of UV-B induced genes have their transcription controlled via UVR8.

*UVR8* has substantial sequence similarity (around 35% identical and 50% similar) to human *RCC1* (regulator of chromatin condensation 1). RCC1 is a nuclear-localised guanine nucleotide exchange factor for the small GTP-binding protein Ran, which plays an important role in nucleocytoplasmic transport and regulation of cell cycle progression and mitosis. This may give an insight into UVR8 function in *Arabidopsis*, but nothing pertaining to this has been published. Brown et al. (submitted for publication, personal comunication) have found that UVR8 has minimal Ran guanine nucleotide exchange activity and concluded that the mechanism of action of UVR8 is different to that of RCC1.

## 1.6. Crosstalk

Signal transduction pathways describe linear interactions between gene products. However, there is mounting evidence for higher-level interactions between pathways sometimes called 'crosstalk' (e.g. Franklin et al. 2004). The consequence of consideration of such crosstalk leads to the adoption of complex network models that probably resemble more closely the way cells work.

Logical models have been developed (Genoud and Metraux, 1999) to encompass many plant biochemical pathways and relate them to one another. This is a brave approach, but has certain problems. It doesn't easily take account of synergism or thresholds and perhaps should include a capacitor function. Consequently, this kind of approach will find it difficult to fully characterise the complexity found in the cell. Difficulties are inevitable but this is still a good place to start. It is probably a good idea to formalise what is understood of the interrelation of pathways. Precedent for this kind of study exists, with modelling of prokaryote and other eukaryote systems using concepts borrowed from symbolic logic and computing science (e.g www.e-cell.org) and it is inevitable that developments in systems biology, microarrays, "omics" technologies and associated improvements in computing are pushing towards whole cell, and whole organism understanding of life.

Crosstalk exists between all the main classes of photoreceptors (Franklin et al. 2004; Wade et al. 2001). Those interactions which pertain to the expression of *CHS* are shown in Figure 1.3 and involve phytochromes, cryptochromes and as yet unidentified UV-B, UV-A and blue light photoreceptors. One of the interactions which awaits elucidation is the synergism seen between UV-B and blue light.

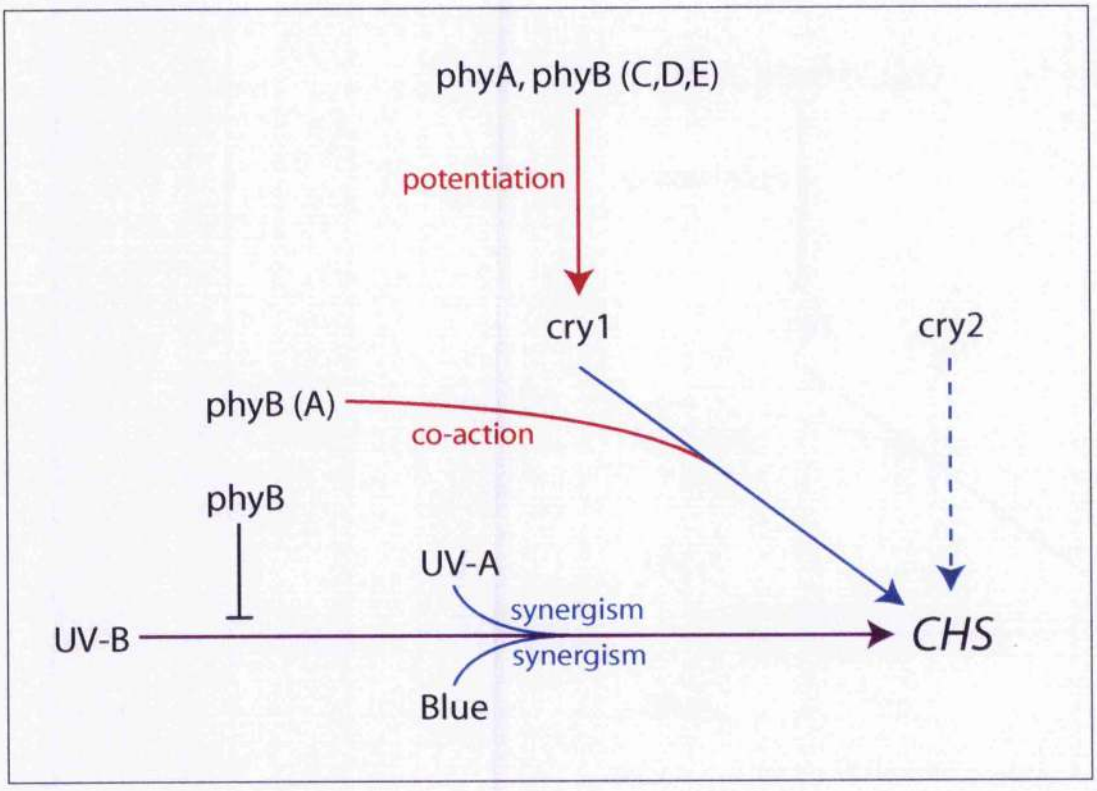


**Figure 1.3 Wade et al (2001) model of photreceptor interactions**

Wade et al (2001) provided a model for photoreceptor interactions in the induction of *CHS* expression. cry1, the main blue light photoreceptor in *CHS* induction, was shown to have its function modulated by phytochromes A and B. In addition, phyB was shown to antagonistically affect UV-B induction of *CHS* expression.

## 1.7. Synergistic induction of *CHS*

Synergism is the name given to the interaction between two stimuli such that they have a combinatorial effect that is greater than the additive effects of both individual stimuli. The interaction may be at any point in the photoreception or signal transduction pathways.

In *Arabidopis*, *CHS* expression is synergistically induced in a range of conditions: mature leaves exposed to UV-B radiation with supplemental UV-A or blue light (Fuglevand et al, 1996) and blue light given in cold (10 °C) conditions.

### 1.7.1. Blue & UV-A and UV-B light synergism

Plants exposed to UV-B radiation along with supplemental UV-A or blue light exhibit synergistic induction of *CHS*. The synergistic interaction between blue and UV-B light with respect to induction of *CHS* transcript, is important and probably is representative of the context in which plants receive these wavelengths of light.

The synergistic stimulation of *CHS* expression with UV-B and either blue or UV-A show differences in signal stability (Fuglevand et al. 1996) suggesting that at least two independent pathways are involved, although these have not been further probed. In addition, there is an implied UV-B photoreceptor responsible for receiving the other interacting signal.

## 1.8. Objectives of this study

The work described in this volume represents an effort to uncover the genetic basis of complex interactions which culminate in the expression of the flavonoid biosynthetic gene *CHS*.

Chapter 3 details a forward genetic approach aimed specifically at the identification of genetic components of the UV-B / blue synergistic induction of *CHS*. The screen was designed to also include mutants in UV-B photoreception as none had been identified at its outset. It was envisaged that this project would identify and initially characterise mutants in these classes and provide transgenic lines which may also be used for further mutant studies.

Chapter 4 adds to the characterisation and proposed mapped-based cloning of *icx2*, an existing mutant exhibiting conditionally aberrant *CHS* expression (see 1.3.1). *icx2* was shown to have a complex pleiotropic phenotype which was investigated. Genetic analysis of the phenotype was also carried out by means of a suppressor screen.

### 1.8.1. UV-B and blue light synergism as the basis of a mutant screen

The forward genetic approach is fundamentally a reductionist approach and as such has certain limitations. It is clear that systems biology and other whole organism and "omics" technologies are becoming ever-more powerful and so also are becoming more popular. The genetic approach can, however be justified by reference to the great discoveries made using a mutant-led approach, which has been very useful in the elucidation and dissection of photoreception mechanisms in *Arabidopsis* since the beginning of the 1980s.

Since in synergistic induction of *CHS*, the blue light signal is more stable than the UV-B signal, it is proposed that the primary screen for mutants should involve imaging plants before any light treatments, after an inductive blue treatment, and again after a subsequent inductive UV-B treatment. This should identify three classes of mutant. Firstly, it should identify mutants constitutively altered in the production of *CHS* (those which don't show any transgene expression at all, although these may be indistinguishable from mutants in the transgene, and are not likely to be very interesting). Secondly, it should identify mutants in blue light signal transduction (i.e. those that don't respond to the inductive blue light treatment). Lastly, it should indicate mutants in the synergism between the blue and UV-B signal transduction pathways, and mutants in UV-B signal transduction together (those that respond normally to blue induction, but not to the subsequent UV-B induction). These could be further classified by a second screen which uses only inductive UV-B light. Those that respond normally will be mutants in the synergism, those that don't will be mutants in UV-B signal transduction.

### 1.8.2. *CHS* as a suitable candidate for reporter gene studies

*CHS* has certain advantages that mark it as a good model for studying complex induction of gene expression in order to elucidate upstream processes. Firstly, *CHS* exists as a single copy gene, with no functional homologues in *Arabidopsis*. Secondly, CHS function is largely controlled at the level of transcription.

### 1.8.2.1. Luciferase

It was important to choose a suitable reporter gene for the experimental work that is described in this volume. The advantages of using luciferase over an alternative reporter are many, and are well reviewed by Michelet and Chua (1996). Briefly, the main features of luciferase which make it suitable for the research proposed here are (1) assay of activity is non-invasive, and incidentally therefore relatively easy to assay using a CCD (charged coupled device) photon counting camera; (2) luciferase has no reported biological function in *Arabidopsis*; and (3) it turns over rapidly in the cell with each luciferase protein molecule reacting only once (a short half-life means that it can be used for applications that look at a change in gene induction over time). The latter gives luciferase an advantage over other reporters such as GUS, which tend to accumulate over time.

Many bioluminescent organisms are known, ranging from jellyfish to fungi, bacteria to fish, algae to worms and fireflies to clams. Enzymes responsible for emission of light are called luciferases. Lampinen et al (1992) divides the action of known luciferases into two categories. Firstly there are bacterial luciferases (coded for by *Lux* genes) exemplified by *Vibrio harveyi*, which catalyze the reaction FMNH2 + O2 + R-CO-H ->FMN + R-COOH + H2O + light (490nm). The second group are eukaryotic luciferases, which require a specific substrate, luciferin, and are typified by the luciferase of the North American firefly (*Photinus pyralis*), commonly called beetle luciferase (*Luc*). Beetle luciferase catalyses the reaction ATP + O2 + D-luciferin -> AMP + PPi + CO2 + oxyluciferin + light (560nm), producing light from the energy stored in ATP. Ford et al (1992) give a two-step equation for this reaction; FL + LH2 + MgATP <-> FL-LH2-

AMP + PPi (1), FL-LH2-AMP + O2 -> FL + oxyluciferin + AMP + CO2 + light (560nm). The firefly luciferase reaction is represented in Figure 1.4.

The kinetics of beetle luciferase light emission are ATP concentration dependent. High ATP concentration leads to a flash release of light where a more even release of light results from lower ATP concentrations. In the firefly lantern, luciferase flashes may be controlled by oxygen availability.

There is a suggestion in the literature that CoA and cytidine nucleotides can stabilize the beetle luciferin reaction (Ford et al., 1992). Most applications rely on endogenous pools of ATP and CoA in the subject tissue to allow the reaction to proceed in a stable manner (e.g. Millar et al. 1992).

Beetle luciferase is about 100 times more luminescent than bacterial equivalents, and as such, has found a great number of applications both in animal and plant research, as can be appreciated from a simple literature search. The first use of luciferase in plant transformations was made in 1986 by Ow et al. (before the first animal transformations). Ow et al. (1986) used a 35S promoter :: luc coding region :: nos terminator fusion to transform (both transiently and stably) plant cells and whole tobacco (*Nicotiana tabacum*) plants. These plants and plant extracts were imaged by placing them in contact with photographic film. Recent applications have used low-light sensing photon counting cameras.

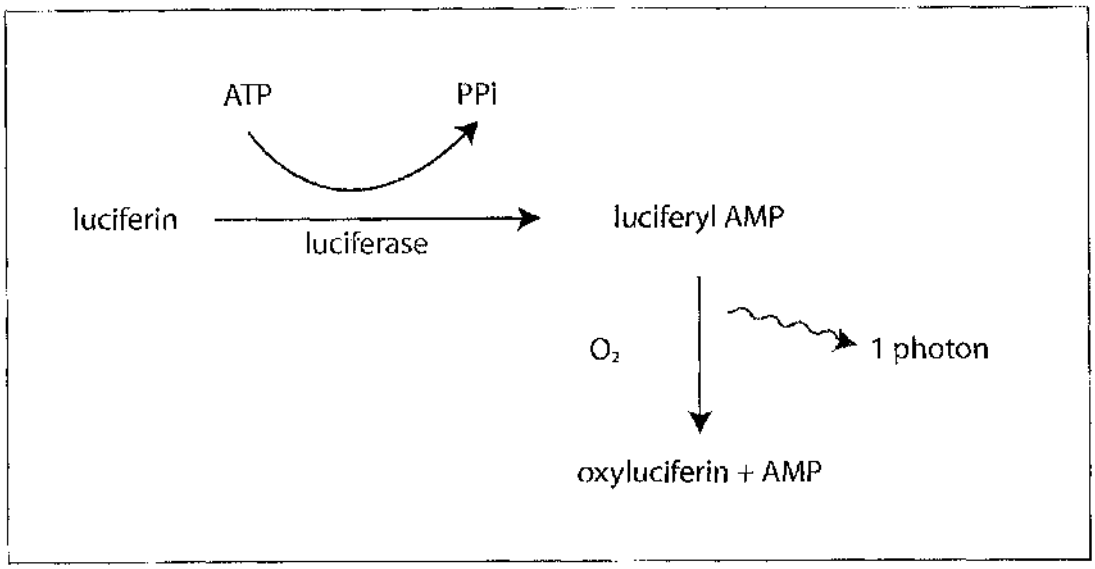


**Figure 1.4 Luciferase reaction diagram**

Firefly luciferase catalyses the conversion of luciferin to oxyluciferin in a two step process which results in the evolution of one photon (560 nm) per molecule converted.

### 1.8.2.2. Reporter gene studies in *Arabidopsis*

It is encouraging to read the work of others who have successfully used comparable genetic screens for mutant isolation. Recent applications of luciferase as a reporter gene used for mutant identification relating to the role of light in plants include the work of Miller et al. (1995, 1996) on circadian rhythms and Michelet and Chua (1996) on phytochrome A signal transducton. This taken with in-house experience and success in mutant isolation with a CHS:GUS reporter line (Jackson et al. 1995) made the prospect of successfully carrying out the proposed screen good.

### 1.8.3. Mutagenesis

The relative merits of EMS (ethyl methane sulphonate), gamma (and other) radiation and T-DNA insertion as agents of mutagenesis in *Arabidopsis* are discussed in section 3.1.3.2 and the relative importance of the arguments depend on the application (and who you talk to).

Briefly, EMS mutagenesis was chosen for a number of reasons. Firstly, it has been used widely and successfully, both in Professor Jenkins lab., and elsewhere in the production of light regulatory mutants found via similar screens to those proposed here.

Although at first glance insertional mutagenesis seems like a good solution to problems of mutagenesis, as you can create mutants with what are essentially tagged mutations, the effort it takes to produce such a population is arguably more than that taken to map mutations made by EMS. Another, perhaps more serious problem with the insertional mutagenesis route is that it does not saturate the genome with mutations as

EMS does as insertional elements used seem to prefer inserting into some genomic sites to others.

EMS was also chosen over radiological methods as EMS produces point mutations whereas radiation (e.g. gamma) tends to produce larger lesions. Single point mutations (once mapped) are then arguably more informative about protein function than a larger lesion.

## Chapter 2. Materials and methods

### 2.1. Materials

#### 2.1.1. Chemicals

Chemicals used were sourced from Sigma (Poole, U.K.), and Fisher (Loughborough, U.K.) unless otherwise stated.

#### 2.1.2. Radiochemicals

[$\alpha$-$^{32}$P dCTP] was obtained from Amersham International (Amersham, U.K.).

#### 2.1.3. Plasmids and bacterial strains

Plasmid maps for plasmids used are shown in Figure 2.1. *CHS:Luc* vector was made by Dr. Matt Shenton.

Electrocompetant *E. coli* and the GV3101 strain of *Agrobacterium* were used.

#### 2.1.4. Enzymes

All enzymes were used with buffers provided and according to manufacturers recommendations. Restriction enzymes were sourced from Promega (Southampton, U.K.) and New England Biolabs (Hitchin, U.K.) and T.aq. DNA polymerase, DNA ligase and reverse transcriptase were obtained from Promega.

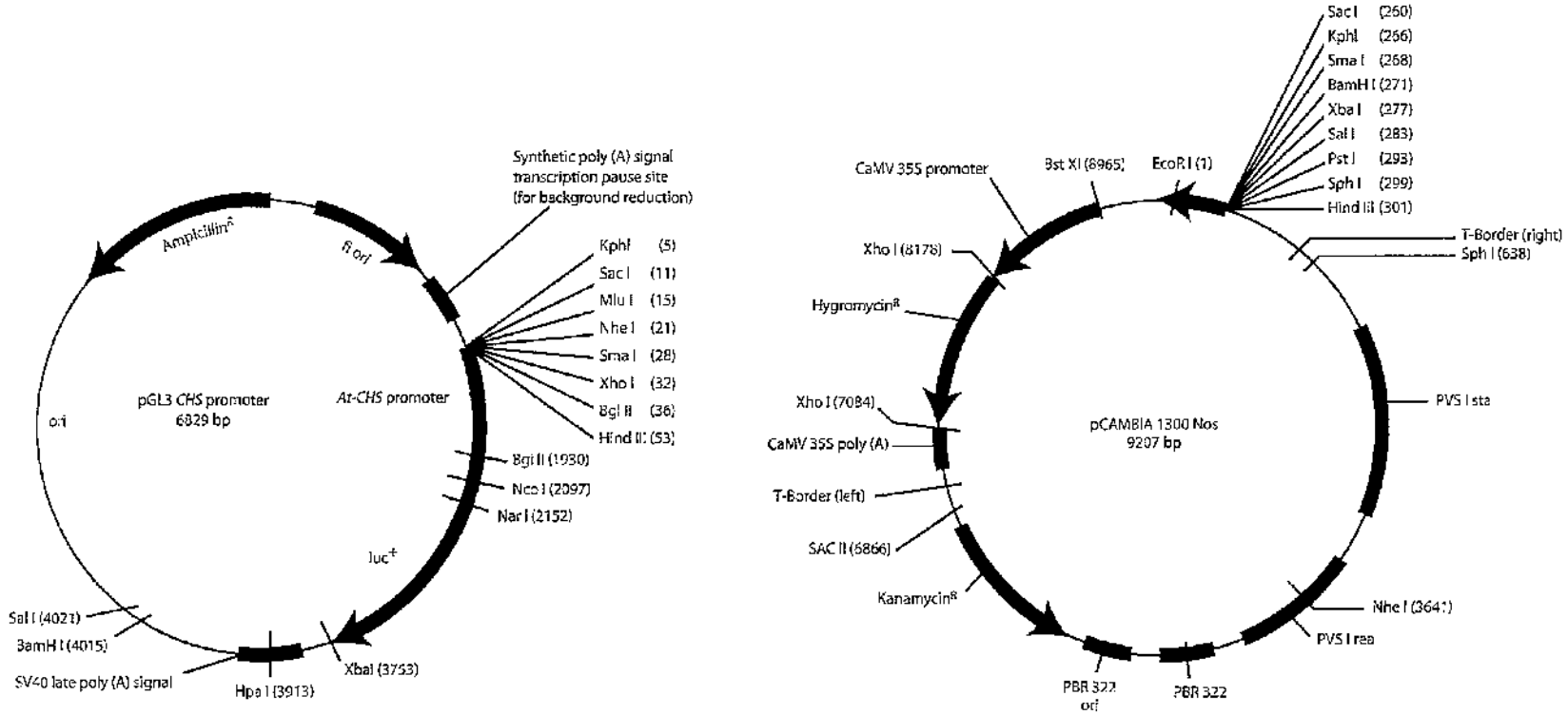


**Figure 2.1 Plasmid maps used**

Maps of plasmids used to produce the vector for transformation of arabidopsis. The 3700 bp fragment from p GL3 and 9163 bp *XbaI*/*HindIII* fragments were ligated to produce the binary vector pBiCHS:Luc+.

### 2.1.5. Oligonucleotides

Oligonucleotides were obtained from M.W.G. (Germany). Primers were designed using Primer3 (http://frodo.wi.mit.edu/cgi-bin/primer3/primer3_www.cgi) software, and checked by hand. Primers were 18-30 bp in length, with the same GC content (about 50%) for both primers of a pair. Annealing temperature ($T_a$) was also matched for both primers of a pair, at around 55-60 °C. For primers < 20 bp, $T_a$ was calculated as [4 (G + C) + 2 (A + T)] -5 °C (Suggs et al., 1981) and for primers > 20 bp, $T_a$ was calculated as 62.3 + 0.41 (%GC) - (500/length (bp)) – 5 °C (Bolton and McCarthy, 1962). Polybase stretches, repeated sequences, complimentary sequences on each primer of a pair and inverted repeats were avoided. Primers were chosen which had 1 or 2 G/Cs at the 3' end to help anchor the primers (despite the added risk of primer dimer formation).

### 2.1.6. Liquid and solid bacterial growth media

LB (Luria – Bertani) medium was used for *E. coli* growth, and consisted of 1% (w/v) tryptone, 0.5% (w/v) yeast extract, and 1% (w/v) sodium chloride, pH 7.0. *E. coli* and *Agrobacterium* were grown on LA plates, i.e. LB medium with 15 g/l agar.

### 2.1.7. Solid plant growth media

The solid plant growth medium used was 0.8% (w/v) agar, 1/2 x Murashage and Skoog (MS) salts, 1 x B5 vitamins, and with or without 1.5% (or other stated) (w/v) sucrose, or antibiotics as appropriate. Media were prepared and made to pH 5.7 without B5 vitamins

and autoclaved. B5 vitamins were added immediately prior to pouring when the medium had cooled to < 50 °C.

### 2.1.8. Antibiotics

Antibiotics were purchased from Sigma (Poole, U.K.). Kanamycin was maintained as a 50 mg / ml stock, and diluted to 50 µg / ml final concentration. Hygromycin stock solution was 15 mg / ml, and diluted to 45 µg / ml. Antibiotic stock solutions were filter sterilised (0.2 µm Nalgene filter), and kept at –20 °C.

### 2.1.9. Soil and pesticides

Autoclaved Growers Potting and Bedding Compost (William Sinclair Horticulture Ltd, Lincoln, U.K.) was used for all applications. Initial watering of all compost was done with the insecticide Intercept (0.15 g $l^{-1}$) (Scott's U.K., Ipswich, U.K.). Serious infestations of thrips led to all compost grown plants being treated with Conserve (Fargro Ltd., Littlehampton, U.K.), diluted according to the manufactures instructions.

## 2.2. General laboratory procedures

### 2.2.1. pH measurement

A Jenway (Felsted, Essex) 3320 pH meter and glass electrode was used for pH measurement of solutions.

### 2.2.2. Autoclaving

All solutions (where appropriate), compost and growth media, plastic-ware, and other equipment, which had to be sterilised for use were autoclaved at 15 psi for 30 minutes (compost for 60 minutes) using a Laboratory Thermal Equipment 225E Autoclave. Biohazardous waste was also autoclaved.

### 2.2.3. Disposal of materials

Glass, sharps, chemicals and radioactive and biohazardous materials, were disposed of according to University of Glasgow procedures. [$\alpha$-$^{32}$P dCTP] use and disposal was logged appropriately.

## 2.3. Plant material and growth

### 2.3.1. Seed stocks

Seed stocks were dried, and stored in 1.5 ml microfuge tubes, labelled appropriately. With the exception of populations produced in the course of this work, unless otherwise stated, seed stocks used were obtained from the Nottingham *Arabidopsis* seed stock centre (NASC). The *tt4icx2* double mutant was generated in Professor Jenkins' lab. (Dr. Mandie Stewart). All mutants used were in the L.*er* ecotype, with the exception of Col-3 and $F_2$ lines derived from crosses with Col-3 Seed was meticulously collected to ensure the reliability of all lines used.

### 2.3.2. Plant growth

All plants used in this work were grown in continuous white light at 20 °C under warm white fluorescent tubes (L36W/30, Osram, Germany). The fluence rates used were 20 μmol $m^{-2}$ $s^{-1}$ low white light (LWL), or 150 μmol $m^{-2}$ $s^{-1}$ high white light (HWL). Plants grown for experiments involving *CHS* induction were grown for 3 weeks in LWL prior to treatment. Plants were watered 3 times a week to ensure damp compost.

### 2.3.3. Seed harvesting

Where seed was to be harvested from plants, plants were grown in approximately 100 μmol $m^{-2}$ $s^{-1}$ white light and allowed to flower. Once flowering was well established and siliques were turning yellow, watering was limited to once per week for two weeks, then stopped (c.f. section 2.3.2), and labelled film negative bags (H. A. West Ltd.) were placed over inflorescences and secured with tape around the base. Bags were not sealed to discourage fungal growth. Plants were then gently bent to one side to avoid seed loss from the open end of the bag. Plants were allowed to dry fully, before harvesting. The contents of negative bags were sieved with a tea strainer to remove all chaff. It is crucial to separate seeds from chaff where they are to be sown by pipette.

### 2.3.4. Seed sterilisation

Seeds were surface sterilised prior to sowing on sterile growth media. Up to approximately 1000 (20 mg) *Arabidopsis* seeds may be sterilised in a 1.5 ml Eppendorf microfuge tube. 1 ml 70% of ethanol (v/v) was added to a 1.5 ml microfuge tube containing seeds to be sterilised. After a 2 minute incubation, the ethanol was removed

(using a sterile pipette tip) and 1 ml of a 10% sodium hypochlorite, 0.01% Triton X-100 solution was added using a sterile pipette tip. Tubes were then closed and inverted several times over the next 5 minutes. The bleach solution was then removed as before, and the seeds were washed 5 times in sterile, distilled water. Sterile 0.1% agar was then added at a ratio of approximately 1 ml per 1000 seeds, as after some experimentation, this proved a suitable density of suspended seeds for pipetting out onto growth media. Seeds were then vernalised at 4 °C, in the dark, for 48 hours.

### 2.3.5. Seed sowing

Seeds sown onto compost were first tapped from the microfuge tube in which they were stored onto a Whatman filter paper. Tapping the edge of the filter paper with the index finger as it is moved across the area to be planted allowed for even and controlled sowing. Seeds sown onto solid, sterile growth media were prepared as described in section 2.3.4. Vernalised seeds, suspended as mentioned, were drawn into a sterile P-1000 pipette tip and pipetted out singly onto the agar surface. This is best achieved using a Gilson pipette and pipetting seeds out slowly by moving the volume setting wheel clockwise between the index finger and thumb.

### 2.3.6. Plant crosses

Plant crosses were performed with the assistance of a binocular microscope. Every effort was taken to allow for easy selection of $F_2$ progeny e.g. use of individuals with a mutant phenotype or carrying a transgene as the male parent. Plants were grown under approximately 100 µmol $m^{-2}$ $s^{-1}$ white light for 4 – 5 weeks, or until flowering begins.

Several buds per female parent were pared down to the stigma (all sepals, petals and male parts removed). All other buds from inflorescences used were removed to avoid contamination or confusion, including pinching out the floral meristem. Stamens from male parents were then collected and used to transfer pollen directly to the stigma of the female parent. Inflorescences used in crosses were labelled and plants placed under a propagator lid for 24 hours to avoid their drying out. After this time, plants were returned to 100 μmol $m^{-2}$ $s^{-1}$ white light until the resultant siliques could be individually harvested. Selection of plants was done in the $F_2$ generation unless otherwise stated.

### 2.4. Plant measurement and representation

All digital images were produced using a 5 megapixel Olympus (Germany, and U.K.) C-50 zoom camera, photon counting camera (section 2.8.3) or scanner (UMAX).

#### 2.4.1. Rosette diameter

To characterise *icx2* rosette growth, individual pots of *icx2*, L.*er* and Col-3 were grown for 1 week under low white light (LWL = 20 μmol $m^{-2}$ $s^{-1}$) in order to allow (particularly *icx2*) plants to become established. After this time, 60 individual plants of each genotype were transplanted to compost (6 x 10 wells of a commercially available gravel tray insert) and further grown under either LWL, or high white light (HWL = 150 μmol $m^{-2}$ $s^{-1}$). High quality digital photographs were taken of each 60 well tray of seedlings to be measured. Each photograph included a scale bar, divided every centimetre, placed in the same plane as the surface level of the compost. Each photograph was digitally manipulated using Adobe Photoshop 6.0 to correct for parallax (using the grid of wells as reference), and

scaled, with reference to the scale bar, so that 1 cm was represented as such within the program. Maximum rosette diameter was then measured by drawing circles with the marquee tool which fully encircled, but touched each plant, and reading off the diameter (to a resolution of 0.1 mm) from the panel labelled "info". Mean rosette diameter and standard deviation were calculated for each genotype in high and low white light and for each time-point.

### 2.4.2. Flowering time

Individual pots of *icx2*, L.er and Col-3 were grown under low white light (LWL = 20 μmol $m^{-2}$ $s^{-1}$) in order to allow (particularly *icx2*) plants to become established, as with those used for rosette measurement. After 1 week, 60 individual plants of each genotype were transplanted to compost (6 x 10 wells of a commercially available gravel tray insert) and further grown under high white light (HWL = 150 μmol $m^{-2}$ $s^{-1}$) until bolting occurred. Chronological age and number of rosette leaves were noted.

### 2.4.3. Root length

Seedlings were grown vertically on solid growth media for 10 days in constant white light (sucrose concentration and light fluence is specified individually for each experiment). This allowed for the easy removal and measurement of seedlings. Root lengths were measured to the nearest mm with a ruler divided every mm. Mean root length and standard error was calculated for each experimental population.

## 2.5. Transformation of *Arabidopsis*

### 2.5.1. *E.coli* transformation and growth

Purified plasmid was added to thawed electrocompetent *E. coli* cells. The mixture (40 µl) was then transferred to an electroporation cuvette, and electroporated (2.5 kV, 21 µF, 6.25 kV / cm). Immediately, 1ml of ice-cold SOC medium was added, and the broth was incubated at 37 °C before being plated out onto LA plates, containing appropriate antibiotics and incubated overnight at 37 °C.

### 2.5.2. *Agrobacterium* transformation and growth

*Agrobacterium* GV3101 cells were transformed by the freeze / thaw method (Mol. & Gen. Genet. (1978), 163:181-7). Cells were grown overnight in 50 ml LB medium (in a 250 ml flask) shaking at 28 °C until $O.D._{600} = 0.5 - 1$. The culture was then chilled on ice for 5 minutes before being centrifuged at 3000g for 5 minutes at 4 °C. Pelleted cells were then suspended in 1 ml of 20 mM ice cold $CaCl_2$. Cells were then competent for transformation. 1 µg plasmid DNA was added to cells immediately before freezing them in liquid nitrogen. Cells were then thawed, and incubated at 37 °C for 5 minutes. 1 ml LB medium was added to the transformed cells, which were then incubated for 4 hours at 37 °C with gentle shaking. Cells were pelleted with centrifugation for 30 seconds in a bench-top microfuge and resuspended in fresh LB medium. Resuspended cells were plated out onto LA plates, containing appropriate antibiotics and incubated for 2-3 days at 28 °C.

### 2.5.3. Vacuum infiltration of *Arabidopsis*

The method of Bent (originally posted to the Arabidopsis bulletin board 11 Jan 1994 and found at http://bionet.hgmp.mrc.ac.uk/hypermail/arab-gen/arab-gen.199401/0009.html) was followed. The only change to this protocol was that 0.01% Silvet L-77 was added to the infiltration medium.

Plants to be transformed were sown in compost with nylon mesh secured with electrical tape around the top of the pot. Mesh was used which allowed plants to grow through it. The first inflorescences were trimmed and plants allowed to produce multiple secondary bolts. Infiltration was performed 4 – 8 days after trimming. For 6 pots, 400 ml culture of *Agrobacterium* was grown up to $O.D._{600} = 0.8$ in LB, and the cells harvested by centrifugation at 1300 g for 10 minutes, then resuspended in 3 volumes of infiltration medium (1/2 M.S. salts, 1 x B5 vitamins, 5% sucrose, 0.044 M benzylamino purine (BAP) and 0.01% Silvet L-77). Resuspended *Agrobacterium* was poured into a large beaker and placed inside a bell jar. Plants to be transformed were placed upside-down in the beaker, submerging all arial parts. The bell jar was then sealed and a vacuum applied until bubbles were visible in the plants. Pressure was quickly released, drawing the *Agrobacterium* suspension into the air spaces of the plants, indicated by darkening of the tissue. Plants were removed from the beaker and placed on their side in a plastic bag over night before being returned to the growth room. Seed was harvested as normal (section 2.3.3). *CHS:Luc* transformations were carried out by Dr. Matt Shenton.

## 2.6. EMS mutagenesis

EMS mutagenesis was carried out according to Leyser and Furner's method (ftp://ftp.arabidopsis.org/home/tair/home/tair/Protocols/compleat_guide/comguidePDFs/6_EMS_mutagenesis.pdf). This method allows for a lot of flexibility in the experimental procedure. In the interests of safety, it is strongly recommended that all procedures involving EMS be carried out in an Atmos bag (Aldrich, Milwaukee, U.S.A., catalogue number Z11, 282-8) inside a fume cupboard and with a back-up supply of sodium thiosulphate (which causes EMS to break down, thereby inactivating it). As the Atmos bag is sealed before the experiment begins, it is also recommended that a full practice run is performed and all necessary equipment and solutions are placed inside before sealing.

60 ml syringes were adapted by removing the end and replacing with two thicknesses of Miracloth (CALBIOCHEM catalogue number 475855, EMD Biosciences, Darmstadt, Germany), secured with electrical tape. Batches of 0.3 g (15000) seeds were then added per syringe and 20 ml 0.1% potassium chloride was drawn into each. Seeds were left to imbibe overnight. Next day, the potassium chloride solution was disposed of and replaced with 60 ml 0.1 M sodium phosphate (pH 5), 5% DMSO, 0.5% EMS. Seeds were incubated for 3 hours, after which time the EMS solution was discarded into a 2 l beaker containing solid sodium thiosulphate and seeds were washed for 15 minutes with 100 mM sodium thiosulphate, twice. Seeds were washed twice more, each time for 15 minutes, with distilled water. The Atmos bag was opened and waste solutions discard in the sink. Water was allowed to run for 30 minutes. Miracloth was cut with a sharp razor blade and mutagenised seeds scraped onto 9 cm filter papers (Whatman (Fisher Scientific U.K. Ltd., Loughborough, U.K.)) and allowed to dry.

### 2.6.1. Collection of $M_2$ batches for screening

$M_1$ seeds were sown directly from filter papers on which they had dried and plants grown and allowed to set seed. Efficacy of mutagenesis was assessed by the observation of a small number (0.5 – 3%) of $M_1$ individuals with white leaf sectors. Seeds were collected from batches of 20 $M_1$ plants and numbered sequentially. Seedlings of the subsequent $M_2$ generation were screened appropriately and appearance of obvious morphological mutants taken to be further evidence of successful mutagenesis.

## 2.7. Illumination of plant material

All light treatments were carried out in temperature controlled growth rooms at 20 °C in the absence of external light and with appropriate eye protection.

### 2.7.1. Light sources and filters

Low (20 μmol $m^{-2}$ $s^{-1}$) and high (150 μmol $m^{-2}$ $s^{-1}$) white light were provided by Osram (Munich, Germany) warm white (L36W/30) fluorescent tubes. The UV-B (3 μmol $m^{-2}$ $s^{-1}$ unless otherwise stated) source was Q-Panel (Q-Panel Co., U.S.A.) UV-B 313 tubes covered with a cellulose acetate filter (West Design Products, London, U.K.) to filter out wavelengths < 280 nm which was changed every 16 hours (or more practically, before each illumination, as no treatments used lasted longer than 16 hours). Blue light (80 μmol $m^{-2}$ $s^{-1}$ unless otherwise stated) was derived from an Osram L36W/67 blue tube with a Lee (Andover, U.K.) Moonlight Blue (No. 183) filter to filter out wavelengths < 390 nm. Sources were those used by Wade et al. (2001).

### 2.7.2. Spectra and fluence measurement

Spectra and fluence rate of light sources used for plant illumination other than white light were measured with a Macam (Livingstone, U.K.) spectroradiometer SR9910. UV-B and blue spectra are shown in Figure 2.2. In all experiments, UV-B fluence rate was measured for wavelengths of 280 – 320 nm and blue light over the interval 390 – 500 nm. White light (400 – 700 nm) fluence rate was measured with a hand-held Skye (Powys, Wales) RS232 meter and quantum sensor.

## 2.8. Anthocyanin extraction and quantification

0.5 g of leaves were frozen in liquid nitrogen, ground in a ceramic mortar and pestle and added to a 15 ml corex tube containing 1.5 ml 1% HCl in methanol. Samples were then shaken overnight at 4 °C before 1 ml sterile, distilled water and 2 ml chloroform were added and the contents thoroughly mixed by vortex. Each sample was then centrifuged at 15 °C for 2 minutes at 15000 g Following centrifugation, the top, aqueous layer was transferred to a fresh microfuge tube. Absorbance was measured at 657 and 530 nm and $A_{530} - A_{657}$ was calculated. Absorbance was reported per g fresh weight.

## 2.9. Imaging luciferase expression

### 2.9.1. Solutions

Beetle luciferin (catalogue number E1603) was obtained as an anhydrous potassium salt from Promega (Southampton, U.K.), and reconstituted with distilled water. 50 µl aliquots of a 150 mM stock solution (250 mg luciferin in 5.235 ml) were kept in total darkness at

(a)

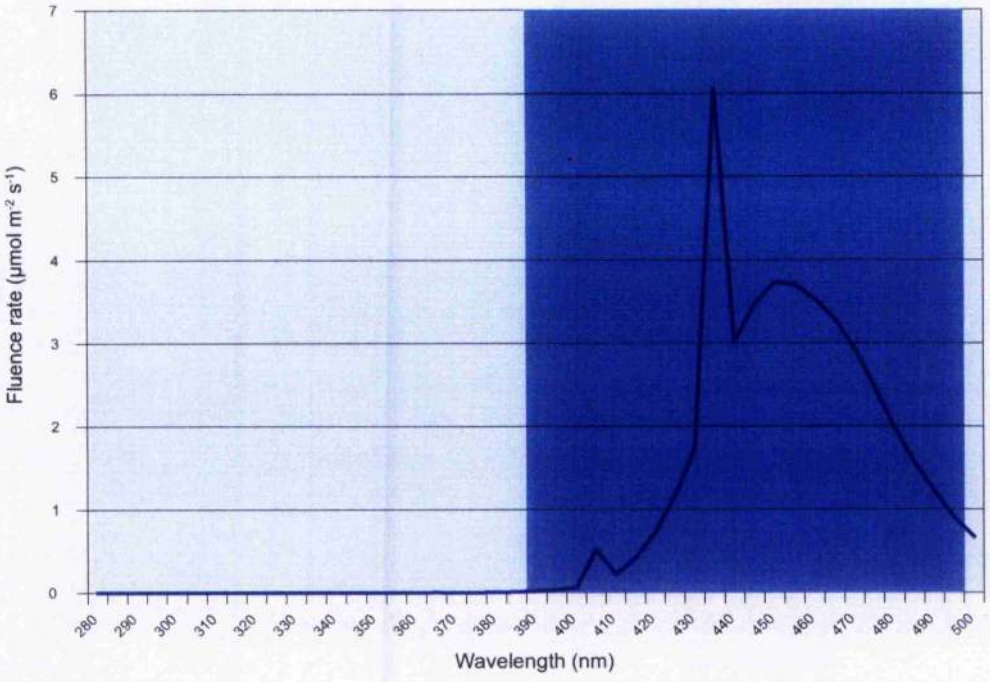


(b)

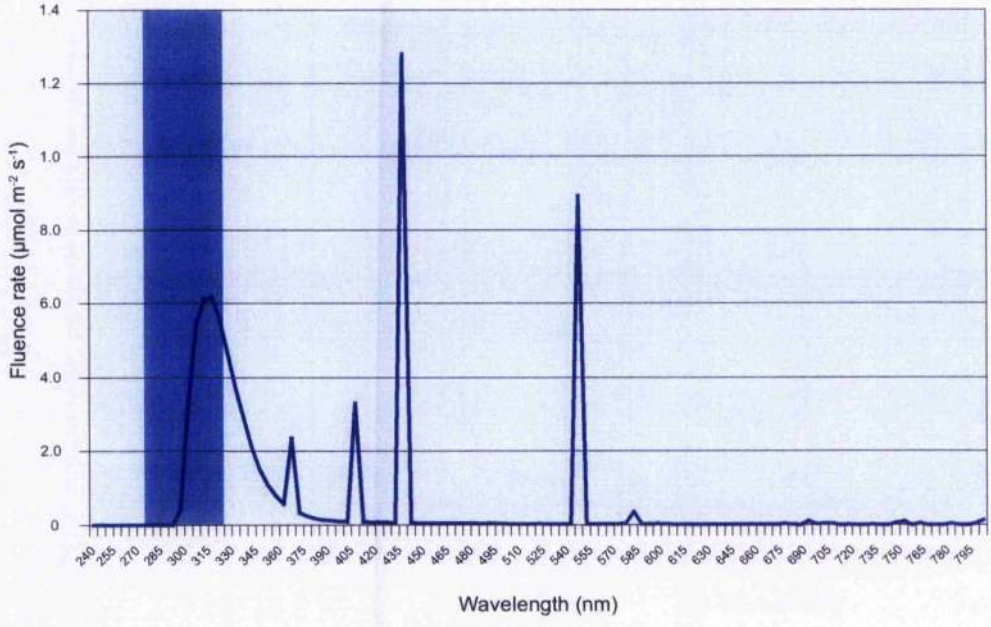


**Figure 2.2 Spectra of light sources used in *CHS* inductive treatments**

80 µmol $m^{-2}$ $s^{-1}$ blue light (a) and 3 µmol $m^{-2}$ $s^{-1}$ UV-B (b) were used. Light was measured using a Macam SR9910 Spectroradiometer. Dark blue areas signify regions defined by the terms UV-B (280-320 nm) and blue (390-500 nm) light.

–80 °C until required. Immediately prior to spraying, 1 or 5 mM working solutions were made up in 0.1% (v/v) Triton X-100.

### 2.9.2. Spraying regime

The method of Miller et al. (1992) was tested for relevance to the proposed application described in Chapter 3 and slightly adapted during the course of the work presented here. Plants to be imaged were sprayed with 5 mM luciferin 12 and 6 hours before inductive light treatments were to begin in order to use up luciferase which may have accumulated in the plant. 20 minutes prior to imaging, plants were sprayed with 1 mM luciferin. In synergistic treatments, 3 rounds of imaging took place (pre-treatment, post-blue and post-UV-B). All experiments described here used an Aztec A470 (Testors Corporation, Rockford IL., USA) airbrush and Ding Hwa Co. Ltd. (Taipei, Taiwan) AC-100 air compressor to apply luciferin solutions form approximately 6 inches directly above study material. The Aztec airbrush has fluid feed rate (mix) and pressure controls, which can be used to ensure even coverage of plants without damaging them. Approximately 150 µl luciferin solution was used per 9 cm Petri dish, or pot. Seed trays used for screening were divided into 5 zones, each of which was sprayed with approximately 500 µl luciferin solution.

### 2.9.3. Photon counting

Luminescence was measured from luciferin-treated transgenic plants using a Photek (East Sussex, U.K.) ICCD 225 Photon Counting Camera (PCC), IFS32 software, darkbox and

lenses appropriate to the sample studied. Integrated images were collected and stored in the software's own .sxy format to facilitate data analysis.

### 2.9.4. PCC image analysis

Photon counting camera images were analysed using the same IFS32 software that was used to gather the data. Three different image analysis methods were used to characterise non-mutant *CHS:Luc* lines. The simplest method (a) was to extract the numerical value of total luminescence (photons detected) collected in a study image and subtract a background value, collected over the same period (but without the presence of luminescent plants). The resultant value was then divided by the total number of plants, thus providing a mean luminescence per plant. This is a valuable method for quickly assessing the effectiveness of a particular treatment but the method doesn't allow the experimenter to calculate standard errors.

The second method (b) used was to produce a set (OAS) of identical circular areas (OAPs), each containing one plant. One background circular area was also taken. The Extract Data tool was then used to produce total luminescence data per selected area, which were transferred to Microsoft Excel. Background was then subtracted from each, and a mean luminescence per plant calculated with a standard error. A problem of this approach is that any variation in size of plants affects the standard error and so exaggerates the reported variation in luminescence.

A way round the problem of variation in plant size was found in the third method (c). Photek's software used with their photon counting camera enables the creation of "learn" files, which carry out a series of image manipulations with parameters defined by

the user. Briefly, this function enables the user to produce a mask based on (exaggerated) luminescence intensity across the image (where threshold may be controlled) and areas of high intensity identified. Areas of high contrast can be recognised as such and the corresponding areas (areas of high luminescence – i.e. plants) automatically selected on the original luminescence image. Luminescence was extracted from these areas as they were from the circular images in method b. In contrast with method b, this method extracts data from areas that differ in size. This was easily overcome by calculating luminescence per pixel.

A method of mutant isolation from luminescence images also had to be developed, where single plants could be isolated from the whole population. Method a, detailed above was obviously unsuitable for this function, as it gives a single mean value per plant for the whole population and cannot distinguish between plants. Methods b and c could each be applied to the problem (method b by statistical means, and method c by subtractive means), but were found to be unnecessary. As each mutant identified is a single plant, the statistical relevance of numerical data collected by methods b and c is questionable, although outliers may be identified. It was quickly realised that where it is useful for luminescence to be quantified in order to characterise the non-mutant *CHS:Luc* lines, this is not necessarily true of mutant isolation.

Visual assessment of the relative change in luminescence between pre-treatment and post-treatment images allowed the selection of mutants without extraction of numerical data. The assumption that most individuals in the screening population should exhibit the wild type response (and so would act as controls for the screening) was made.

Mutants were selected by rapidly flicking between pre-treatment and post-treatment images and selecting individuals that differed from those around them.

### 2.10. Harvesting and storing tissue

Tissue to have DNA or RNA extracted was frozen in liquid nitrogen and ground with a ceramic mortar and pestle (cooled with liquid nitrogen) either at the time of harvesting or after storage at -- 80 °C.

### 2.11. Isolation and manipulation of DNA

Autoclave sterilised plasticware and water was used throughout. Samples were concentrated where required by sodium acetate / ethanol precipitation. 0.1 volumes of 3 M sodium acetate (pH 5.2) and 2.5 volumes ethanol were added, and tubes placed at –20 °C overnight, before tubes were centrifuged at 15000 g at 4 °C for 30 minutes. DNA pellets were then washed twice with 70% ethanol, air dried for 1 hour and resuspended in an appropriate volume of sterile, distilled water.

#### 2.11.1. Qiagen DNeasy DNA extraction kit

*Arabidopsis* genomic DNA was isolated from frozen tissue, finely ground in liquid nitrogen with a ceramic mortar and pestle. The Qiagen (Crawley, U.K.) DNeasy Plant Mini DNA extraction kit was used according to manufacturer's instructions. Frozen, ground tissue was transferred to a microfuge tube and 400 µl of buffer AP1, and 4 µl Rnase A stock solution were added to the tube. The tube was vortexed to mix and incubated for 10 minutes at 65 °C with occasional agitation. 130 µl buffer AP2 was then

added and the tube inverted several times to mix, before being placed on ice for 5 minutes. The lysate was removed from the tube and placed onto the QIAshredder spin column and collection tube, which was then centrifuged for 2 minutes at 15000 g. The liquid supernatant was then transferred to a fresh microfuge tube and 1.5 volumes buffer AP3/E was added and mixed by gentle pipetting. This mixture was passed through the DNeasy spin column (650 µl at a time), which binds DNA, by centrifugation at 15000 g for 1 minute. The DNeasy column was placed in a new collection tube and washed twice with 500 µl buffer AW. The first wash was spun through by centrifugation at 15000 g for 1 minute and an extra minute of centrifugation was allowed in the second wash to help dry the column. The column was then transferred to a fresh microfuge tube and 100 µl of elution buffer AE (pre-heated to 65 °C) was added. The column was incubated an room temperature for 5 minutes with the elution buffer, before being passed through by centrifugation for 1 minute at 15000 g, carrying the purified DNA with it. The elution step was repeated to yield 200 µl DNA solution which was stored at 4 °C until required.

### 2.11.2. Plasmid preparation

The Promega (Southampton, U.K.) Wizard Plus Miniprep kit was used exactly as directed by the manufacturer's instructions.

### 2.11.3. Restriction digests

Restriction enzymes were used in compliance with the vendors' guidelines and with buffers provided. Reactions were allowed to proceed for 4 hours at 37 °C.

### 2.11.4. DNA ligation

Enzymes were used in compliance with the vendors' guidelines and with buffers provided. Reactions were allowed to proceed for 2 hours at 20°C.

## 2.12. Isolation and manipulation of RNA

### 2.12.1. Preparation of materials and solutions

Solutions for use with RNA were made with distilled water which had been DEPC-treated (0.5% (v/v) diethyl pyrocarbonate) and then autoclave sterilised. Autoclave sterilised, disposable plasticware was also used.

### 2.12.2. Gentra Purescript RNA extraction kit – modified protocol

RNA was isolated with a Gentra Purescript RNA isolation kit, but with an extended protocol which included chloroform, isopropanol and ethanol clean-up steps. 5 - 10 mg of frozen tissue per sample (about half a microfuge tube) was finely ground in liquid nitrogen with a ceramic mortar and pestle and transferred to a fresh, labelled microfuge tube. 300 µl cell lysis solution was added per sample (3 or 4 at a time). Samples were inverted to mix before continuing with other samples. 100 µl protein / DNA precipitation solution was then added before the tube inverted 10 times before being placed on ice for 5 minutes and centrifuged at 15000 g for 5 minutes. The supernatant was removed and added to a fresh, labelled tube containing 500 µl chloroform and inverted to mix. Tubes were then centrifuged at 15000 g for 20 minutes before the upper aqueous phase was transferred to a fresh, labelled tube containing 300 µl isopropanol, which was again

inverted several times to mix. Waste chloroform was disposed of suitably. Tubes containing the aqueous phase and isopropanol were centrifuged at 15000 g for 3 minutes to pellet the RNA. The RNA pellets were then washed with 200 µl 70% ethanol (made with DEPC treated water) and centrifuged again at 13000 r.p.m. for 1 minutes before the ethanol was drained. Tubes were left open to air dry for approximately 1 hour before being re-suspended in 20 - 25 µl DEPC treated water for 1 hour on ice. Re-suspended RNA was stored at – 80 °C.

**2.12.3. Preparation of cDNA**

The protocol of Dr. Bobby Brown (University of Glasgow) was followed. RNA was first DNase treated before being reverse transcribed. Frozen RNA samples were thawed and stored on ice. 2 units DNase 1 per 10 µg RNA was added in a total volume of 35 µl (including DEPC-treated water and DNase buffer). Tubes were incubated at 37 °C for 30 minutes. 5 µl DNase inactivation slurry was added to each tube and flicked to mix before a 2 minute incubation at room temperature. Tubes were microcentrifuged at 15000 g for 1 minute to pellet the inactivation slurry. A 35 cycle PCR was then carried out on each sample to confirm the removal of contaminating DNA. cDNA was synthesised from 10 µl of each DNase-treated sample. The DNase-treated RNA sample was mixed with 5.8 µl DEPC-treated water and 0.6 µl of 0.24 µM oligo dT before being incubated at 70 °C for 10 minutes. Samples were immediately cooled on ice and made up to 25 µl with 5x AMV reverse transcriptase buffer (Promega, Southampton, U.K.), 1 mM final concentration dNTPs (Promega), 0.4 u / µl final concentration AMV reverse transcriptase, 1 u / µl final concentration RNase inhibitor (Promega) and 1 mM final concentration of DTT in

DEPC-treated water. Reactions proceeded at 48 °C for 45 minutes, followed by enzyme inactivation at 95 °C for 5 minutes.

### 2.13. Spectrophotometric quantification of RNA and DNA

DNA and RNA were quantified spectrophotometrically. 2 µl RNA or 1 µl DNA was made up to 100 µl with sterile distilled water. Absorbance was read at 260, 280 and 320 nm. The ratio of $A_{260} - A_{320}$ to $A_{280} - A_{320}$ gave an estimation of purity and $A_{260} - A_{320} = 1$ was taken to represent double stranded DNA of concentration 50 µg / ml, and single stranded DNA or RNA at 40 µg / ml.

### 2.14. Amplification of genomic DNA

All routine PCRs (e.g. with genomic or plasmid DNA) were performed in 25 µl volumes and included both positive and negative controls. Master mixes were used such that each reaction tube contained 0.1 nmol / µl dNTPs, 5 pmol / µl each primer, 1.5 mM $MgCl_2$, 1 u T.aq. polymerase, 1 x T.aq. buffer, and 2 µl DNA in sterile, distilled water. PCRs reaction conditions were: 95 °C for 3 minutes, followed by 30 cycles of (94 °C for 30 seconds, then 58 °C for 30 seconds, then 72 °C for 1 minute) and lastly 72 °C for 5 minutes. All PCR was performed with DYAD DNA Engine PTC-220 and PTC-200 thermal cyclers (Genetic Research Instrumentation, Braintree, Essex).

### 2.15. Amplification of cDNA (RT-PCR)

Total cDNA was amplified in 25 µl. Master mixes were used such that each reaction tube contained 0.2 nmol / µl dNTPs, 5 pmol / µl each primer, 1.5 mM $MgCl_2$, 1 u T.aq.

polymerase, 1 x T.aq. buffer, and 2 µl DNA in sterile, distilled water. PCR reaction conditions were: 94 °C for 2.5 minutes, followed by 22 to 25 cycles of (94 °C for 45 seconds, then 55 °C for 1 minute, then 72 °C for 1 minute) and lastly 72 °C for 5 minutes. All PCR was performed with DYAD DNA Engine PTC-220 and PTC-200 thermal cyclers (Genetic Research Instrumentation, Braintree, Essex).

### 2.16. Agarose gel electrophoresis

All agarose gels were cast with 1x TBE (0.1 M Tris-borate, 2 mM EDTA, pH 8.3), and 1 mg / ml ethidium bromide. 0.8% agarose gels were used for all applications with the exception of those used for *icx2* mapping, which were cast with 4% agarose in order to separate polymorphic INDELS, which differed by as little as 11 in 200 bp. Gels were run in TBE buffer under an appropriate current and voltage for the size and agarose content of the gel. Gels were generally run until the loading dye front had progressed at least two thirds of the length of the gel before the desired separation of fragments was observed.

#### 2.16.1. Molecular size markers

Promega (Southampton, U.K.) 25 bp DNA Step Ladder (catalogue number G4511) and Roche (Mannheim, Germany) Marker X (catalogue number 1 498 037) were used.

#### 2.16.2. Visualisation of DNA on agarose gels

6 x DNA loading buffer (50% glycerol, 0.25% (w/v) bromophenol blue, 0.25% (w/v) xylene cyanol FF) was used to ensure proper loading of DNA gels. The addition of the DNA intercalator ethidium bromide to agarose gels allows DNA to be visualised with the

use of UV light. Gels were photographed either on a (Spectroline TC-312A) transluminator with a Polaroid camera, or in a specialised gel documentation system (Gel Doc 2000, Bio-Rad, Hemel Hempstead, UK with Quantity One (4.3.0) software).

### 2.16.3. Recovery of DNA fragments from agarose gels

DNA bands of interest were identified by means of the molecular size marker used, and excised using a sharp razor blade. Purification of DNA from excised bands was effected by the use of the QIAquick (Qiagen, Crawley, U.K.) Gel Extraction Kit, following the vacuum manifold protocol.

## 2.17. Southern blotting

Restriction digested (37 °C for 4 hours) genomic DNA was run on a 0.6% agarose gel at a low voltage (45 V) overnight. The gel was then washed with denaturation (1.5 M NaCl, 0.5 M NaOH) buffer for 45 minutes, then rinsed with distilled water and finally washed with neutralisation buffer (1 M Tris (pH 7.4), 1.5 M NaCl) for 30 minutes, and again for 15 minutes. All washing was done with constant agitation. Hybond-N (Amersham, U.K.) nylon filter was cut to size and well positions and orientation marked with a pencil. A glass plate was placed across a photographic developing tray and wick of Whatman 3MM filter paper was positioned such that the ends overhung the glass plate and into the tray. The tray was then filled with 20 x SSC (3 M NaCl, 0.3 mM *tri*-sodium citrate) so that the wick was in contact with the solution and allowed to get wet. The gel was then placed on top of the wick, supported by the glass plate. The Hybond-N filter was then wetted with water and placed on the gel so that there were no air bubbles between them. Several more

thicknesses of 3MM paper were placed directly on top of the nylon filter, taking pains not to short circuit the apparatus by allowing them to contact the wick. Paper towels were then placed on top of the 3MM paper before another glass plate and 1 kg weight was used to compress the apparatus, which was left overnight.

The apparatus was disassembled and the nylon filter carefully removed. The filter was then gently washed in 6 x SSC, blotted on filter paper, and UV crosslinked.

## 2.18. Radiolabelling DNA

### 2.18.1. Probe selection and preparation

In hybridisation of Southern blots, the luciferase probe used was a 1670 bp fragment digested from the p1300 CHS Luc plasmid with *Nco*I and *Sac*I, and gel purified. This was chosen as it would allow the copy number to be ascertained in genomic DNA of transgenic lines, digested with either *Nco*I or *Sac*I, Southern blotted and probed.

### 2.18.2. DNA radiolabelling

DNA was radiolabelled using the Amersham (Little Chalfont, U.K.) rediprime II (catalogue number RPN 1633) random prime labelling kit. 2.5 – 25 ng DNA to be labelled was prepared in 45 µl TE buffer (10 mM Tris HCl, pH 8.0 and 1 mM EDTA) and denatured by heating for 5 minutes in a boiling water bath, before being snap cooled on ice for 5 minutes. The sample was then pulse centrifuged to bring the contents of the tube to the bottom. The contents were added to the reaction tube (supplied), along with 5 µl Redivue (Amersham) [$^{32}$P] dCTP, mixed by gentle pipetting and incubated at 37 °C for 10 minutes. The reaction was then stopped by the addition of 5 µl 0.2M EDTA.

Stratagene's Push Column and β–shield device were used to separate the newly synthesised probe from unincorporated radio-nuclides. Heat denaturation of the probe was carried out by incubation in a boiling water bath for 5 minutes, followed by snap cooling on ice for 5 minutes before the probe was added to hybridisation buffer.

## 2.19. Hybridisation of Southern blot

### 2.19.1. Hybridisation of nylon filters

Nylon filters from Southern blots were prehybridised with 25 ml IPSR (20 mM PIPES (pH 6.8), 4 mM EDTA, 0.6 M NaCl, 0.2% (w/v) Ficoll 400, 0.2% (w/v) PVP, 1% (w/v) SDS, 0.5% sodium pyrophosphate) buffer at 65 °C for at least 2 hours with 500 µg salmon sperm DNA (denatured at 95 °C for 8 minutes and snap cooled on ice before adding) before the probe was added. 15 ng of probe DNA was added directly to the hybridisation solution and left overnight.

### 2.19.2. Washing nylon filters

The probe was then disposed of and the filter washed. The washing regime was 5 minutes 2x SSC, 0.5% SDS at 20 °C, 15 minutes 2x SSC, 0.1% SDS at 20 °C, 1 hour 0.1 x SSC, 0.5% SDS at 37 °C, 1 hour 0.1 x SSC, 0.5% SDS at 68 °C and lastly a rinse with 0.1% SSC at room temperature.

### 2.19.3. Autoradiography

Filters were heat sealed in plastic and placed in contact with Fuji RX X-ray film, between two intensifying screens in a film cassette for an appropriate length of time before the film was developed and fixed.

## 2.20. Statistical analysis

Appropriate statistical analyses were used. Yates's correction, $\chi^2 = (O - E - 0.5)^2 / E$, was used in $\chi^2$ tests, where O = observed numbers, and E = expected. Standard deviation and standard error were calculated in Microsoft Excel.

## 2.21. Figure construction and manuscript preparation

Once data and images had been collected, figures were made using Microsoft Excel, Adobe Photoshop 6.0, and Illustrator 10.0 and set with Adobe InDesign 2.0. Manuscript preparation was done with Microsoft Word (Mac OS 9, and Windows XP editions). Endnote 5 was used to manage references.

## Chapter 3: Identification and characterisation of mutants altered in the UV-B / blue light induction of chalcone synthase.

### 3.1. Introduction

Given independently, both UV-B (λ = 280 – 320 nm) and blue (λ = 390 – 500 nm) light induce transcription of chalcone synthase (*CHS*). Given together, UV-B and blue light induce the transcription of *CHS* to a greater than additive or synergistic, degree (Fuglevand et al. 1996).

It has been shown previously (Fuglevand et al. 1996) that the synergistic induction of *CHS* can be achieved by giving both blue and UV-B light simultaneously, or by giving each of these light conditions sequentially, with a short interval between. This requires the photoreception mechanism involved to exhibit the ability to be cocked and later fired (in effect, to have a "memory"). The sequence of light treatments is, however, important.

Synergistic induction is seen only when blue light is given before UV-B meaning that the cellular "memory" is primed by blue light but not by UV-B. A clear implication of this observation is that more than one photoreception pathway is involved in the synergistic induction of *CHS* by UV-B / blue light.

Interestingly, UV-A light also has the ability to synergistically enhance the induction of *CHS* when given with UV-B light, although the dynamics of this interaction are different from those of the UV-B / blue synergism (Fuglevand et al. 1996; Wade, 1999). The UV-A signal is transient (i.e. cannot prime the response) whereas the blue signal is relatively stable. This suggests a complex network of interactions involving separate UV-B, UV-A and blue light pathways. In addition, there is evidence that blue

light and cold induce expression of *CHS* synergistically (Dr. Mandie Stewart, unpublished, personal communication). Neither the UV-A / UV-B nor the blue / cold synergistic induction of *CHS* were studied, as for various reasons, they were found to be unsuitable for assessment using *CHS:Luc* reporter lines.

### 3.1.1. An opportunity for mutant discovery

The observation that chalcone synthase (*CHS*) gene expression could be induced synergistically, by UV-B and blue (or UV-A) light in *Arabidopsis* (Fuglevand, 1996) suggested that mutants specifically altered in crosstalk between these interacting photoreception pathways may be amenable to discovery by forward genetic means, using a reporter gene system driven by the *CHS* promoter to report endogenous *CHS* expression. If designed correctly, a screen conducted to identify such mutants would be expected to yield only novel functional mutants as no gene products have yet been implicated in this interaction. Furthermore, both UV-B signal perception and signal transduction are poorly understood, and so a properly designed screen might also uncover novel mutants involved in general UV-B photoreception or signalling.

When this project was conceived, no genetic element of UV-B photoreception or signalling had been identified. Since then, it has become clear that the gene *UVR8* (Kliebenstein et al. 2002; Kliebenstein et al. 2002) (and possibly *ULI3* (Suesslin et al. 2001) is involved. There is some evidence that brassinosteroids are involved in UV-B signalling. In addition, pharmacological evidence suggests that calcium may be involved in UV-B signalling. UV-B responses are discussed more fully in Chapter 1.

As well as there being no known UV-B receptor, none of the photoreceptors identified in *Arabidopsis* (5 phytochromes, 2 (or 3) cryptochromes, and 2 phototropins, as detailed in chapter 1), have been specifically implicated as the photoreceptor responsible for the blue light sensing component of UV-B / blue synergistic induction of *CHS* (Wade, 1999; Wade et al. 2001). CRY1 is the main mediator of blue light induction of *CHS* expression, but mutant studies have shown UV-B / blue synergistic induction to be unaffected by the absence of CRY1 and other photoreceptors. The possibility exists, then, to find novel blue and UV-B photoreceptors, and signal transduction elements.

### 3.1.2. Aim of mutant screen

The aims of the work detailed in this chapter were to develop and carry out a robust mutant screen which would identify *Arabidopsis* mutant lines altered in UV-B / blue light (synergistic) or UV-B mediated induction of *CHS* and to characterise those mutants, in this regard.

### 3.1.3. Experimental approach

The experimental approach taken was first to generate and characterise at least one non-mutant transgenic line containing a single (i.e. corresponding to a single insertional event in the host genome), homozygous copy of a *CHS:Luc* reporter construct (where the *Arabidopsis thaliana CHS* promoter is used to drive the Luciferase coding sequence from *Photinus pyralis*). It was considered important to choose a line that was homozygous for a single insertion of the transgene, as it would reduce potential for variation in the non-mutant lines used for mutant discovery.

The resultant transgenic line would then be characterized with regard to luminescence and used to select screening conditions. It might then be shown that it faithfully reports endogenous *CHS* transcript levels, under screening conditions by comparing transcript levels in wild type and transgenic lines with one another and with luminescence data for appropriate light treatments.

A population of $M_2$ plants, derived (using EMS mutagenesis) from a line characterized as suggested above would then be used to identify putative mutants in blue / UV-B synergistic signalling to *CHS* by monitoring *CHS* expression in appropriate light conditions, as reported by luciferase luminescence. Mutants found in this way may then be cloned using traditional map based cloning. A forward genetic approach was chosen as there were no extant mutants nor candidate genes shown to have any involvement in the UV-B / blue signalling pathway.

### 3.1.3.1. Choice of reporter

The luciferase enzyme (Luc) from the firefly (*Photinus pyralis*) was first used to report gene expression in eukaryotes in 1986, when Ow et al. expressed the gene, controlled by a CaMV 35S promoter in carrot protoplasts, and transgenic tobacco plants. Since then, it has been used successfully in plant and animal systems, and has been used to great effect in similar screens to that described here (Michelet and Chua 1996; Millar et al. 1996).

Luciferase uses a substrate, luciferin, along with ATP, $Mg^{2+}$, Co-A, and oxygen to catalyse the formation of oxyluciferin and evolution of light ($\lambda$=535nm). Since the other reaction ingredients exist in endogenous intracellular pools, only the addition of luciferin is required for the reaction to take place in transgenic plants.

Theoretically, a single photon is evolved from the conversion of each molecule of luciferin to oxyluciferin but, empirical measurements show only about 90% of reactions give off light (Van Leeuwen et al, 2000). The evolution of light means that luciferase activity may be easily (i.e. with a luminometer or photon counting camera) and non-invasively visualized *in planta* without negative effect on the life of the plant.

The firefly luciferase reaction involves three forward steps, and regeneration of the enzyme in a subsequent step (Figure 1.4). The completion of the regeneration step is slow and the half-life of luciferase is short. This means that each luciferase protein molecule only acts (i.e. causes luminescence) once before being degraded. Hence, given the presence of all the reactants, luciferase can accurately and dynamically report both qualitative and quantitative changes in gene expression (promoter activity) in (almost) real time and should not accumulate in the presence of luciferin *in planta.*

It is important to note that luciferase has no demonstrated biological function in *Arabidopsis* (although luciferin has been shown to induce *PR* gene expression (Jorda and Vera, 2000).

Luciferase has, then, certain advantages as the reporter for mutant screens where high throughput and the ability to rescue selected plants are important.

### 3.1.3.2. Choice of mutagen

The successful execution of a mutant screen requires careful planning and the selection of an appropriate mutagen requires a clear view of the expected results of an inquiry. Chemical, radiological, and biological mutagens have associated benefits and drawbacks, which make them suitable for different kinds of projects. For example, different methods

of mutagenesis produce different kinds of mutation. This may also be exploited in the design of a mutant screen.

Factors which might influence the selection of a mutagen are the kind of mutation desired, number of mutants wanted, expected phenotype (i.e. ease of mapping), basis of selection, possibility of future screens using the same biological materials and resources and time available. If a large number of mutants are expected, and sufficient resources are available to characterise many of them, then T-DNA insertional mutagenesis is appropriate.

Screening a large insertionally mutagenised population has certain strong advantages over traditional chemical or radiological methods of mutagenesis. Perhaps chief amongst these is the fact that the agent of mutagenesis (i.e. DNA of known sequence) tags the mutation and can be used directly to sequence adjacent host DNA. Newly sequenced host DNA can then be compared (using the BLAST algorithm at http://www.ncbi.nlm.nih.gov/BLAST/, (Altschul et al. (1990))) against the whole genome thereby giving chromosomal location and gene identity without the need for map based cloning. This is, of course, only possible since the whole *Arabidopsis* genome has been sequenced (analysed in Kaul et al. 2000) and is freely available.

T-DNA mutagenised populations are commercially available and are suited to search for mutants with a clear physical (developmental or morphological) phenotype or altered survival in particular environmental circumstances. These populations have been used successfully by other researchers and although this does not guarantee success, it is helpful to know that the biological materials you are to use have been successful in other screens.

If a biochemical phenotype (not physically manifested or characterised) is being studied, and a reporter gene is to be used to identify mutants, it becomes necessary to generate a new T-DNA mutagenised population, using the reporter line. In this case, it is important to know what is to be expected from the mutant screen to be undertaken. A balance has to be struck between the effort of producing such a population and the effort involved in mapping and cloning eventual mutants identified from the screen. Where it is important to produce mutants quickly and it is likely that only one or a few will be mapped and cloned, non-tagged mutagenesis is probably the better choice. Where many mutants are expected and all will be looked at in great detail, or if future genetic screens are to be carried out on the same population of mutants, then insertional mutagenesis may be the favoured alternative. This is time-consuming and is not a trivial exercise, but will only have to be done once and will ultimately save time in the mapping and cloning of mutants generated by other means.

The experimental strategy outlined in section 3.1.3 required the generation of new transgenic lines of *Arabidopsis* and so an insertionally mutagenised population was not already available. Of course, it would be possible to first produce the transgenic line, and subsequently create an insertionally mutagenised population from this line, which could then be screened for aberrant *CHS* expression. On balance, this was not considered the best route to mutant discovery as it would involve considerable time and effort to produce such a population and it was deemed important to gain mutants quickly. This, taken with the facts that only one or a very few mutants could realistically be studied and that all the components of the pathway were still to be found (and so new mutants might

reasonably be expected to be novel) added weight to the argument in favour of the traditional route of mutagenesis.

Other common methods of mutagenesis suitable for production of a mutant population are radiological or chemical. Radiological methods, such as the use of gamma or X-rays or fast neutron bombardment use high energy radiation to physically damage DNA, which can cause large lesions and chromosomal re-arrangements. Although these are potentially (although not necessarily) more amenable to map-based cloning, the expression of many genes may be affected. By far the most common method of chemical mutagenesis is the use of ethyl methane sulphonate (EMS).

EMS was chosen as the mutagen for this work as it is technologically easy to use and has been used successfully in similar screens (for example, the screen that produced icx2, the mutant discussed in Chapter 4), so established protocols exist. In addition, EMS causes specific lesions (usually G/C to A/T substitutions), which result in discrete mutants, which can then be map-based cloned. Chemical mutagenesis (usually performed with EMS) is also an ideal method to use if new alleles of a known gene are desired. Methods such as TILLING make good use of EMS to generate new mutant alleles of known genes.

### 3.1.3.3. Mapping strategy

Mapping likely classes of mutants should be thought about before embarking on a programme of mutant screening. When using a reporter gene to expose a biochemical phenotype, it should be remembered that there may be no associated physical phenotype. A strategy has to be in place to map mutants not exhibiting a physical phenotype.

Any mutants arising from the screen developed here may have no physical phenotype to facilitate mapping. The biochemical phenotype (i.e. the alteration of *CHS* expression) might be used to map-based clone any such mutants. After considering more complex schemes, it became obvious that the best route to a mapping population for these mutants would be to select individuals from the $F_2$ of Col x mutant (L.er) crosses. In such an $F_2$, 1/4 of the progeny would be homozygous for the mutation (high likelihood that it would be recessive), and 3/4 would be hemizygous or homozygous for the transgene. This would make a mapping population of 3/16 of the progeny, rather than 1/4, as expected based on a recessive physical phenotype. This strategy requires that individuals could be distinguished based on their transgene and mutation status (i.e. homozygous, hemizygous). Also the difference between high and low *CHS* expressors, as reported, might not be as obvious in a mixed Col / L.er background. If these problems were found to be real, then the use of reference images taken of each $F_2$ batch given low white light (LWL < 20 μmol $m^{-2}$ $s^{-1}$) and an inductive treatment might allow these to be distinguished.

### 3.2. Generation of non-mutant *CHS:Luc* primary transformants

The generation and verification of the non-mutant lines is illustrated in Figure 3.1. *Arabidopsis thaliana* (ecotype Landsberg erecta) was transformed via the *Agrobacterium* tumefaciens vacuum infiltration method using plasmids, *Agrobacterium* strain, and method detailed in Materials and Methods. T-DNA included a luciferase transgene driven by the *AtCHS* (*Arabidopsis thaliana CHS*) promoter and $Hyg^r$ (hygromycin resistance) transgene to allow for easy selection of primary transformants. Plasmids

containing either *CHS:Luc* or *CHS:Luc*$^{+}$ in their T-DNA were used for transformation. *CHS:Luc* vector construction and transformations were carried out by Dr. Matt Shenton.

Growth of the resultant $T_1$ generation (i.e. primary transformants) on selection medium (0.8% agar + 1/2 MS + 1xB5 vitamins) containing (50 µg/ml) hygromycin resulted in the identification of eight primary *CHS:Luc* transformants, designated *CHS:Luc* 1-8 and five *CHS:Luc*$^{+}$ primary transformants, designated *CHS:Luc*$^{+}$ 1-5. The presence of luciferase transgenes were confirmed using *in planta* imaging of $T_2$ plants (Figures 3.3 and 3.4). Only lines containing the *CHS:Luc* sequence were used, as these transformants were generated and characterised as *CHS:Luc*$^{+}$ transformations were carried out. *CHS:Luc*$^{+}$ transformations were only performed as insurance against *CHS:Luc* transformants being unsuitable. *Luc*$^{+}$ individuals would be expected to give a stronger signal than those containing *Luc* . Figure 3.2 shows that contrary to expectations both *CHS:Luc* and *CHS:Luc*$^{+}$ $T_2$ individuals did not differ significantly in luminescence on exposure to 8 hours, 80 µmol $m^{-2}$ $s^{-1}$ blue light.

Figure 3.3, shows an integrated luminescence image (180 seconds), laid over a bright field image (i.e. a photographic image taken with the photon counting camera in "bright field" mode and using room light) of a single *CHS:Luc* 3.4 (see below) seedling exposed to 8 hours, 80 µmol $m^{-2}$ $s^{-1}$ blue light and sprayed with 1mM luciferin 20 minutes prior to imaging. It is clearly seen that luminescent regions observed correlate exactly with the position of the seedling. This was found to be the case for all transformed lines with the exception of *CHS:Luc*$^{+}$ 7. Overlayed images such as this were used to assess the segregation of the transgene in *CHS:Luc* lines.

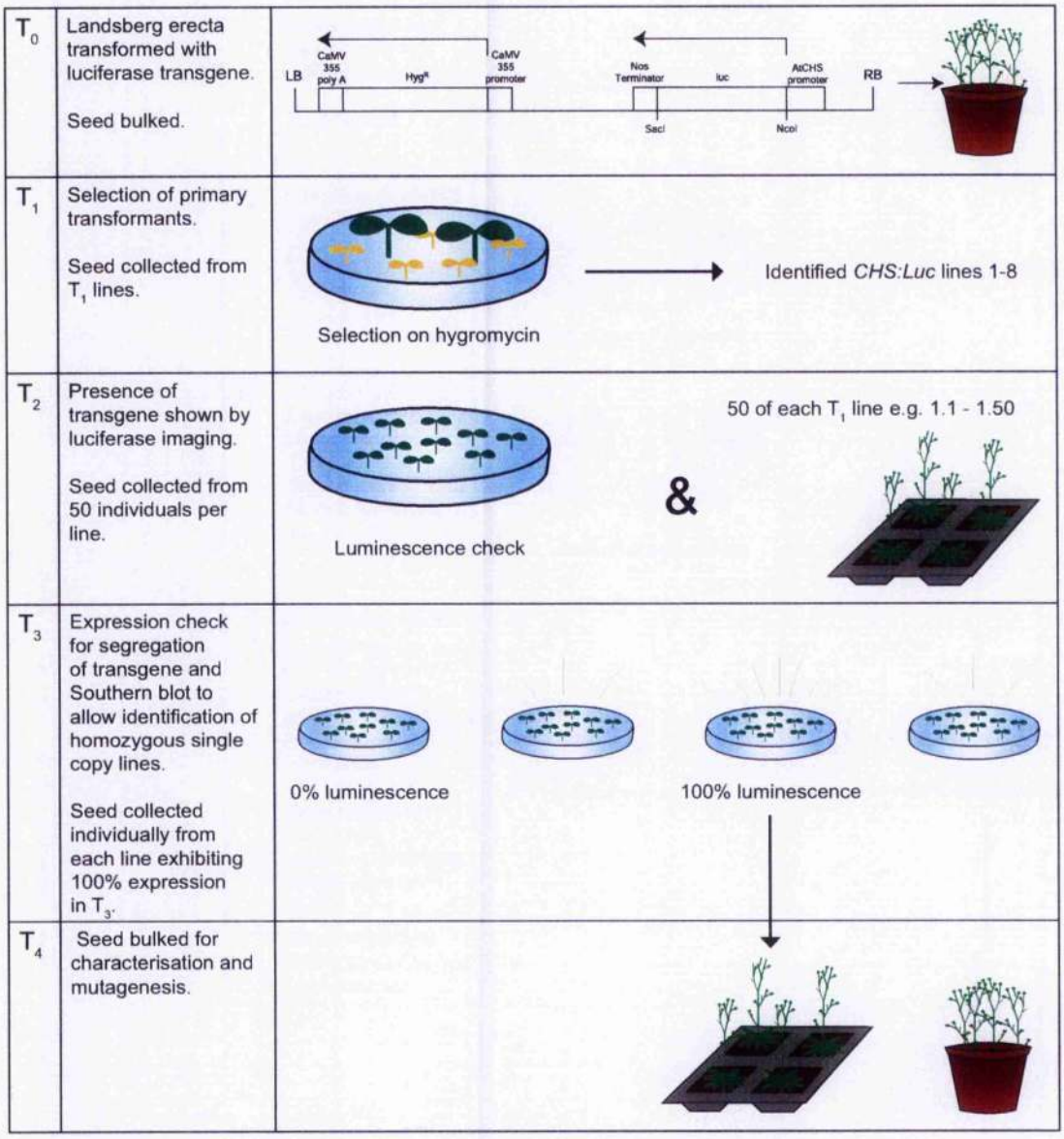


**Figure 3.1 Schematic representation of selection of a *CHS:Luc* transgenic line**

*Arabidopsis CHS:Luc* primary transformant seedlings were selected on solid growth medium in low white light (LWL < 20 μmol $m^{-2}$ $s^{-1}$), based on their hygromycin resistance. Seed was collected and sown to check for luminescence in light conditions known to induce chalcone synthase (*CHS*), i.e. 8 hours of 80 μmol $m^{-2}$ $s^{-1}$ blue (λ = 390 – 500 nm) light. Homozygosity of the transgene was demonstrated by selection of an appropriately segregating line (Figure 3.6) and single copy status was assessed by Southern blot (Figure 3.5).

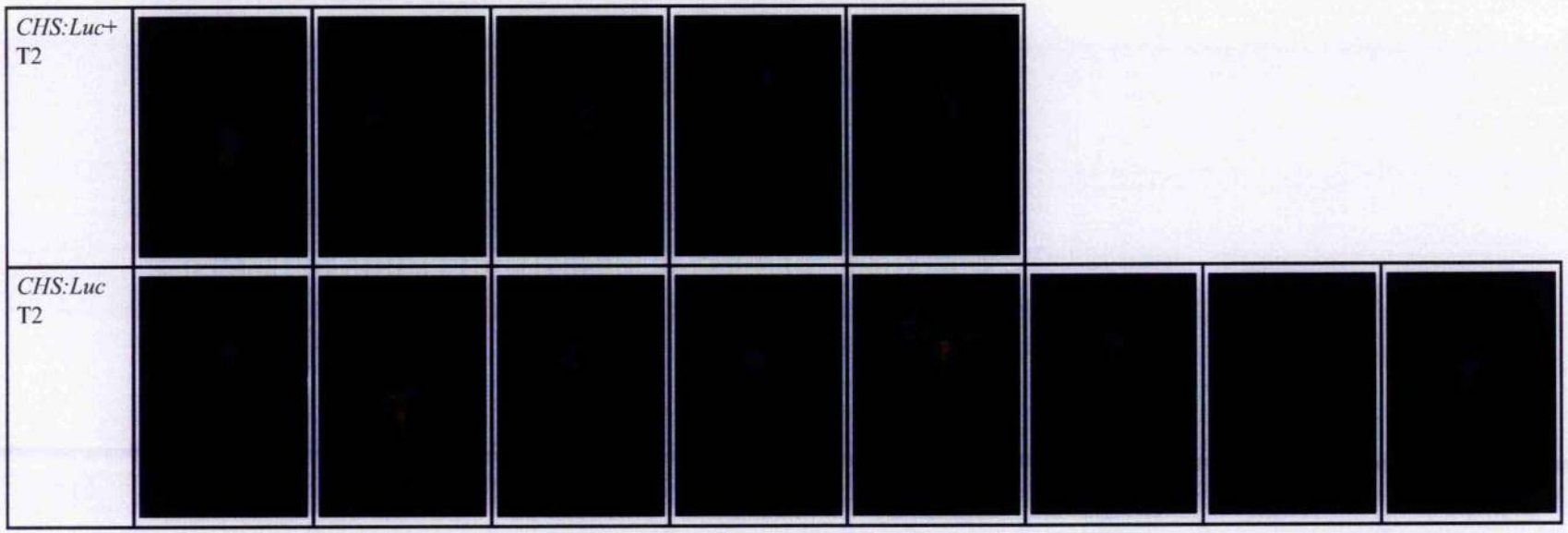


**Figure 3.2 *CHS:Luc* and *CHS:Luc*$^+$ T2 express luciferase**

*Arabidopsis CHS:Luc* and *CHS:Luc*$^+$ T2 seedlings were grown on solid growth medium in low white light (LWL < 20 µmol $m^{-2}$ $s^{-1}$) for 14 days. Seedlings were then exposed to light conditions known to induce chalcone synthase (*CHS*), i.e. 8 hours of 80 µmol $m^{-2}$ $s^{-1}$ blue ($\lambda$ = 390 – 500 nm) light. Plants were sprayed with 5 mM luciferin 12 and 6 hours before the experiment began, and with 1 mM luciferin immediately prior to imaging. Images were collected with a photon counting camera for 180 seconds. False colour images are shown, where colours represent a logarithmic scale from black (no luminescence), through blue, green, yellow, red, purple to white (saturated pixels).

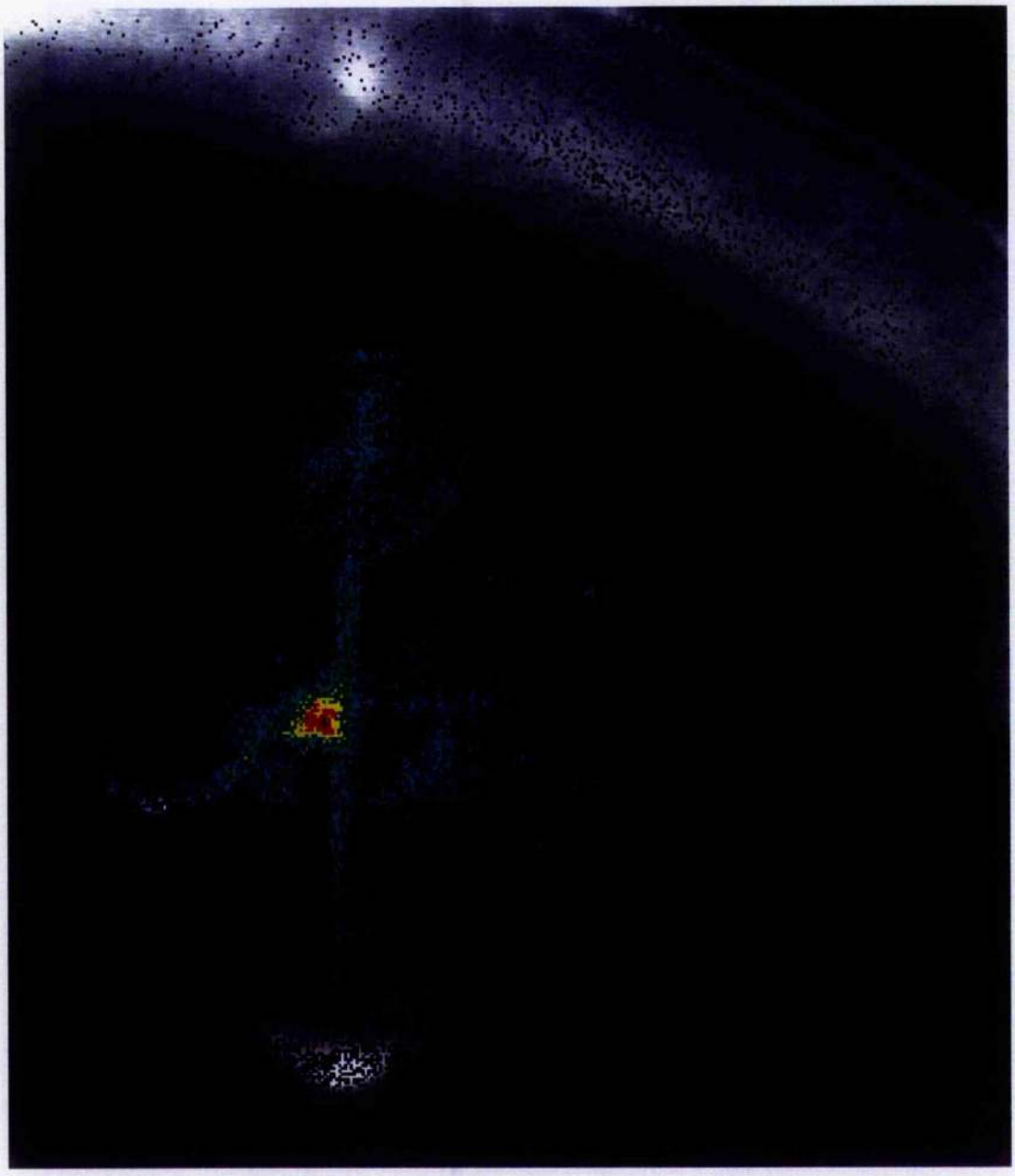

**Figure 3.3 Luminescence correlates with seedling position**

*Arabidopsis CHS:Luc* 3.4 seedlings were grown on solid growth medium in low white light (LWL < 20 μmol $m^{-2}$ $s^{-1}$) for 14 days. Seedlings were then exposed to light conditions known to induce chalcone synthase (*CHS*), i.e. 8 hours of 80 μmol $m^{-2}$ $s^{-1}$ blue ($\lambda = 390 - 500$ nm) light. Plants were sprayed with 5 mM luciferin 12 and 6 hours before the experiment began, and with 1 mM luciferin immediately prior to imaging. Images were collected with a photon counting camera for 180 seconds and in brightfield mode (which produces a standard black and white photographic image with ambient light). The luminescence image was then superimposed on the brightfield image. False colour images are shown, where colours represent a logarithmic scale from black (no luminescence), through blue, green, yellow, red, purple to white (saturated pixels).

### 3.2.1. *CHS:Luc* lines 1.7 and 3.4 are homozygous for the transgene

A single site of *CHS:Luc* transgene insertion per genome was assumed (based on $\chi^2$ tests for luminescence in $T_2$) for each $T_1$ individual (lines 1, 3, 4, 6 and 8) until it was satisfactorily demonstrated to be true or false by Southern blot (section 3.2.2). Lines (2, 5 and 7) that had transgene insertions numbering greater than one were discarded.

Seed was collected from fifty $T_2$ individuals per $T_1$ line, and each $T_2$ line given an identifying number 1-50, separated from the parental ($T_1$) line number by a decimal point (e.g. *CHS:Luc* 1.1 – 1.50). This was done in order to select at least one $T_2$ line where the transgene was present and homozygous (i.e. with no segregation). Where a single insertional event is seen, $T_3$ lines would be expected to exhibit either no luminescence, luminescence in 75% plants, or luminescence in 100% plants, respectively representing, $T_2$ individuals lacking the transgene, hemizygous for the transgene and homozygous for the transgene (i.e. exhibiting Mendelian segregation of the transgene).

Amongst others, *CHS:Luc* 1.7 and 3.4 were selected and assumed homozygous for the transgene, as shown in Figure 3.4, which demonstrates 100% luminescence in images of lines *CHS:Luc* 1.7 and 3.4. The veracity of this position was dependent on the transgene copy number, which was assessed using Southern blotting.

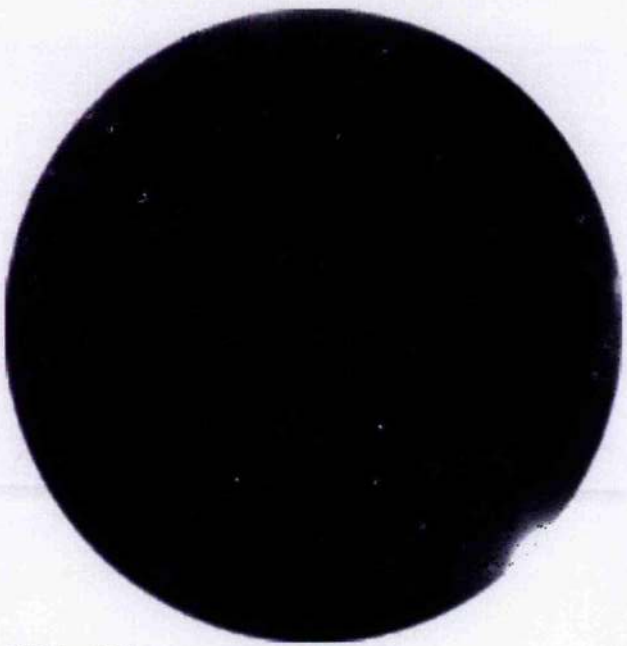

*CHS:Luc* 1.7 $T_3$

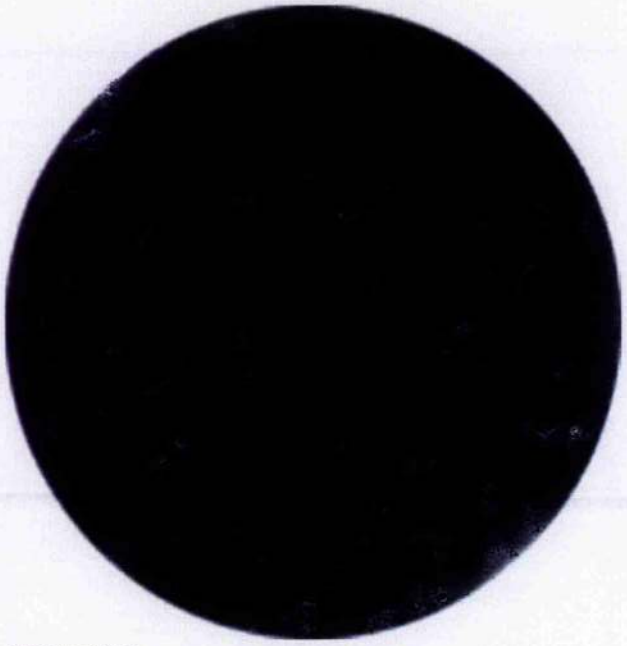

*CHS:Luc* 3.4 $T_3$

**Figure 3.4 100% of *CHS:Luc* 1.7 and 3.4 $T_3$ show luminescence**

*Arabidopsis CHS:Luc* 1.7 and 3.4 $T_3$ seedlings were grown for 21 days on solid growth medium in low white light (LWL < 20 µmol $m^{-2}$ $s^{-1}$). Seedlings were then exposed to 8 hours of 80 µmol $m^{-2}$ $s^{-1}$ blue ($\lambda$ = 390 – 500 nm). Plants were sprayed with 5 mM luciferin 12 and 6 hours before the experiment began, and with 1 mM luciferin immediately prior to imaging. Images were collected with a photon counting camera for 360 seconds. False colour images are shown and superimposed on bright field images, where colours represent a logarithmic scale from black (no luminescence), through blue, green, yellow, red, purple to white (saturated pixels).

### 3.2.2. *CHS:Luc* lines 1.7 and 3.4 contain a single copy of the transgene

Southern blotting of restriction digested (*Nco*I or *Sac*I) genomic DNA from transgenic lines selected as described in Figure 3.1 was carried out. A 1670 b.p (base pairs) fragment corresponding to the luciferase coding sequence cut with *Nco*I and *Sac*I from plasmid p1300 CHSLuc (sections 2.1.3, 2.10.3) was gel purified (section 2.10.4) and used to probe digested genomic DNA (as described in section 2.18). Southern blotting genomic DNA from each candidate line digested with either *SacI* or *NcoI* allowed the number of transgene insertions to be ascertained. Figure 3.5 shows the autoradiograph of the probed Southern blot.

Two lines containing only a single insertion of the transgene were identified in the host genome corresponding to primary transformants ($T_1$) 1 and 3. These were designated *CHS:Luc* 1.7 and *CHS:Luc* 3.4, according to their $T_2$ line numbers.

Both lines were mutagenised and screened, but *CHS:Luc* 3.4 was favoured, as the level of reporter gene expression, as visualised in non-mutant individuals was higher than in *CHS:Luc* 1.7 and it was decided that under expressor mutants would be easier to identify in the *CHS:Luc* 3.4 background. All further characterisation shown relates to *CHS:Luc* 3.4 as all mutants discussed in any detail were isolated in this background. Characterisation of *CHS:Luc* 1.7 was carried out and it behaved as *CHS:Luc* 3.4.

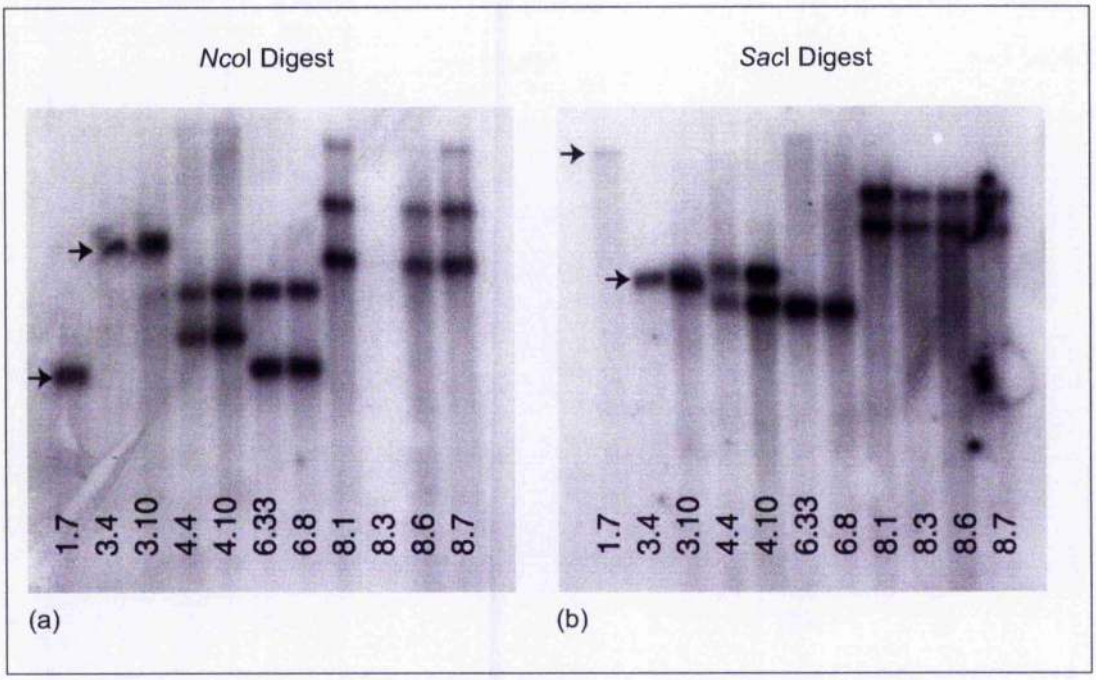


**Figure 3.5 *CHS:Luc* 1.7 and 3.4 carry single copies of the *CHS:Luc* reporter fusion**

Genomic DNA was extracted from selected *CHS:Luc* $T_3$ lines and digested to completion with either *Nco*I (a) or *Sac*I (b) before being run out on a 0.8% agarose gel. Southern blots were made of these gels and probed with a 1670 bp *Nco*I / *Sac*I fragment of *Luc* sequence from p1300CHSluc, the plasmid vector used in initial transformations. Arrows indicate lines carrying single copies of the luciferase transgene.

## 3.3. Selection of screening conditions

### 3.3.1. Optimisation of screening conditions

Most optimisation went into variation in spraying and light treatment methodologies and image analysis but attempts were made to improve the method of substrate delivery and to assess the merits of growth media.

An initial recommendation of baby hair de-tangling spray bottles as a means of luciferin delivery led to trials of various atomising and spray devices. Eventually, it was found that an ordinary artist's airbrush (with compressor) perfectly suited the requirements of the experimental approach as it gave easy control of pressure, volume, rate of flow and direction of a fine, dense mist, which resulted in even coverage of plant material. It later appeared in the literature that Van Leeuwen et al (2000) had come to the same conclusion.

Some experimentation with solid agar growth media, sowing seeds in grids, multi-cell and large plates etc was also tried, but plants dried out, as lids had to be left off for light treatments and imaging. Plants grown on plates were also easily damaged. On balance, sowing out on compost at a reasonable density and thinning out, so that plants did not overlap and so could be distinguished from one another in luminescence images worked best.

All plants used in the course of optimisation were three weeks old (21 days) and grown in constant LWL (low white light, < 20μmol $m^{-2}$ $s^{-1}$), which does not induce *CHS*. Some experiments were carried out with two week old plants, and while synergism was seen it was not as clear as that seen in three week old plants (Figure 3.6), the surface area

of mature leaf tissue was sufficiently low as to hamper easy identification of individual mutant plants in subsequent screening. It should also be noted that reproducible results were obtained from plants subjected to light treatments expected to induce expression of *CHS*. An example of the uniformity of response is seen in figure 3.7.

| | 14 days old | 21 days old |
|---|---|---|
| LWL<br>< 20 µmol $m^{-2}$ $s^{-1}$ | 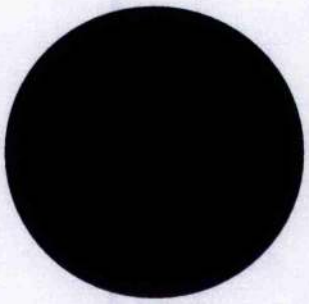 |  |
| Blue<br>8 hours, 80 µmol $m^{-2}$ $s^{-1}$ |  |  |
| UV-B<br>4 hours, 3 µmol $m^{-2}$ $s^{-1}$ |  |  |
| SYN<br>8 hours, 80 µmol $m^{-2}$ $s^{-1}$<br>4 hours, 3 µmol $m^{-2}$ $s^{-1}$ |  |  |

**Figure 3.6 Selection of seedling age for synergism screening**.

*Arabidopsis CHS:Luc* 3.4 seedlings were grown on solid growth medium in low white light (LWL < 20 µmol $m^{-2}$ $s^{-1}$) for either 14 or 21 days. Seedlings were then exposed to light conditions to be used for screening, i.e. 8 hours of 80 µmol $m^{-2}$ $s^{-1}$ blue light, 4 hours of 3 µmol $m^{-2}$ $s^{-1}$ UV-B, or 8 hours blue followed by 4 hours UV-B. Plants were sprayed with 5 mM luciferin 12 and 6 hours before the experiment began, and with 1 mM luciferin immediately prior to imaging. Images were collected with a photon counting camera for 180 seconds.False colour images are shown, where colours represent a logarithmic scale from black (no luminescence), through blue, green, yellow, red, purple to white (saturated pixels).

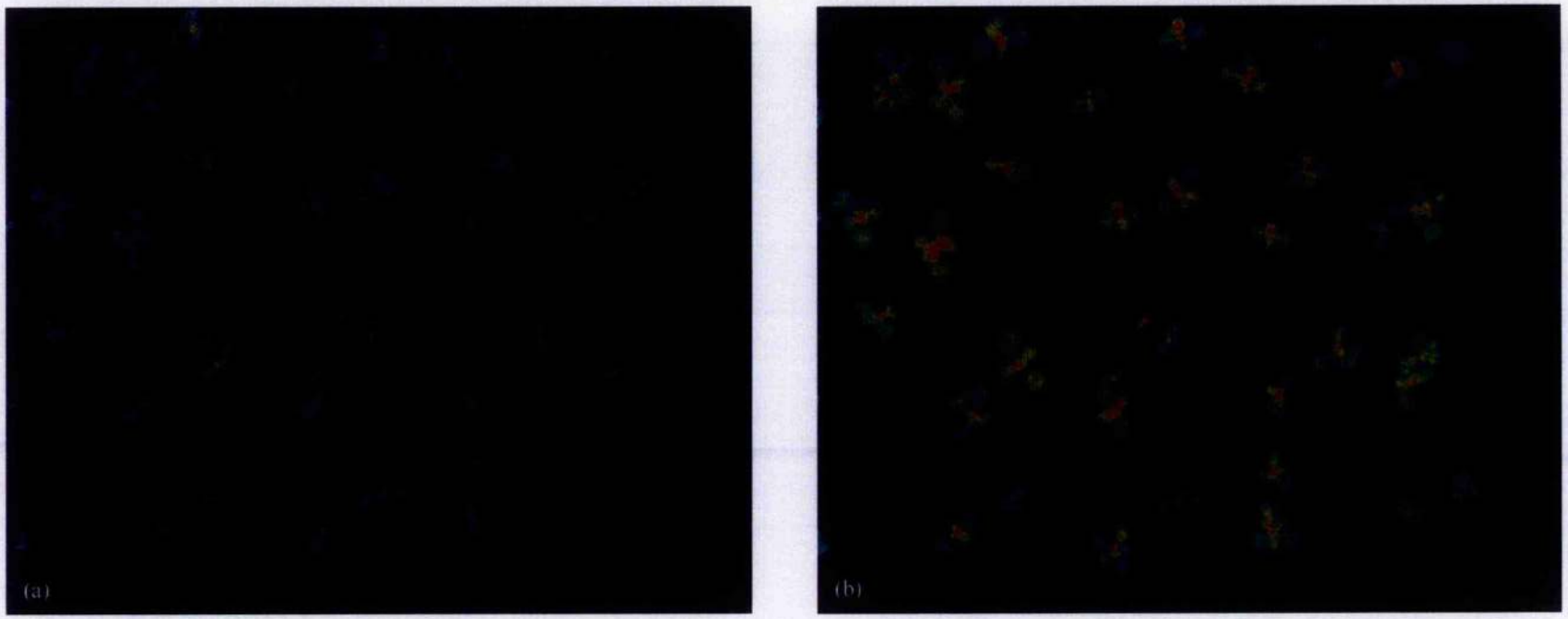


**Figure 3.7 UV-B light treatment gives reproducible results**

*Arabidopsis CHS:Luc* 3.4 seedlings were grown for 21 days on solid growth medium in low white light (LWL < 20 μmol $m^{-2}$ $s^{-1}$). Seedlings were then exposed to 4 hours of 3 μmol $m^{-2}$ $s^{-1}$ UV-B ($\lambda$ = 280 – 320 nm). Plants were sprayed with 5 mM luciferin 12 and 6 hours before the experiment began, and with 1 mM luciferin immediately prior to imaging. Images were collected with a photon counting camera for 360 seconds (a) before and (b) after UV-B light treatment. False colour images are shown, where colours represent a logarithmic scale from black (no luminescence), through blue, green, yellow, red, purple to white (saturated pixels).

### 3.3.1.1. Image analysis

The software used for image capture and manipulation (Photek's IFS32) allows collection of luminescence data in three dimensions; time and the X and Y co-ordinates (as the file extension name .SXY suggests). The best way to think of the integrated image presented to the user is as a series of transparent sheets, each representing a time point, onto which photons detected are plotted, where the whole pile is flattened and viewed from above. Any group of these notional "sheets" may be selected and viewed independently. This means that dynamic changes in luminescence may be observed from the luminescence collected in a single integrated image. Sensitivity of the camera and timing and duration of image capture may be defined by the user.

The matter of how best to process images produced in characterisation and screening to accurately quantify luminescence was investigated. Three different image analysis methods were used to characterise non-mutant lines *CHS:Luc* 3.4 and 1.7. These are described in Materials and Methods (section 2.8.4) and their reliability compared in Figure 3.8.

The simplest method (method a) was to extract the numerical value of total luminescence (photons detected) collected in a study image and subtract a background value collected over the same time period (but without the presence of luminescent plants). The resultant value was then divided by the total number of plants, thus providing a mean luminescence per plant. This is a valuable method for quickly assessing the effectiveness of a particular treatment, but the method doesn't allow the experimenter to calculate standard errors.

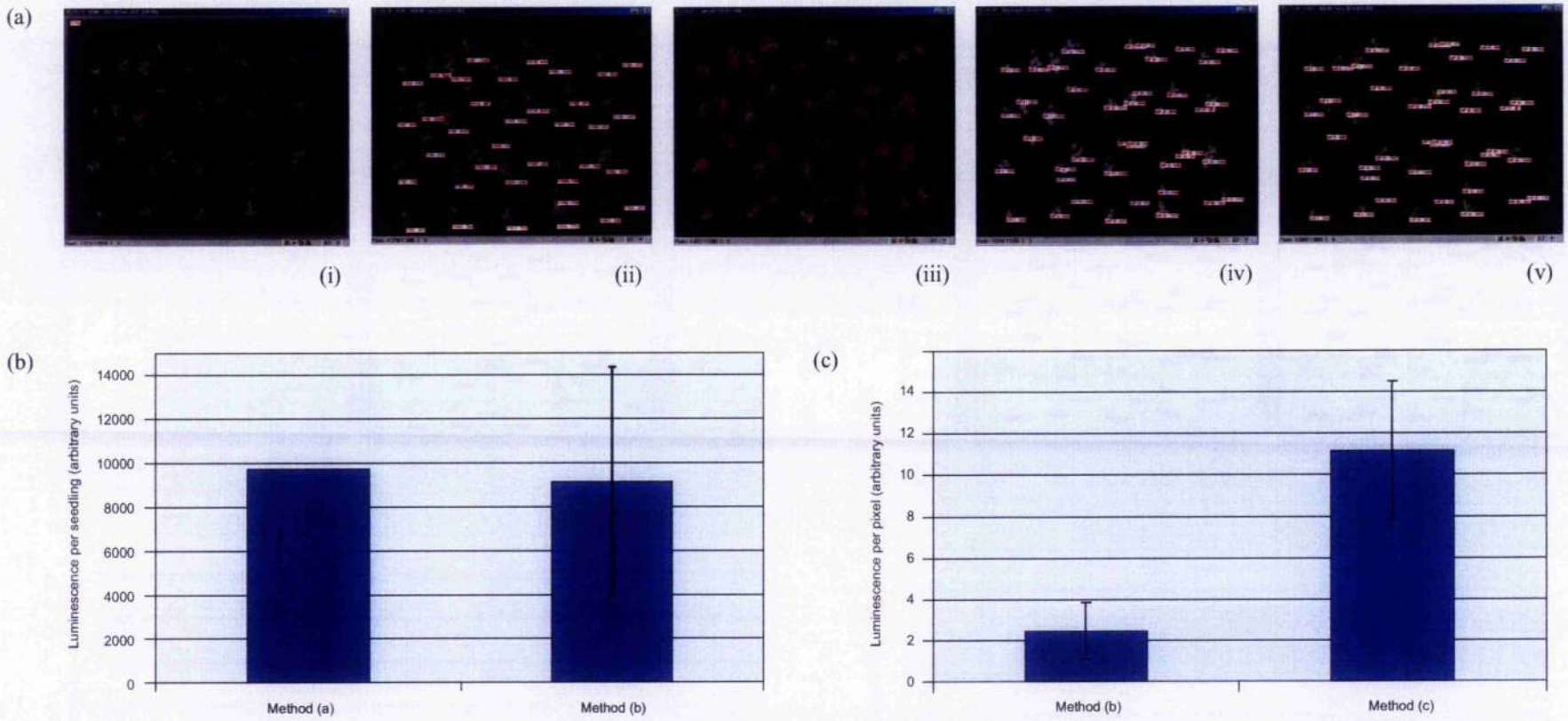


**Figure 3.8 Imaging protocols compared**

Three methods of image analysis were used to interperate luciferase luminescence data numerically. Details of each method are given in the text. (a(i)) raw image with OAP encompassing full data set. (a(ii)) data set overlaid with identical circular OAPs. (a(iii)) despeckled spread image. (a(iv)) threshold mask made corresponding to seedling positions. (a(v)) mask applied to raw data image. (b) methods (a) and (b) compared; note the inability of method (a) to provide error bar. (c) methods (b) and (c) compared. The disparity seen between these two methods is a direct result of the better fit of OAPs to seedling shapes in method (c).

The second method (method b) used was to produce a set (OAS, Photek software) of identical circular areas (OAPs), each containing one plant. One background circular area is also taken. The Extract Data tool can then be used to produce total luminescence data per selected area, which can be transferred to Microsoft Excel. Background can then be subtracted from each, and a mean luminescence per plant can be calculated with a standard error. A problem of this approach is that any variation in size of plants affects the standard error, and so exaggerates the reported variation in luminescence.

A way round the problem of variation in plant size is found in the third method (method c). Photek's software used with their photon counting camera enables the creation of "learn" files, which carry out a series of image manipulations with parameters defined by the user. Briefly, this function enables the user to produce a mask based on (exaggerated) luminescence intensity across the image (where threshold may be controlled) and areas of high intensity identified. Areas of high contrast can be recognised as such and the corresponding areas (areas of high luminescence – i.e. plants) automatically selected on the original luminescence image. Luminescence can then be extracted from these areas as they were from the circular images in method b. In contrast with method b, this method extracts data from areas that differ in size. This is easily overcome by calculating luminescence per pixel. Full details are given in Materials and Methods (section 2.8.4).

A method of mutant isolation from luminescence images also had to be developed, where single plants could be isolated from the whole population. Method a, detailed above was obviously unsuitable for this function, as it gives a single mean value

per plant for the whole population, and cannot distinguish between plants. Methods b and c could each be applied to the problem (method b by statistical means, and method c by subtractive means), but were found to be unnecessary. As each mutant identified is a single plant, the statistical relevance of numerical data collected by methods b and c is questionable, although outliers may be identified. It was quickly realised that where it is useful for luminescence to be quantified in order to characterise the non-mutant *CHS:Luc* lines, this is not necessarily true of mutant isolation.

Visual assessment of the relative change in luminescence between pre-treatment and post-treatment images allowed the selection of mutants without extraction of numerical data. The assumption that most individuals in the screening population should exhibit the wild type response, and so would act as controls for the screening, was made. Mutants were selected by rapidly flicking between pre-treatment and post-treatment images and selecting individuals that differed from those around them. Subjectivity is inherent in this approach, but it did prove a powerful, flexible and economical technique for the discovery and differentiation of several mutant classes, as discussed in section 3.4.2.

### 3.3.1.2. Spraying regimes

Plants expressing luciferase must be pre-sprayed with luciferin before subjecting them to an inductive treatment. This exhausts pools of luciferase that have built up during the life of the plant (see section 3.1.3.1), thereby "re-setting" the plant's reporter function. Further spraying after inductive treatments can then be used to develop the signal from the reporter. The spraying regime used was based on that of Millar et al (1992) and is

detailed in Materials and Methods. This entails giving two pre-sprays, 6 hours apart and beginning 12 hours before the start of the experiment. 5 mM luciferin was used for each pre-spray and 1 mM for each imaging spray.

Luciferase activity was found to reach a plateau 10 minutes after spraying, and this level of activity is maintained for more than 1 hour, after which time it tails off. Some activity is still observable after several hours with no further spraying. All images used in this work were taken 20 minutes after the imaging spray.

#### 3.3.1.3. Light regimes

All light sources used are detailed in Materials and Methods and were measured with a spectroradiometer. UV-B ($\lambda$= 280-320 nm), UV-A ($\lambda$= 320-390 nm) and blue ($\lambda$= 390-500 nm) light have defined wavelengths, which were strictly observed in the work presented here.

##### 3.3.1.3.1. Wavelength optimisation

Figure 3.9 shows luminescence from *CHS:Luc* 3.4 plants treated with UV-A or blue light. As can be seen, treatment with blue light induces *CHS:Luc* expression, but UV-A seemingly does not. It was assumed that the lack of luminescence was caused by an effect of UV-A on the luciferase protein and UV-A was not used further. An implication of this was that the synergistic interaction between UV-A and UV-B could also not be studied. This was not disadvantageous to the project, as it had already been decided that UV-B / blue synergism ought to be the focus of screening as the blue light signal involved in the synergistic response is stable in comparison with the UV-A signal. This

meant that luminescence images may be collected from synergistic treatments where blue and UV-B light qualities are given sequentially rather than at the same time. Comparison of images taken before treatment (i.e. in non-inductive conditions) between blue and UV-B light treatments (the post-blue image), and after the UV-B treatment (synergistic) would allow for detailed classification of mutants from the primary screen (as discussed in section 3.4.2).

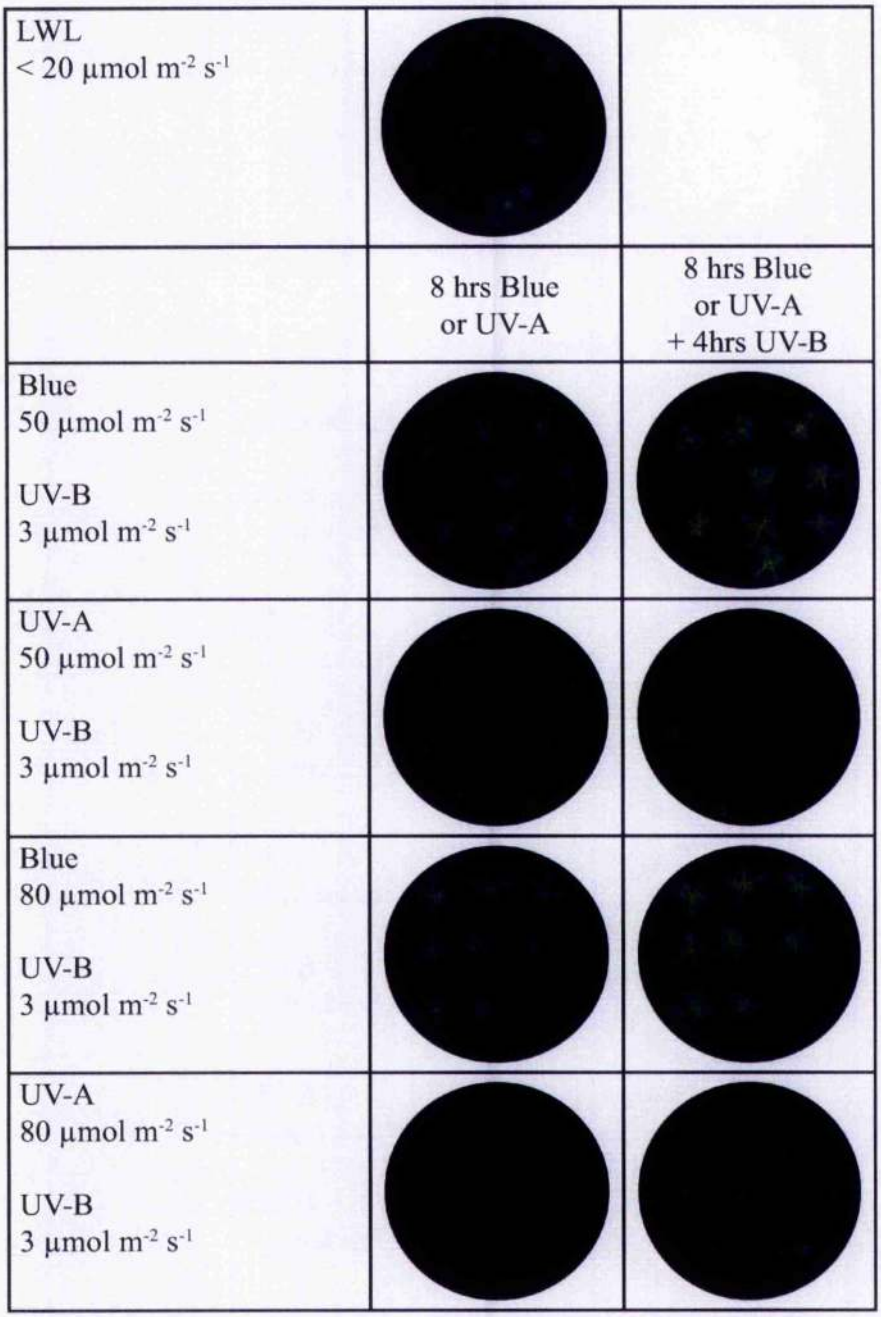


**Figure 3.9 Selection of UV-A or blue light fluence for synergism screening.**

*Arabidopsis CHS:Luc* 3.4 seedlings were grown on solid growth medium in low white light (LWL < 20 μmol $m^{-2}$ $s^{-1}$) for 21 days. Seedlings were then exposed to light conditions potentially to be used for synergism screening, i.e. 8 hours of 50 or 80 μmol $m^{-2}$ $s^{-1}$ UV-A ($\lambda$ = 320 – 390 nm) or blue light ($\lambda$ = 390 – 500 nm), or 8 hours UV-A or blue followed by 4 hours of 3 μmol $m^{-2}$ $s^{-1}$ UV-B ($\lambda$ = 280 – 320 nm). Plants were sprayed with 5 mM luciferin 12 and 6 hours before the experiment began, and with 1 mM luciferin immediately prior to imaging. Images were collected with a photon counting camera for 180 seconds. False colour images are shown, where colours represent a logarithmic scale from black (no luminescence), through blue, green, yellow, red, purple to white (saturated pixels).

#### 3.3.1.3.2. Fluence optimisation

Precedents exist for fluence rates used to induce *CHS* expression, based on light levels found in ambient light on a clear day (Wade, 1999; Brown, 2005). Luminescence was recorded from 3 week old, LWL (low white light, < 20μmol $m^{-2}$ $s^{-1}$) grown *CHS:Luc* 3.4 plants exposed various fluence rates of blue light, imaged and subjected to a further treatment of UV-B light (3 μmol $m^{-2}$ $s^{-1}$), or given a single treatment of UV-B light. Figure 3.10 shows that 80 μmol $m^{-2}$ $s^{-1}$ blue light would be used for screening.

#### 3.3.1.3.3. Timing optimisation

Full time-courses were carried out, where 3 week old, LWL grown *CHS:Luc* 3.4 plants were exposed to 80 μmol $m^{-2}$ $s^{-1}$ blue or 3 μmol $m^{-2}$ $s^{-1}$ UV-B. Figure 3.11 shows luminescence time-courses for single UV-B or blue light treatments.

#### 3.3.1.3.4. UV-B / blue light synergism is reproducibly observable

Figure 3.12 shows that UV-B / blue light synergistic induction of *CHS* can be seen under a range of light treatment combinations. This is not entirely unexpected, as synergistic induction of *CHS* is probably the most biologically relevant, since UV-B and blue light are found together in ambient light. The most pronounced differences between the treatments LWL, blue (80 μmol $m^{-2}$ $s^{-1}$), UV-B (3 μmol $m^{-2}$ $s^{-1}$) and synergistic were seen where a blue light treatment of 8 hours was followed by a UV-B light treatment of 4 hours. These conditions were consequently chosen as the screening conditions to be used for mutant isolation.

| | | |
|---|---|---|
| LWL<br>< 20 μmol $m^{-2}$ $s^{-1}$ | 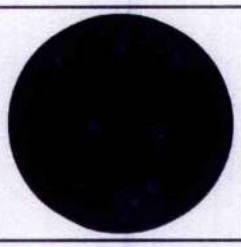 | |
| | 8 hrs Blue | 8 hrs Blue<br>+ 4hrs UV-B |
| Blue<br>50 μmol $m^{-2}$ $s^{-1}$<br><br>UV-B<br>3 μmol $m^{-2}$ $s^{-1}$ | 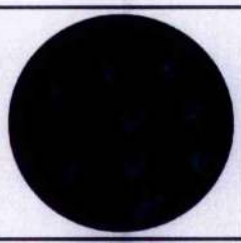 | 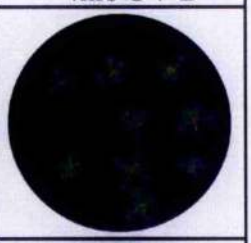 |
| Blue<br>65 μmol $m^{-2}$ $s^{-1}$<br><br>UV-B<br>3 μmol $m^{-2}$ $s^{-1}$ | 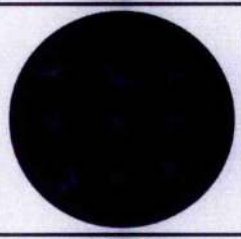 | 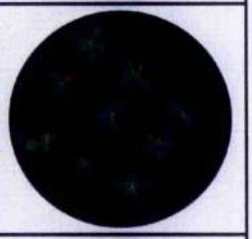 |
| Blue<br>80 μmol $m^{-2}$ $s^{-1}$<br><br>UV-B<br>3 μmol $m^{-2}$ $s^{-1}$ | 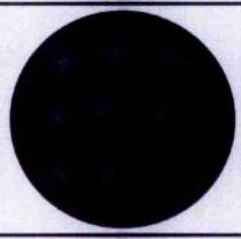 | 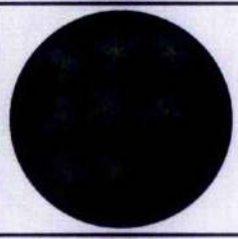 |
| Blue<br>95 μmol $m^{-2}$ $s^{-1}$<br><br>UV-B<br>3 μmol $m^{-2}$ $s^{-1}$ | 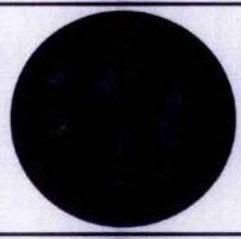 | 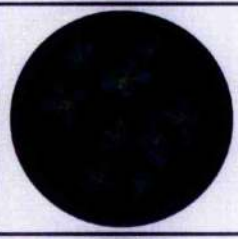 |
| Blue<br>110 μmol $m^{-2}$ $s^{-1}$<br><br>UV-B<br>3 μmol $m^{-2}$ $s^{-1}$ | 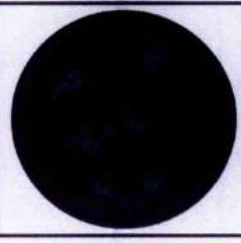 | 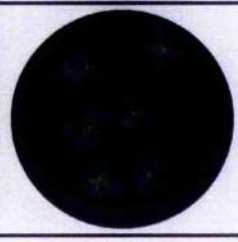 |

**Figure 3.10 Selection of blue light fluence for synergism screening.**

*Arabidopsis CHS:Luc* 3.4 seedlings were grown on solid growth medium in low white light (LWL < 20 μmol $m^{-2}$ $s^{-1}$) for 21 days. Seedlings were then exposed to light conditions potentially to be used for screening, i.e. 8 hours of 50, 65, 80, 95 or 110 μmol $m^{-2}$ $s^{-1}$ blue ($\lambda$ = 390 – 500 nm) light, or 8 hours blue followed by 4 hours of 3 μmol $m^{-2}$ $s^{-1}$ UV-B. Plants were sprayed with 5 mM luciferin 12 and 6 hours before the experiment began, and with 1 mM luciferin immediately prior to imaging. Images were collected with a photon counting camera for 180 seconds. False colour images are shown, where colours represent a logarithmic scale from black (no luminescence), through blue, green, yellow, red, purple to white (saturated pixels).

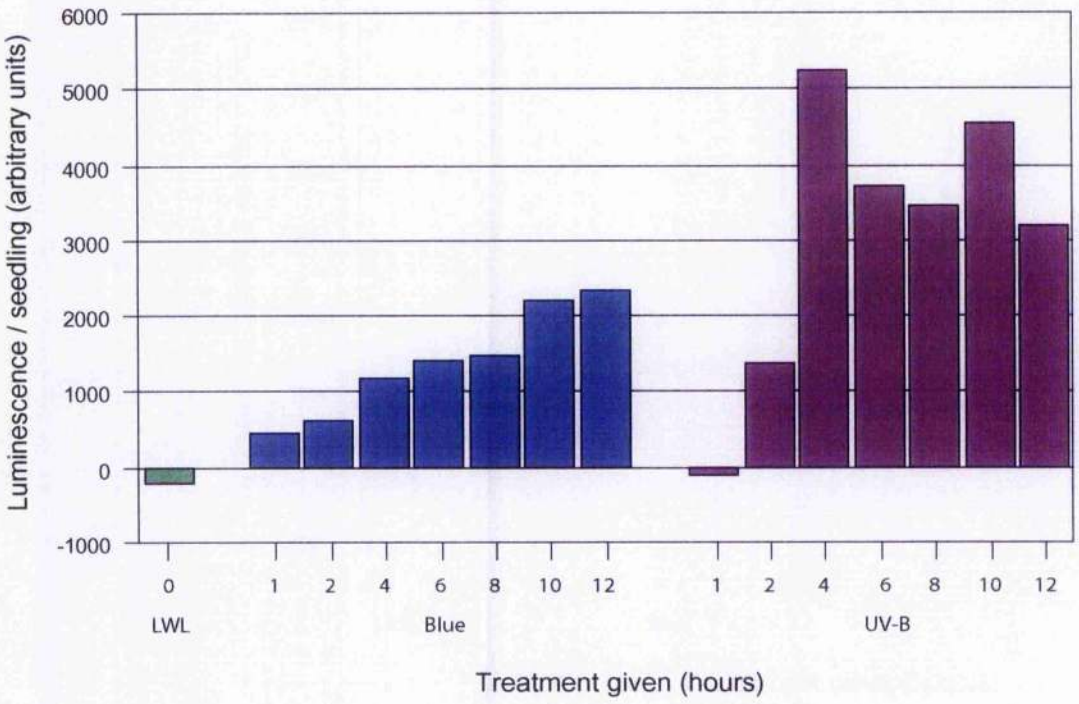


**Figure 3.11 UV-B and blue light induce luminescence in *CHS:Luc* 3.4**

*Arabidopsis CHS:Luc* 3.4 seedlings were grown for 21 days on solid growth medium in low white light (LWL < 20 μmol $m^{-2}$ $s^{-1}$). Seedlings were then exposed to 0, 1, 2, 4, 6, 8, 10 or 12 hours of 3 μmol $m^{-2}$ $s^{-1}$ UV-B (λ = 280 – 320 nm) or 80 μmol $m^{-2}$ $s^{-1}$ blue (λ = 390 – 500 nm) light. Plants were sprayed with 5 mM luciferin 12 and 6 hours before the experiment began, and with 1 mM luciferin immediately prior to imaging. Images were collected with a photon counting camera for 180 seconds. Mean luminescence was calculated by dividing (total luminescence – background luminescence) by the number of seedlings. Luminescence is shown in arbitrary units. Data were collected using method (a) described in section 3.3.1.1.

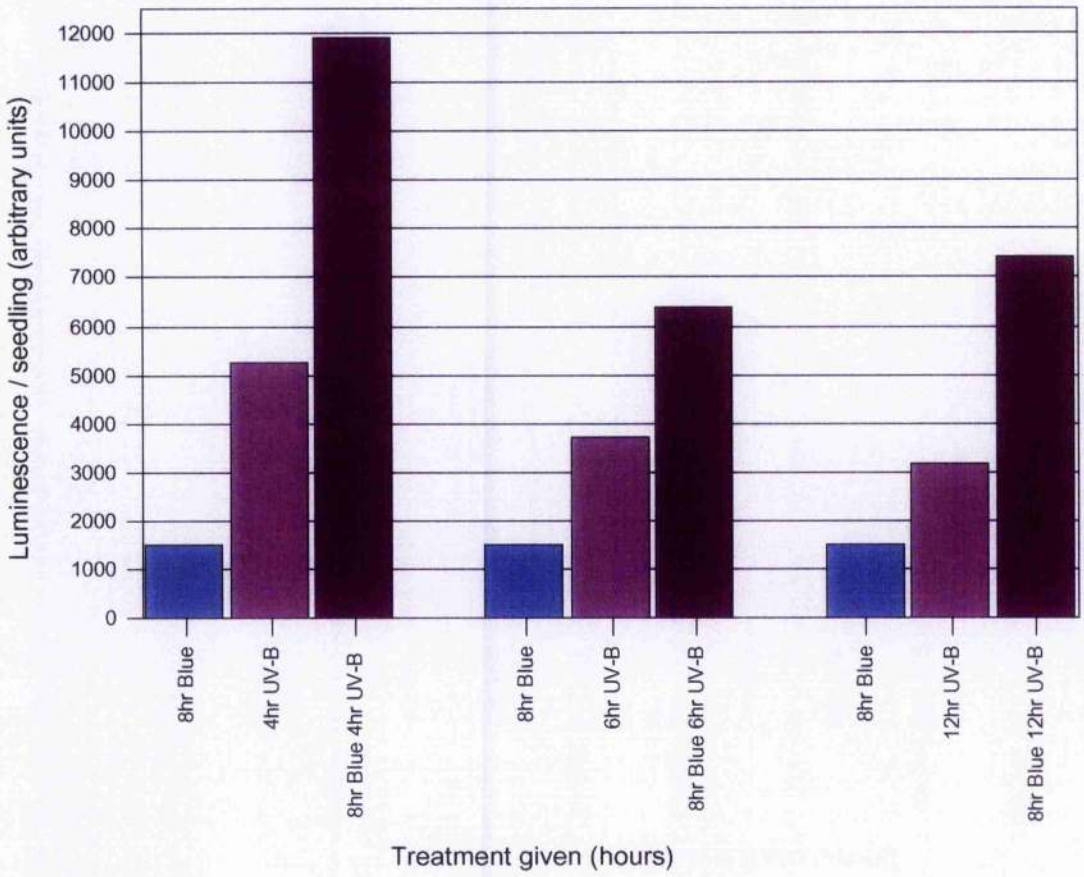


**Figure 3.12 UV-B and blue light synergism is seen in various conditions**

*Arabidopsis CHS:Luc* 3.4 seedlings were grown for 21 days on solid growth medium in low white light (LWL < 20 μmol $m^{-2}$ $s^{-1}$). Seedlings were then exposed to 8 hours of 80 μmol $m^{-2}$ $s^{-1}$ blue (λ = 390 – 500 nm) light or 4, 5, or 12 hours of 3 μmol $m^{-2}$ $s^{-1}$ UV-B (λ = 280 – 320 nm), or 8 hour blue light followed by 4, 5, or 12 hours UV-B. Plants were sprayed with 5 mM luciferin 12 and 6 hours before the experiment began, and with 1 mM luciferin immediately prior to imaging. Images were collected with a photon counting camera for 180 seconds. Mean luminescence was calculated by dividing (total luminescence – background luminescence) by the number of seedlings . Luminescence is shown in arbitrary units. Data were collected using method (a) described in section 3.3.1.1.

An example of how luminescent images of plants subjected to these conditions look is seen in Figure 3.13. It now was important to demonstrate that synergism reported by luciferase corresponds to a synergistic increase in *CHS* transcript levels.

## 3.4. Characterisation of non-mutant *CHS:Luc* line

It was important to demonstrate that the *CHS:Luc* 1.7 and 3.4 transgenic lines behaved as wild type with respect to blue and UV-B light induction of *CHS*.

### 3.4.1. *CHS:Luc* activity follows *CHS* transcript response

Figure 3.14 shows that *CHS* transcript production, assayed by RT-PCR, in *CHS:Luc* 3.4 parallels that of wild type. It demonstrates that the trends in transcript production are reflected in the associated levels of luciferase luminescence seen in *CHS:Luc* 3.4 under the same light conditions. Plants were grown in LWL for 3 weeks before being subjected to various durations of blue or UV-B light as detailed.

## 3.5. Anticipated classes of mutants

The screen, 8 hours blue light followed by 4 hours UV-B light, with images taken at every stage, was designed and executed in such a way that it maximised yield of relevant mutants, and sorted them by classification automatically. The screen design allowed mutants to be classified, with regard to their reported expression of *CHS*, as:

*(i) constitutive over-expressors*

*(ii) constitutive under-expressors*

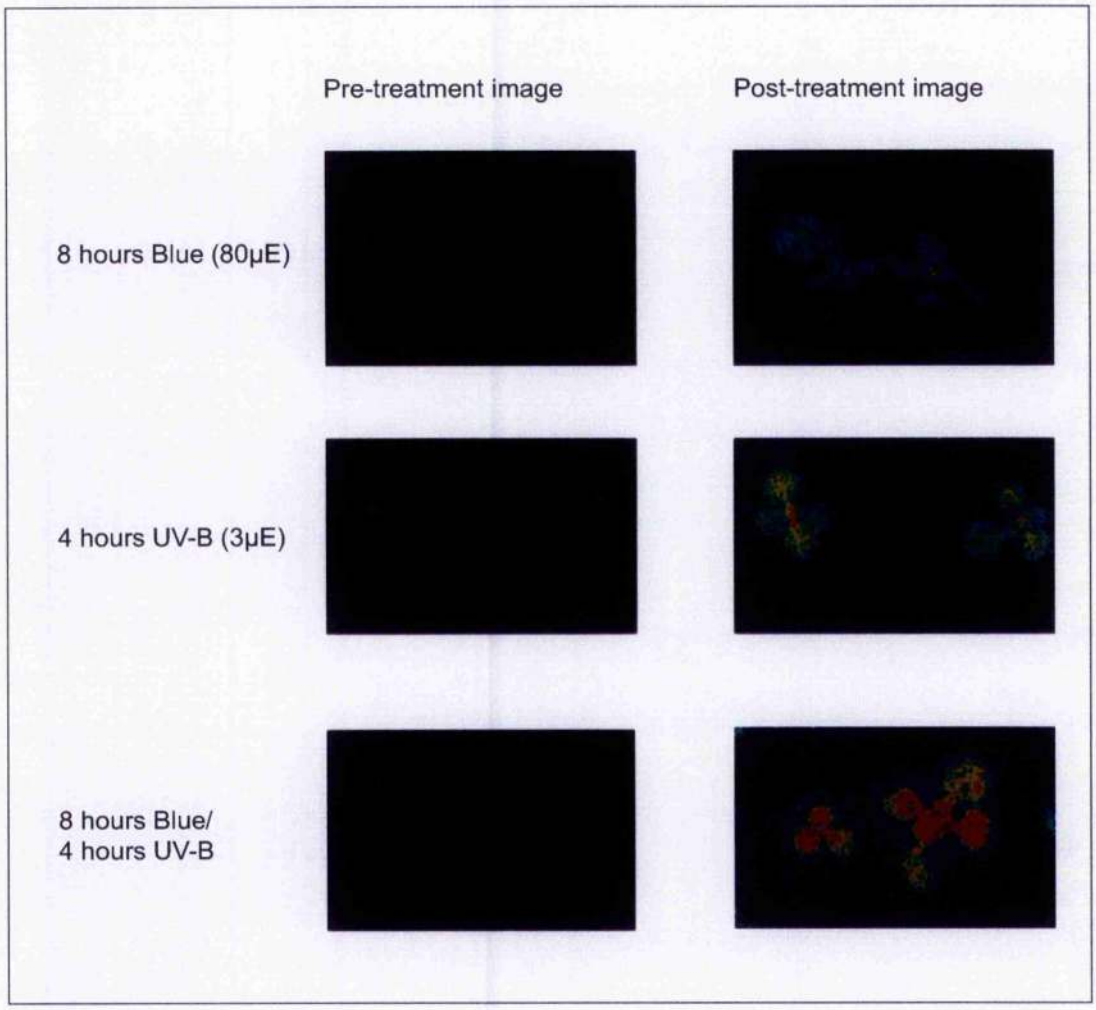


**Figure 3.13 8 hours blue, 4 hours UV-B synergism is ideal for screening conditions**

*Arabidopsis CHS:Luc* 3.4 seedlings were grown for 21 days on solid growth medium in low white light (LWL < 20 μmol $m^{-2}$ $s^{-1}$). Seedlings were then exposed to 8 hours of 80 μmol $m^{-2}$ $s^{-1}$ blue ($\lambda$ = 390 – 500 nm) light or 4 hours of 3 μmol $m^{-2}$ $s^{-1}$ UV-B ($\lambda$ = 280 – 320 nm), or 8 hour blue light followed by 4 hours UV-B. Plants were sprayed with 5 mM luciferin 12 and 6 hours before the experiment began and with 1 mM luciferin immediately prior to imaging. Images were collected with a photon counting camera for 180 seconds. False colour images are shown, where colours represent a logarithmic scale from black (no luminescence), through blue, green, yellow, red, purple to white (saturated pixels).

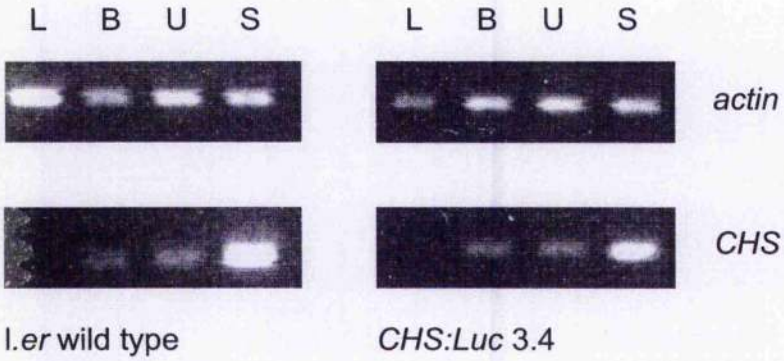


**Figure 3.14 *CHS* expression in *CHS:Luc* 3.4 follows that of wild type for the screening conditions**
Wild type Landsberg *erecta* (L.*er*) (left) and *CHS:Luc* 3.4 (right) were grown for 3 weeks in 20 μmol $m^{-2}$ $s^{-1}$ low white light. Plants were subjected to a range of light treatments, low white light (L), 80 μmol $m^{-2}$ $s^{-1}$ blue light (B), 3 μmol $m^{-2}$ $s^{-1}$ UV-B (U) or 80 μmol $m^{-2}$ $s^{-1}$ blue light followed by 3 μmol $m^{-2}$ $s^{-1}$ UV-B light (S). RNA was extracted and cDNA made in preparation for RT-PCR. PCR was carried out and according to Materials and Methods.

*(iii) blue light specific over-expressors*

*(iv) blue light specific under-expressors*

*(v) UV-B light specific over-expressors*

*(vi) including synergistic over-expressors*

*(vii) UV-B light specific under-expressors*

*(viii) including synergistic under-expressors*

*(viiii) low white light (LWL) under-expressors*

*(x) LWL over-expressors*

The experimental classification of mutants is illustrated in Figure 3.15. In reality, it would be very unlikely to find mutants in LWL (classes (*viiii*) and (*x*)), as this is the non-inductive condition. These would be likely to be members of another class (constitutive classes (*i*) and (*ii*)), but are included for completeness, as the screen did have the resolving power to isolate mutants of these classes.

Mutant classes (*vi*) and particularly (*viii*) are those primarily sought in this screen, and represent synergism mutants. As designed, this screen would separate these mutants along with classes (*v*) and (*vii*), i.e. UV-B specific mutants. It was possible that synergism mutants may be distinguishable from UV-B specific mutants, as the level of wildtype induction is different under these two conditions, but it was anticipated that mutants in these classes would have to be further sorted. This was not considered problematic, as UV-B specific mutants were considered equally valuable, as discussed in section 3.1.1.

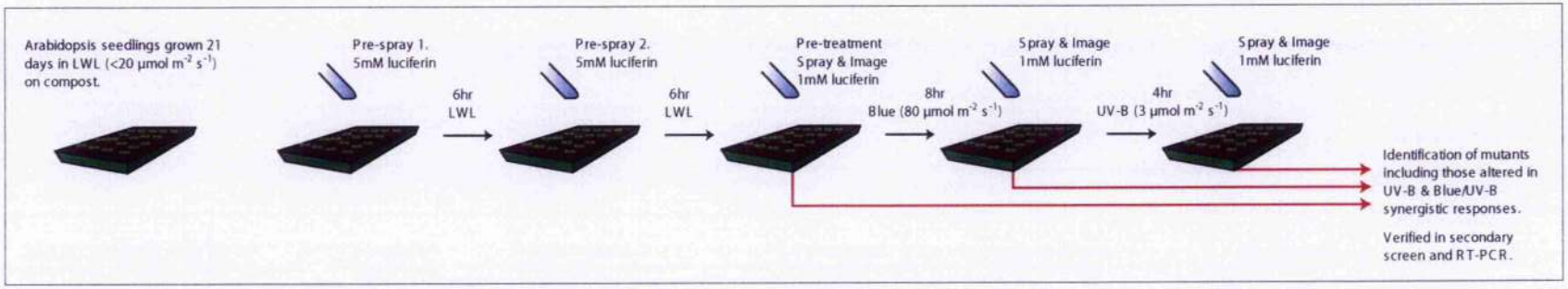


**Figure 3.15 Schematic diagram of screening protocol**

*Arabidopsis CHS:Luc* 1.7 and 3.4 $M_2$ seedlings were grown for 21 days compost in low white light (LWL < 20 µmol $m^{-2}$ $s^{-1}$). In primary screening, *CHS:Luc* $M_2$ seedlings were sown out at a density that ensured no overlapping of seedlings, then exposed to 8 hours of 80 µmol $m^{-2}$ $s^{-1}$ blue ($\lambda$ = 390 – 500 nm) light followed by 4 hours of 3 µmol $m^{-2}$ $s^{-1}$ UV-B ($\lambda$ = 280 – 320 nm). Plants were sprayed with 5 mM luciferin 12 and 6 hours before the experiment began and with 1 mM luciferin immediately prior to imaging. Images of luminescence were captured before inductive treatments began, after blue light treatment, and again after UV-B exposure. Red arrows indicate collection of images in the diagram. Images were collected with a photon counting camera for 180 seconds, and compared visually to select and categorise putative mutants. Selected putative mutant seedlings were transplanted to fresh compost, and grown up for seed. $M_3$ seed (progeny of selected $M_2$) was densely sown out alternately with wild type in a chess board pattern in 60 well gravel tray inserts, and treated and imaged as in the primary screen. This allowed selection for mutants to be verified by RT-PCR.

## 3.6. Screening for mutants in synergistic induction of *CHS:Luc* by UV-B and blue light

### 3.6.1. The dimensions of the primary screen

EMS mutagenesis was carried out according to the protocol of Leyser and Furner (see Materials and Methods). As recommended, a concentration of 80 mM EMS and an incubation time of 3 hours was used per 0.3g *CHS:Luc* seeds, as described in Materials and Methods. Batches of $M_2$ plants were prepared for screening by collecting seed from 20 $M_1$ plants per $M_2$ batch. Approximately 160-170 (mean =169) seedlings were imaged per $M_2$ batch, corresponding to 8.45 $M_2$ seedlings per $M_1$ plant. As neither the number of gene products involved in the synergistic induction of *CHS,* nor the efficiency of mutation of these genes was known, the probability of generating relevant mutants cannot be calculated in this instance. The probability of isolating recessive and dominant mutants generated (i.e. present) was $P = 1-(0.75)^{8.45}$ or 0.912, and $P = 1-(0.25)^{8.45}$ or <0.999 respectively.

143 batches of *CHS:Luc* 3.4 and 44 batches of *CHS:Luc* 1.7 $M_2$ seedlings were screened, corresponding to 30000 - 33000 $M_2$ seedlings. This number probably does not represent saturation of the genome, but as was stated in section 3.1.2, the strategy for mutant discovery was such that only one or a few mutants might be studied and at the end of the primary screen, over 200 putative mutants (of all classes, including 132 under-expressors in UV-B) had been isolated (section 3.5.2).

Seed was collected from each of the putative mutants for use in further verification and characterisation, where appropriate.

#### 3.6.1.1. Typical results of the primary screen

Figure 3.16 shows selection of primary mutants. The visual method of selection worked well with these images and led to the isolation of both over-expressors and under-expressors. Mutants were numbered according to their batch number and the order in which they were selected from that batch, given in parenthesis (numbers for *CHS:Luc* 3.4, and letters for *CHS:Luc* 1.7). Image names and co-ordinates were noted for each mutant isolated for future reference. Any strong phenotypes associated with mutants selected were also noted. Unfortunately, all *CHS:Luc 1.7* mutants were lost in a thrips infestation.

### 3.6.2. Classes of putative mutants found in the primary screen

The classes of putative mutants to come from the primary screen are tabulated in Table 3.17. 210 putative mutants were isolated from *CHS:Luc* 1.7 and 3.4 $M_2$ batches, of which 132 reported underexpression of *CHS:Luc* in UV-B (or synergistic conditions) only. All but 7 of the putative mutants isolated were in the CHS:Luc 3.4 background, including all the UV-B specific under-expressors.

It was encouraging to find that putative UV-B specific underexpressing individuals had been isolated several times from the same line. This suggested that although this probably reduced the number of independent mutants represented, those that had been isolated more than once were arguably more likely to represent real mutants.

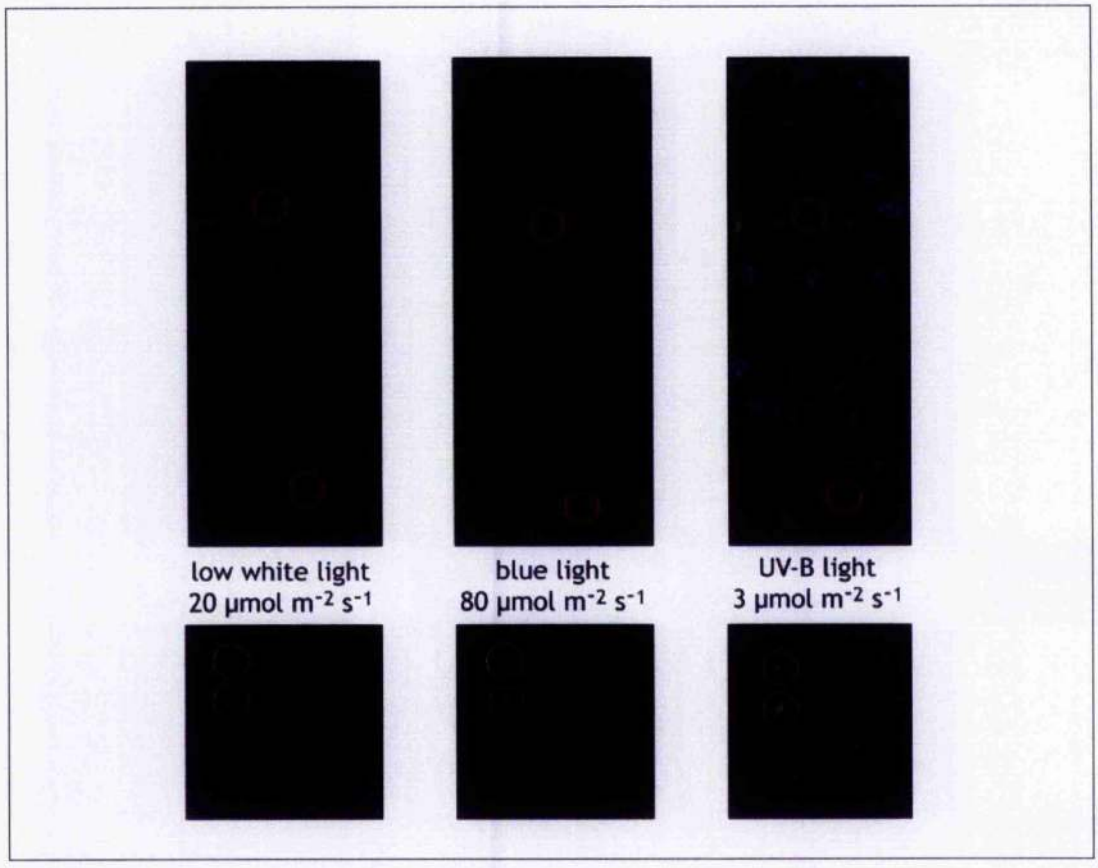


**Figure 3.16 Typical isolation of under-expressing and over-expressing mutants based on *CHS:Luc* luminescence in primary screening**

*Arabidopsis CHS:Luc* 3.4 $M_2$ seed was sown out at a density that ensured no overlapping of seedlings and grown for 21 days in compost in low white light (LWL < 20 µmol $m^{-2}$ $s^{-1}$). Seedlings were then exposed to 8 hours of 80 µmol $m^{-2}$ $s^{-1}$ blue ($\lambda$ = 390 – 500 nm) light followed by 4 hours of 3 µmol $m^{-2}$ $s^{-1}$ UV-B ($\lambda$ = 280 – 320 nm). Plants were sprayed with 5 mM luciferin 12 and 6 hours before the experiment began and with 1 mM luciferin immediately prior to imaging. Images were collected with a photon counting camera for 180 seconds before inductive light treatments, after blue, and again after UV-B. Red circles show typical isolation of under-expressing mutants, and yellow circles show isolation of over-expressors. False colour images are shown, where colours represent a logarithmic scale from black (no luminescence), through blue, green, yellow, red, purple to white (saturated pixels).

| | *CHS:Luc* 3.4 $M_2$ | *CHS:Luc* 1.7 $M_2$ |
|---|---|---|
| Total selected | 215 | 50 |
| Total surviving | 203 | 7 |
| UV-B specific under expressors | 139 (7 very marginal) | - |
| UV-B specific over expressors | 13 | - |
| Blue specific under expressors | 5 | - |
| Constitutive under expressors | 16 | - |
| Constitutive over expressors | 28 | - |
| Mutants with spatial alteration in expression | 2 | - |

**Table 3.17 Classes of putative mutants found in the primary screen**

*Arabidopsis CHS:Luc* 3.4 and 1.7 $M_2$ seedlings were grown on compost in low white light (LWL < 20 μmol $m^{-2}$ $s^{-1}$) for 21 days before being screened as described in section 3.3. It is worth noting that the stringency for selection of UV-B specific underexpressors was low as this was the class most desired in this screen. This accounts for the high number of putative mutants identified in this class.

### 3.6.3. The dimensions of the secondary screen

Each putative mutant isolated from the primary screen had been isolated based on gene expression reported by only one seedling. In order to confirm each putative mutant, secondary screening was undertaken, according to the conditions of the primary screen. The progeny of each putative mutant selected in the primary screen ($M_3$ generation) were sown out, alternately with "wild type" (*CHS:Luc* 3.4) in compost, in wells of seed tray inserts in a chess-board pattern, with wild type on the white squares. Each seed tray insert had 10 x 6 wells, allowing 30 putative mutants to be screened per seed tray, with at least three control wells immediately adjacent to each one. Each well held around 20 seedlings. Each putative mutant was screened at least twice.

The overwhelming majority of putative mutants selected in the primary screen were rejected at this stage. Of 201 putative mutants selected in primary screening, all but 52 were discarded in secondary screening, reducing the number of candidate UV-B (or synergism) specific under expressors from 139 to 5. All putative mutants carried past the secondary screen were successfully selected from images, where the investigator did not know the identity of the wells scored until scoring was complete. As a control for the quality of selection, *chum31* (*uvr8-2* allele, isolated in *CHS:Luc 3.4* (Brown, 2005)) was used. *uvr8* individuals show under expression of *CHS* in UV-B light (Kliebenstein et al. 2002). Under these experimental conditions, *chum31* was selected 5 of 6 times, as under expressing in UV-B. *chum31* also exhibited slight reduction of reported *CHS* expression in blue light. *CHS* transcript levels in *uvr8* under these experimental conditions are discussed more fully in section 3.6.2.

### 3.6.4. Results of the secondary screen

Figure 3.18 shows typical results collected in secondary screening. Luminescence images taken after UV-B (i.e. corresponding to synergistic illumination) are shown on the left hand side of the figure and each putative mutant's designation and classification given in the grid on the right hand side of the figure. Green filled boxes denote mutants which behaved as wild type. These false positives make up the majority of those mutants screened. This is a sample of the images taken. All putative mutants were tested at least twice. After secondary screening, a number of classes of mutants had been identified and stored for further characterisation. Only seven UV-B (or synergism) specific putative mutants remained. These fell into two catagories; under-expressors (*CHS:Luc* 068(1), 068(2), 068(3), 134(3) and 136(2) and over-expressors 111(1) and 93(1).

#### 3.6.4.1. *CHS:Luc* 136(2)

One mutant, *CHS:Luc* 136(2), selected from the primary screen elicited considerable excitement, as it was classified as a putative UV-B (or UV-B / blue light synergism) specific under expressor of *CHS:Luc* and it had a striking visible phenotype, which would help facilitate future map-based cloning. Figure 3.19 (a) lists the mutants identified in primary screening which also exhibited a physical phenotype and Figure 3.19 (b) shows *CHS:Luc* 136(2).

| | | | | | | | | | |
|---|---|---|---|---|---|---|---|---|---|
| 3.4 | 057(5) ? | 3.4 | 100(1) | 3.4 | 128(4) | 3.4 | 135(1) | 3.4 | 129(2) |
| 132(1) | 3.4 | 030(2) | 3.4 | 126(1) | 3.4 | 134(1) | 3.4 | 134(2) | 3.4 |
| 3.4 | 061(2) ? | 3.4 | 128(3) | 3.4 | 126(2) | 3.4 | 139(2) | 3.4 | 129(1) |
| 068(2) | 3.4 | 086(1) | 3.4 | 054(1) | 3.4 | 128(1) | 3.4 | 136(1) | 3.4 |
| 3.4 | 136(3) | 3.4 | 131(2) | 3.4 | 030(1) | 3.4 | 125(1) | 3.4 | 057(4) |
| 132(2) ? | 3.4 | - | 3.4 | 134(3) ! | 3.4 | 052/3 | 3.4 | 139(3) | 3.4 |

| |
|---|
| Wild type |
| Constitutive under-expressor |
| Constitutive over-expressor |
| UV-B specific under-expressor |
| UV-B specific over-expressor |
| Blue specific under-expressor |
| Too few or no plants |
| ? Marginally exhibiting phenotype |
| ! Strongly exhibiting phenotype |

| | | | | | | | | | |
|---|---|---|---|---|---|---|---|---|---|
| 3.4 | 1.7 101/2 | 3.4 | 057(1) | 3.4 | 099(1) | 3.4 | 057(3) | 3.4 | 061(1) |
| 103(2) | 3.4 | 1.7 103/4 | 3.4 | 107(2) | 3.4 | 050(2) | 3.4 | 060(3) | 3.4 |
| 3.4 | 1.7 | 3.4 | 100(2) | 3.4 | 052(1) | 3.4 | 051(2) | 3.4 | 051(1) |
| CHUM 31 ! | 3.4 | 130(1) | 1.7 | 1.7 103/1 | 3.4 | CHUM 31 ! | 3.4 | 109(1) | 3.4 |
| 3.4 | 136(2) ! | 3.4 | 1.7 101/3 | 1.7 | 060(1) | 3.4 | 110(1) | 3.4 | 052(2) |
| 128(2) | 3.4 | 142(1) | 3.4 | CHUM 31 ! | 3.4 | 106(1) | 3.4 | 060(2) | 3.4 |

| | | | | | | | | | |
|---|---|---|---|---|---|---|---|---|---|
| 3.4 | 092(1) ? | 3.4 | 094(1) | 3.4 | 078(1) | 3.4 | 050(2) | 3.4 | 025(2) ? |
| 068(1) ? | 3.4 | 093(3) | 3.4 | 057(2) | 3.4 | 093(1) | 3.4 | 016(2) | 3.4 |
| 3.4 | 023(4) ? | 3.4 | 108(1) | 3.4 | 091(1) | 3.4 | 078(1) | 3.4 | H/D(2) |
| 068(3) | 3.4 | CHUM 31 | 3.4 | 056(1) | 3.4 | 043(2) | 3.4 | 088(2) | 3.4 |
| 3.4 | 097(1) ? | 3.4 | 105(1) | 3.4 | 085(1) | 3.4 | 081(3) | 3.4 | 013(1) |
| 061(2) | 3.4 | 097(2) ? | 3.4 | 095(1) | 3.4 | 078(1) | 3.4 | 025(1) | 3.4 |

| | | | | | | | | | |
|---|---|---|---|---|---|---|---|---|---|
| 024(2) | 020(1) | 3.4 | 123(3) ! | 3.4 | 118(2) | 3.4 | 121(1) | 3.4 | 113(2) |
| 016(1) | 3.4 | 021(2) | 3.4 | 123/4 | 3.4 | 116(1) | 3.4 | 124(3) | 3.4 |
| 3.4 | 000(1) | 3.4 | 098(2) | 3.4 | 113(3) | 3.4 | 114(1) | 3.4 | 115(1) |
| 023(1) ? | 3.4 | CHUM 31 ! | 3.4 | 098(1) | 3.4 | CHUM 31 ! | 3.4 | 122(2) | 3.4 |
| 3.4 | 027(1) | 3.4 | 088(4) | 3.4 | 113(1) ! | 3.4 | 119(1) | 3.4 | 118(1) |
| 050(1) ? | 3.4 | 000(2) | 3.4 | 000(3) | 3.4 | 111(2) ! | 3.4 | 123(2) | 3.4 |

**Figure 3.18 Typical results gained in secondary screening of *CHS:Luc* 3.4 $M_3$**

*Arabidopsis CHS:Luc* 3.4 and 1.7 $M_3$ seedlings were grown on compost in low white light (LWL < 20 µmol $m^{-2}$ $s^{-1}$) for 21 days before being screened as described in section 3.3.

? denotes marginal luminescence phenotype

! denotes strong candidate mutant

(a)

| Mutant | Visible phenotype | Luminescence phenotype |
|---|---|---|
| 128 (1) | Pale leaves | Over-expressor |
| 125 (1) | Small, dark green plants | UV-B specific under-expressor |
| 023 (4) | Dark green leaves | Constitutive under-expressor |
| 013 (1) | Pale leaves | Over-expressor |
| 093 (1) | Long petioles, narrow leaves | UV-B specific over-expressor |
| 136 (2) | Pale leaves with green veining | UV-B specific under-expressor |
| 061 (1) | Pale leaves | UV-B specific under-expressor |

(b)

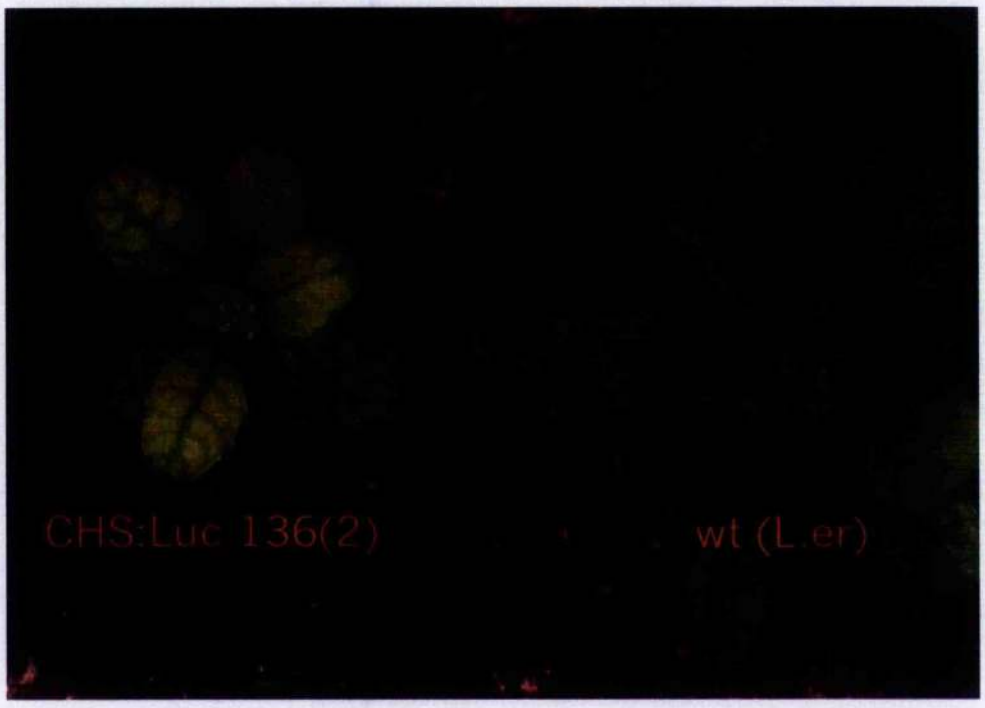


**Figure 3.19 Visible phenotypes of putative mutants isolated**

Several putative mutants identified in the primary screen exhibited a visible phenotype. (a), Of those putatives listed, only 093(1) and 136 (2) (labelled in blue) came through the secondary screen. (b), 136(2) exhibits a strong visible phenotype and was identified in the class of mutants which was the primary target of the screen. Both 093(1) and 136(2) were found to show wild type transcript production in RT-PCR analysis.

### 3.6.5. Selection by RT-PCR of the best candidate mutants

All the mutants which came through secondary screening were assessed for native *CHS* expression under four light conditions, relating to those used in screening (LWL, 4 hours UV-B, 8 hours blue and 4 hours UV-B followed by 8 hours blue). None of those mutants tested were found to have a specific response to synergism. Figure 3.20 shows the RT-PCR results of those mutants that were rejected at this stage. Of the strongest mutants to come through the secondary screen, RT-PCR selected two only as UV-B specific under-expressors of *CHS*. These were *CHS:Luc* 068(1) and 068(2)shown in Figure 3.21. *CHS:Luc* 068(3) is also shown on this gel image.

## 3.7. Verification of mutants

### 3.7.1. Complementation groups

The mutants *CHS:Luc* 068(1) and 068(2) were selected through RT-PCR as mutants in the UV-B and UV-B / blue synergism. These mutants were crossed to one another, and the $F_1$ was tested for allelism via luciferase luminescence. Luminescence data for these crosses is shown in Figure 3.22. These were found to be allelic.

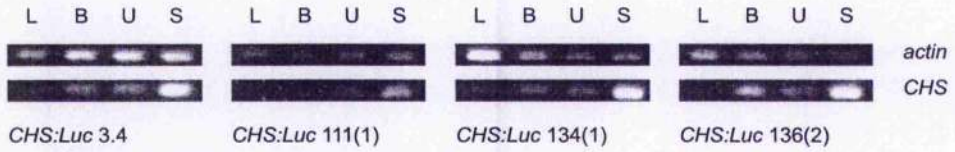


**Figure 3.20 RT-PCR of mutants**

Wild type *CHS:Luc* 3.4 and mutants shown were grown for 3 weeks in 20 μmol $m^{-2}$ $s^{-1}$ low white light. Plants were subjected to a range of light treatments, low white light (L), 80 μmol $m^{-2}$ $s^{-1}$ blue light (B), 3 μmol $m^{-2}$ $s^{-1}$ UV-B (U) or 80 μmol $m^{-2}$ $s^{-1}$ blue light followed by 3 μmol $m^{-2}$ $s^{-1}$ UV-B light (S). RNA was extracted and cDNA made in preparation for RT-PCR. PCR was carried out and according to Materials and Methods.

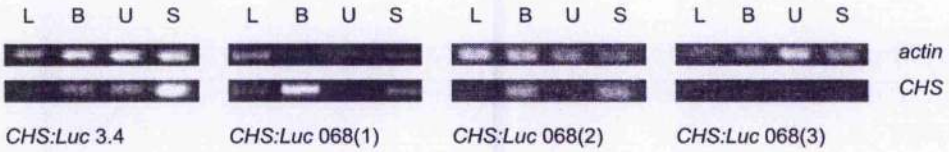


**Figure 3.21 *CHS:Luc* 068 mutants are altered in *CHS* expression**

Wild type *CHS:Luc* 3.4 and mutants shown were grown for 3 weeks in 20 μmol $m^{-2}$ $s^{-1}$ low white light. Plants were subjected to a range of light treatments, low white light (L), 80 μmol $m^{-2}$ $s^{-1}$ blue light (B), 3 μmol $m^{-2}$ $s^{-1}$ UV-B (U) or 80 μmol $m^{-2}$ $s^{-1}$ blue light followed by 3 μmol $m^{-2}$ $s^{-1}$ UV-B light (S). RNA was extracted and cDNA made in preparation for RT-PCR. PCR was carried out and according to Materials and Methods.

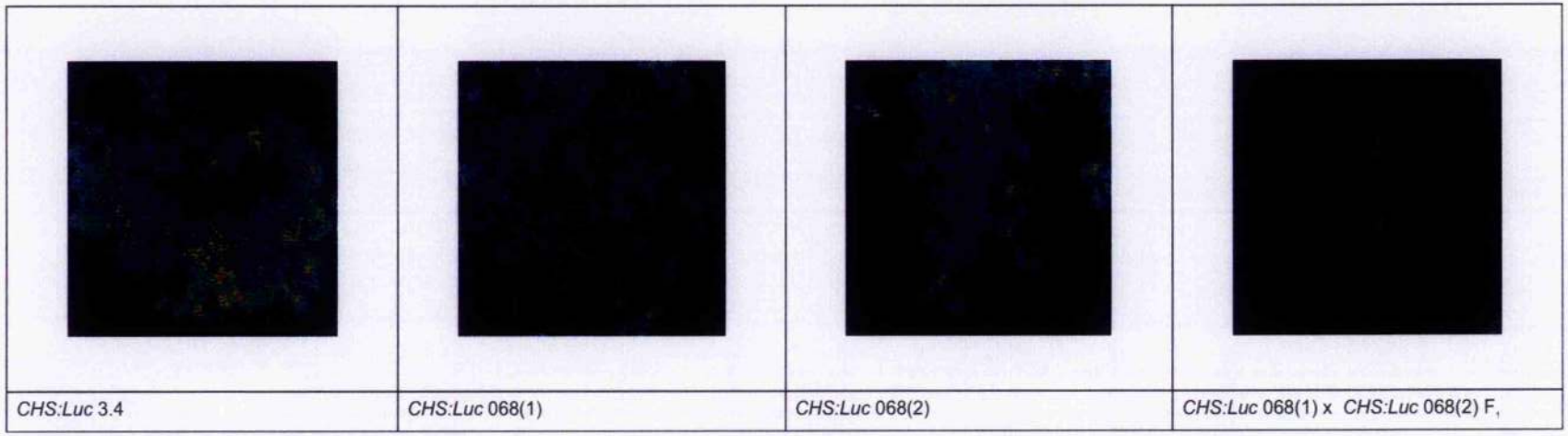

| *CHS:Luc* 3.4 | *CHS:Luc* 068(1) | *CHS:Luc* 068(2) | *CHS:Luc* 068(1) x *CHS:Luc* 068(2) $F_1$ |
|---|---|---|---|

**Figure 3.22 *CHS:Luc* 068(1) appears to be allelic with *CHS:Luc* 068(2)**

CHS:Luc 068(1) x *CHS:Luc* 068(2) $F_1$ plants were grown in compost, under 20 µmol $m^{-2}$ $s^{-1}$ low white light before being illuminated with 3 µmol $m^{-2}$ $s^{-1}$ UV-B ($\lambda$=280-320nm) for 4 hours. Plants were sprayed with 5 mM luciferin 12 and 6 hours before the experiment began, and with 1 mM luciferin immediately prior to imaging. Images were collected with a photon counting camera for 180 seconds. False colour images are shown, where colours represent a logarithmic scale from black (no luminescence), through blue, green, yellow, red, purple to white (saturated pixels).

### 3.7.2. UV-B / blue light synergism is abolished in *uvr8*

The UV-B sensitive mutant *uvr8* has been shown to exhibit reduced expression of *CHS* when exposed to UV-B light (Kliebenstein et al. 2002). A mutant, *chum31* (*chalcone synthase under expressing mutant 31*), corresponding to a novel allele of *uvr8* (*uvr8-2*) has been isolated in a similar screen to that described here, which looked for mutants exhibiting aberrant *CHS* expression in UV-B, using the *CHS:Luc* 3.4 reporter line (Brown, 2005). These are the only described mutants from either of these screens, suggesting that *uvr8* plays a very important role in the photoreception of UV-B and / or the transduction of the signal.

Figure 3.23 shows that as well as having reduced UV-B induction of *CHS*, UV-B / blue synergistic induction of *CHS* gene expression in *uvr8* (both described alleles) is abolished. *CHS:Luc* 068(2) has been included for reference. This clearly indicates that the *uvr8* allele might be expected to be isolated from this synergism screen, given the screening conditions. Selection of *chum31,* as a control, under these screening conditions was reported in section 3.5.3.

### 3.7.3. Allelism with *uvr8*

Since the new mutant identified in this Chapter and *uvr8* were so alike in their *CHS* transcript accumulation and since *uvr8* has been the only mutant to come from two other UV-B specific screens (Kleibenstein et al. 2002; Brown, 2005), allelism was assessed for these two in the same way as it was established for *CHS:Luc* 068(1) and 068(2). Figure 3.24 shows that *CHS:Luc* 3.4 068(1) is allelic to *uvr8*.

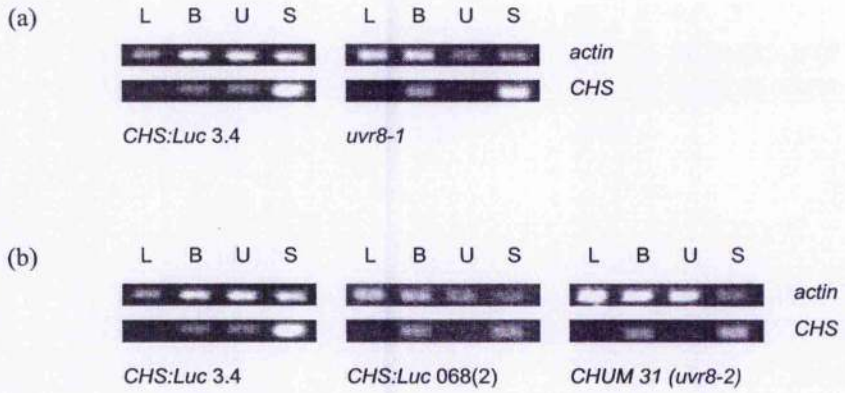


**Figure 3.23 UV-B/blue synergism is abolished in *uvr8***

Wild type *CHS:Luc* 3.4 and mutants shown were grown for 3 weeks in 20 μmol $m^{-2}$ $s^{-1}$ low white light. Plants were subjected to a range of light treatments, low white light (L), 80 μmol $m^{-2}$ $s^{-1}$ blue light (B), 3 μmol $m^{-2}$ $s^{-1}$ UV-B (U) or 80 μmol $m^{-2}$ $s^{-1}$ blue light followed by 3 μmol $m^{-2}$ $s^{-1}$ UV-B light (S). RNA was extracted and cDNA made in preparation for RT-PCR. PCR was carried out and according to Materials and Methods.no evidence in *icx2*.

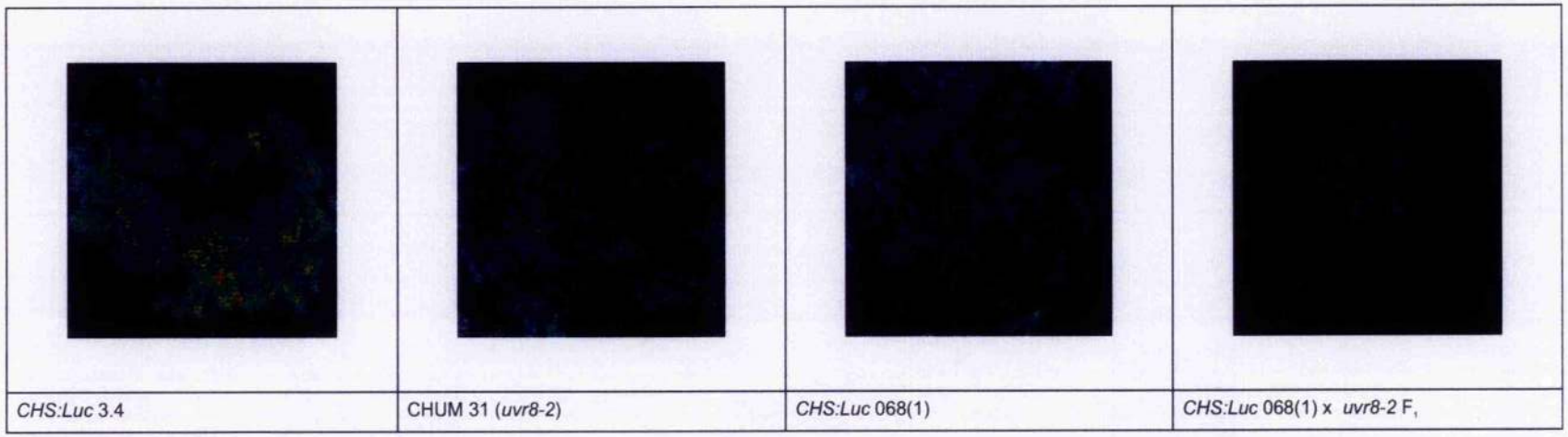


**Figure 3.24 *CHS:Luc* 068(1) appears to be allelic with *uvr8***

CHS:Luc 068(1) x uvr8-2 $F_1$ plants were grown in compost, under 20 µmol $m^{-2}$ $s^{-1}$ low white light before being illuminated with 3 µmol $m^{-2}$ $s^{-1}$ UV-B (λ=280-320nm) for 4 hours. Plants were sprayed with 5 mM luciferin 12 and 6 hours before the experiment began, and with 1 mM luciferin immediately prior to imaging. Images were collected with a photon counting camera for 180 seconds. False colour images are shown, where colours represent a logarithmic scale from black (no luminescence), through blue, green, yellow, red, purple to white (saturated pixels).

### 3.7.4. Overview of the mutant screen

Table 3.25 shows the fate of all putative mutants selected in the primary screen. Of 265 putative mutants selected in the primary screen, 215 were in the *CHS:Luc* 3.4 line and the other 50 in *CHS:Luc* 1.7 line, with respectively, 203 and 7 surviving. A thrips infestation in the growth room in which the *CHS:Luc* 1.7 plants were growing meant that few survived. None of the *CHS:Luc* 1.7 derived mutants passed secondary screening, and so won't be discussed further. Primary screening selected 139 putative UV-B (or synergism) specific under-expressing mutants, which was reduced to 5 after secondary screening and finally only 1 after RT-PCR and a subsequent allelism test. It should be noted that far more putative UV-B (or synergism) specific under-expressing mutants were isolated in the primary screen, and selection in this category was less stringent to avoid loss of valuable mutants. This was because this was the main class of mutants of interest in this study. Stringency was introduced in subsequent secondary screening and RT-PCR. Other mutants were selected only where they looked strong candidates and were carried through secondary screening. RT-PCR of these mutants would be the next step in their verification.

| | *CHS:Luc* 3.4 $M_2$ | | | *CHS:Luc* 1.7 $M_2$ | | |
|---|---|---|---|---|---|---|
| | Primary Screen | Secondary Screen | RT-PCR | Primary Screen | Secondary Screen | RT-PCR |
| UV-B specific under expressors | 139(7)† | 5 | 2(1)* | 7 | 0 | - |
| UV-B specific over expressors | 13 | 2 | - | - | - | - |
| Blue specific under expressors | 5 | 4 | - | - | - | - |
| Blue specific over expressors | - | - | - | - | - | - |
| Constitutive over expressors | 16 | 4 | - | - | - | - |
| Constitutive under expressors | 28 | 16 | - | - | - | - |
| Mutants with spatial alteration in expression | 2 | 0 | - | - | - | - |
| Other marginals | 21 | - | - | - | - | - |
| Total | 203 | 52 | 1 | 7 | 0 | - |

**Table 3.25 Fate of all putative mutants selected**

*Arabidopsis CHS:Luc* 3.4 and 1.7 $M_2$ seedlings were grown on compost in low white light (LWL < 20 µmol $m^{-2}$ $s^{-1}$) for 21 days before illumination and assessment. Figures denote the number of putative mutants in a mutant class at any stage of screening.

† number in parenthesis indicates number of very marginal individuals

* number in parenthesis indicates number of complementation groups

## 3.8. Discussion and further work

### 3.8.1. A novel *CHS:Luc* reporter resource

A resource has been established in the generation and characterisation of *CHS:Luc 1.7* and *3.4* lines, and M2 populations which might be exploited in future mutant screens and has been used by Brown (2005) to screen for mutants in UV-B induction of *CHS*. Luciferase expression in these lines reflects wild type *CHS* transcription in blue, UV-B and blue / UV-B synergistic conditions in three week old mature leaves. Synergism does not appear to be as obvious in two week old plants as in three week old plants. It is known that *CHS* expression is differently controlled in very young seedlings (up to 6 days old) and adult plants (three weeks old) and it is possible that photoreception or signalling mechanisms involved in the synergistic induction of *CHS* are yet to become fully established in two week old seedlings. This observation is of course based on luciferase luminescence so might not represent any real difference in *CHS* expression between two and three week old plants. It is however, recommended that three week old plants be used in any subsequent use of these lines to report mature *CHS* expression.

It should also be noted that UV-A induction of *CHS:Luc* is not seen in these lines. The reason for this phenomenon is not clear, but as the main photoreceptor for blue and UV-A light (CRY1) does not seem disturbed in its function or signalling (i.e. blue light is still inductive), it seems likely that luciferase activity in these lines is compromised by UV-A light. Luciferase's substrate luciferin is light labile, but as it is added to the plants after inductive light treatments, the possibility that UV-A might promote its destruction can be dismissed. Although there is no clear explanation of the phenomenon, the lack of

luciferase activity in plants exposed specifically to UV-A means that the *CHS:Luc* lines could not be used for a genetic screen involving this type of illumination.

### 3.8.2. Critical assessment of the experimental approach

A lot of time was spent at the beginning of this project in the optimisation of screening conditions. For the sake of the work described, it was only necessary to demonstrate that the reporter lines used were representative of *CHS* transcription and perhaps some of this time may have been better spent pushing on with screening. The various manipulations and trials did serve three useful functions, though. Firstly, the new transgenic lines were quite thoroughly tested which helped establish confidence in them, and saved wasted effort in screening with an unsuitable line. Secondly, these pilot experiments allowed the researcher to become familiar with the biological material, techniques and critical assessment of the types of data produced before progressing with the screen, thereby cutting experimental variability and consequently increasing the chances of success of such a screen. Lastly, a fairly elegant and robust screen was developed which successfully allowed isolation of putative mutants in all anticipated classes. It was essential to the success of the screen that conditions were properly established before screening began.

In optimising conditions for the screen, various light qualities, fluence rates and durations were tested. Screening conditions were set as 8 hours blue (80 μmol $m^{-1}$ $s^{-2}$) light followed by 4 hours UV-B (3 μmol $m^{-1}$ $s^{-2}$) as these showed a maximal difference between luminescence seen in synergism and single light treatments. A photon counting camera was used to measure luciferase luminescence before each inductive light

treatment and at the end of the experiment. Efforts were made to develop analytical methods for interpreting the luminescence data produced. Three approaches were taken which relied on extracting numerical data from the images. Although these techniques were useful in demonstrating the suitability of the screening procedures used, visual assessment proved best for analysis of multiple images (which could be viewed in quick succession to make putative mutants more obvious). Three week old plants were used as they exhibited luminescence better than individuals of two weeks old.

Screening conditions were such that mutants were imaged three times before selection, which allowed for the assignment of mutants to several mutant classes in primary screening. This was only possible as a consequence of the stability of the blue light signal, which allowed synergism to be seen in plants exposed to sequential light treatments (i.e. blue light followed by UV-B). In retrospect, it may be argued that a strategy which used a quicker screen such as co-incident illumination with UV-B and blue light, followed by secondary screening as conducted (section 3.5.3) may have proved more economical. Consideration of the number of mutants isolated suggests that this is probably true, but without this prior knowledge, it is the considered view of the researcher that the screen as executed was the best approach.

The screen produced a very large proportion of false positives. Each putative mutant was selected based on the phenotype of only one individual plant. Secondary screening drastically cut the number of putative mutants, but still contained a majority which did not differ significantly from wild type with respect to *CHS* transcription. It may be expected that a proportion of false positives would be attributable to mutations in the transgene or in cellular components affecting the functionality of luciferase or ability

of luciferin to enter the cell (which is very unlikely, as cell membranes are permeablised with Triton X-100 to allow luciferin in) or even in cell shape or cuticle thickness which could conceivably influence the optical (light scattering) properties of the cell. All these examples would be expected to have something in common, though. They would not be expected to behave as wild type under any inductive conditions when assessed via luciferin luminescence.

These possibilities were anticipated before the commencement of the screen. The screen was designed in such a way as to image $M_3$ plants three times before classification, allowing all "constitutive under and over-expressors" to be identified and not pursued further. The example given in this chapter of the putative mutant *CHS:Luc* 136(2) is typical of most putative mutants identified in this screen. Here, the $M_3$ seedling was a strong candidate for classification as a UV-B / synergism specific under-expressor (the class most desired in the screen). This classification was confirmed in secondary screening, but RT-PCR showed it to have wild type *CHS* transcript production under experimental conditions. *CHS:Luc* 136(2) was thought particularly promising when it was first identified as it had a clear associated variegated leaf phenotype, which would have facilitated mapping. This phenotype may be key to understanding why so high a proportion of putative mutants eventually prove themselves false. It may be that while endogenous *CHS* expression can be maintained, putative mutants may suffer from compromised general fitness (in this case, the root cause of variegation) and this might reduce the level of luciferase luminescence, perhaps because of a reduced availability of ATP.

### 3.8.3. Implications of the screen

The genetic screen described in this chapter successfully identified 210 putative mutants, which were further screened and selected based on larger numbers of $F_3$ plants. This cut the number of putative mutants drastically to only 52 which did not behave as wildtype. Of these, none were specifically altered in UV-B / blue light synergism and only 7 looked like genuine UV-B specific under or over-expressing mutants. RT-PCR of these mutants reduced the number to only two, both derived from *CHS:Luc* 3.4 $M_2$ 068. This made it likely, as was confirmed in an alleleism test, that these mutants derived from the same mutagenic event. There are, then some mutants remaining uncharacterised from the current screen, which may be exploited for further study.

Only one complementation group was reliably shown to have altered UV-B and UV-B / blue synergistic induction of *CHS*. This mutant was also shown to be allelic to *uvr8*. The most obvious conclusion to be drawn here is that *UVR8* is specific to, and very important in, UV-B photoreception or signalling. The screen, as described, probably did not saturate the genome but two previous screens, conducted by (Kliebenstein et al 2002 and Brown 2005) also each isolated only *uvr8* mutants, with no other UV-B photoreception or signalling mutants described. This suggests that the likelihood of obtaining novel genetic components of UV-B or UV-B / blue photoreception or signalling by extension of this screen may be low.

It would seem logical that since UV-B / blue synergism is observed, there must be some gene products involved and in principle these could be identified by the type of approach employed here. Since such mutants were not isolated it is natural to draw into question the sensitivity of the screen. It is possible that several mutants exist which have

subtle effects on the system and as such are less amenable to discovery. The screen, as devised, was able to distinguish LWL, blue, UV-B and synergistic induction of *CHS*, as measured via luciferase luminescence. One possible way to pick up synergism-specific mutants is to extend the scale of luminescence (perhaps by selecting a new transgenic line with higher inducible luminescence), where the differences between each inductive treatment are magnified.

The fact though that the work detailed in the current screen has again only identified *UVR8* suggests that there was some common flaw in the three screens discussed (Kliebenstein et al. (2002), Brown (2005) and the present study), which could account for the outcomes. Alternatively, it may be that the pathways being probed use components which are highly redundant with those of other pathways. There is a temptation to suggest that the repeated identification of *UVR8* and no other components in UV-B and UV-B / blue light photoreception and signalling suggests that the pathway is a short one, and this may well be true, but cannot be asserted until the level of redundancy is known.

*uvr8* was shown to have lost its capacity for synergistic induction of *CHS*, just as it had lost its ability to express *CHS* in response to UV-B. This has clear implications for the understanding of this synergistic interaction. Firstly, UVR8 acts downstream of the interacting pathways. Secondly, this data suggests that there is only one UV-B inductive pathway responsible for UV-B and synergistic induction of *CHS*, unless there exist two (or more) separate photoreception pathways, which each act through UVR8. Thirdly, *uvr8* showed wild type induction of *CHS* under illumination with blue light, indicating that UVR8 is not required for blue light induction of *CHS*. As this work was done in a

line with wild type *cry1* (the main blue light photoreceptor involved in *CHS* expression), the logical possibility exists that a non-*cry1* blue light signal (the signal involved in synergistic induction of *CHS*) is disrupted. *uvr8* exhibits (seemingly) wild type *CHS* expression under blue light. It is possible that disruption of the blue light signal involved in synergism is masked by the *cry1* blue light signal. Indeed, it is curious that no mutants were found with specific disruption of the synergistic interaction where the disruption was based in the blue light specific component.

### 3.8.4. Further work

#### 3.8.4.1. How might genetic components of UV-B / blue synergism be found?

The first and most obvious route to discovery of genetic components of the UV-B / blue light synergistic induction of *CHS* would be to use further genetic screens. Some suggestions for such a screen are made above. It may be necessary to illuminate plants with UV-B and blue light simultaneously and vary the conditions of the screen (e.g. duration or fluence rate of illumination). In addition, the synergism-specific blue light photoreception and signalling components may be amenable to discovery in a similar screen which assesses blue light induction of *CHS* via *CHS:Luc* in a *cry1cry2* mutant background. As very little *CHS* expression is seen in the *cry1cry2* double mutant, there could be a problem with luminescence levels not being high enough to conduct a screen. In addition, there is no evidence to suggest that the synergism-specific blue light photoreceptor works inductively in the absence of UV-B. Any putative mutants that were, however, isolated from such a screen may then be assessed for synergism.

### *3.8.4.2. uvr8*

A range of mutants came from the genetic screen conducted in this chapter. These fell into a number of classes. Unfortunately, no mutants with specific lesions in UV-B / blue light synergistic induction of *CHS* were found. One mutant (isolated twice) was *CHS:Luc 068*. It did have altered synergistic induction of *CHS* expression, but was also altered in UV-B induction. This mutant is likely to be a new *uvr8* allele. Sequencing of this new allele is planned for the immediate future.

UVR8 has only recently been shown to have a role in UV-B induction of *CHS* expression. It has been shown though, that UVR8 localises to the nucleus and associates with chromatin, similarly to RCC1 and the significance of chromatin binding seems to be that it facilitates the UV-B regulation of target genes (Brown, Cloix, Jiang, Kaiserli, Herzyk, Kliebenstein and Jenkins, submitted). This study also shows that UVR8 has very little Ran GEF (guanine exchange factor) activity, indicating that it functions differently to RCC1. The study of further mutant alleles, such as that identified in the work described in it this chapter will help to characterize the structure / function relationship of UVR8.

Assessment of interactions of the UVR8 protein with other cellular components, may provide a means of identifying components concerned with synergism. Mutants in components interacting with UVR8 would need to be examined for the synergistic response.

# Chapter 4 Characterisation and mapping of *icx2*

## 4.1. Introduction

### 4.1.1. The isolation and previous characterisation of *icx2*

Chalcone synthase (*CHS*) is an essential gene for the production of plant flavonoids and is induced by a range of light qualities, including UV-B (λ = 280-320 nm), in mature (3 week old) leaf epidermis of wild type *Arabidopsis thaliana*. The *icx2* (*increased chalcone synthase expression 2*) mutant (originally designated 4L13) was isolated from an EMS mutagenised population as a high expressor of chalcone synthase (*CHS*) under UV-B light (Dr. G. Fuglevand, unpublished). *CHS* expression was reported in this screen via a *CHS:GUS* reporter line (NM4 (non-mutant line 4)) which utilised the *Sinapis alba CHS* promoter fused to the coding sequence of the *GUS* gene.

*CHS* transcript expression has been extensively characterised for a double backcrossed line (4L13BC2) of the *icx2* mutant (Dr. M. R. Shenton, personal communication, unpublished data). These experiments show that the amplitude of *CHS* expression is increased under the same inductive light conditions as wild type in the *icx2* mutant (i.e. blue (λ = 390-500 nm), UV-A (λ = 320-390 nm), UV-B, and white light in 3 week old leaves).

*icx2* plants also retain synergistic induction of *CHS* (as described in sections 1.6 and 3.1) with blue / UV-B and UV-A / UV-B light, and the total *CHS* transcript level is greater still in *icx2* than in wild type when induced synergistically. In low white light (i.e. < 20 μmol $m^{-2}$ $s^{-1}$) or in darkness there is little difference in *CHS* expression between wild type and *icx2*.

*DFR* (*di-hydroflavonol reductase*) and *PAL* (*phenylalanine ammonia lyase*) gene expression behave similarly to that of *CHS* in *icx2* (i.e. hyper-induction in response to blue, UV-A or UV-B light).

All of these expression data suggest that the ICX2 gene product must be involved in the negative regulation of *CHS* and other genes important to the production of flavonoid secondary metabolites, including anthocyanins, in *Arabidopsis* via repression or other means. It is clear that *icx2* does not give rise to constitutive over-expression, but rather has its involvement in the magnitude of *CHS* response to various light conditions, rather than in the specificity or quality of the response.

*icx2* individuals were initially characterized as having reduced stature and a deep purple leaf colour, corresponding to an associated increase in anthocyanin accumulation in leaf epidermal cells, under white light with fluence > 100 μmol $m^{-2}$ $s^{-1}$, as exemplified in Figure 4.1. This phenotype was described as being recessive, and monogenic. During the course of the work presented here, these assertions were questioned.

*icx2* has also been shown to be more resistant than wild type to UV-B radiation (Dr. G. Fuglevand, unpublished data). Under damaging levels of UV-B, the *icx2* mutant displays a higher rate of survival. *icx2* also exhibits reduced formation of CPDs (cyclic pyramidine dimers) and 6-4 photoproducts, indicative of damage to DNA, compared to wild type when subjected to 16 hour exposures of ambient (3 μmol $m^{-2}$ $s^{-1}$) or higher (6 μmol $m^{-2}$ $s^{-1}$) fluence rates of UV-B.

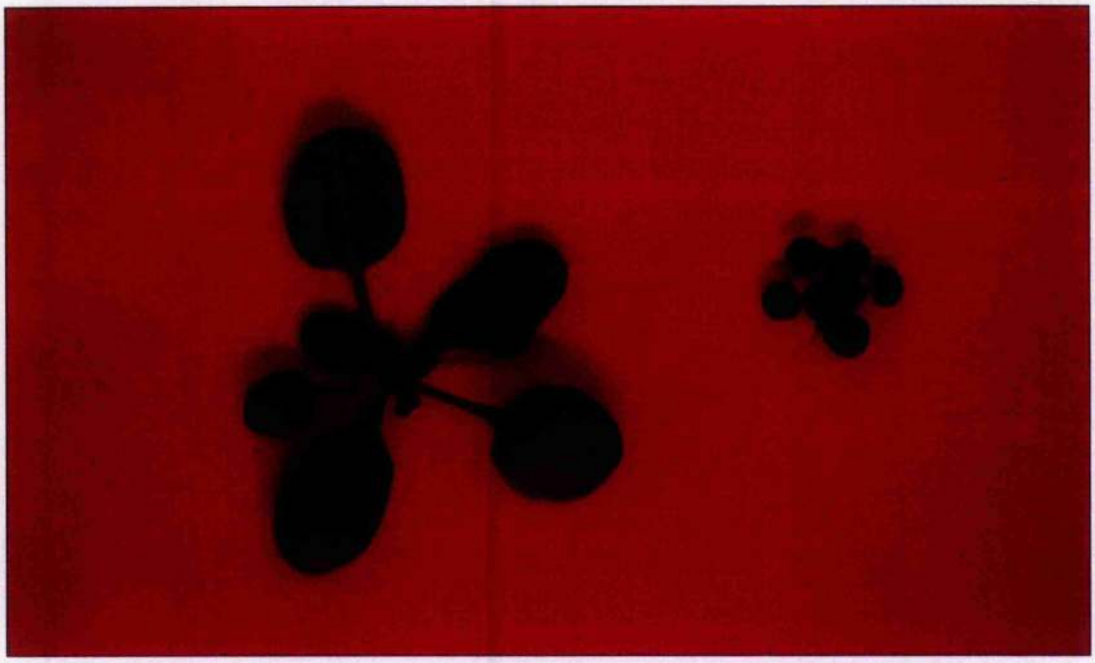

**Figure 4.1 *icx2* leaf phenotype**

Wild type Landsberg *erecta* (L.*er*) (left) and *icx2* (right) grown for 4 weeks in 150 μmol $m^{-2}$ $s^{-1}$ white light. *icx2* individuals exhibit stunted growth, dark purpling of the leaves, and have produced 6 mature leaves where wildtype has produced 8. Wildtype is beginning to produce a flower bolt, of which there is no evidence in *icx2*.

In *Arabidopsis,* ICX2 is clearly implicated in protection from harmful UV-B radiation and the control of *CHS* expression, which is an interesting model of gene regulation, as it lies at a biochemical crossroads, which represents the interaction of multiple biotic and abiotic inputs. This makes *icx2* an intriguing subject for further research. Characterisation of the pleiotropic phenotype of this mutant should assist in understanding the processes in which ICX2 is involved.

### 4.1.2. Aims

The aims of the work described here were threefold. First was to further characterise the phenotype of the *icx2* mutant against wild type. This was done using a range of developmental and morphological traits. Second was to advance mapping of the mutation, and if possible clone the gene. The third aim was to gain an understanding of the function of *ICX2*. Full realisation of the third aim was largely reliant on the successful completion of the second aim.

### 4.1.3. Experimental approach

Defining the *icx2* visible phenotype should help probe the function(s) of the wild type gene and facilitate map-based cloning of the mutation. The experiments reported here were used to characterise the phenotype of *icx2*, against two wild type ecotypes (Landsberg *erecta* (L.*er*) and Columbia (Col-3), as appropriate) and to advance mapping of the gene.

Landsberg *erecta* is the background ecotype in which the *icx2* mutant was isolated and so was used as wild type. Columbia was also characterised because it was the ecotype used in crosses with *icx2* for the production of an $F_2$ mapping population. Columbia was the ecotype used to generate the *Arabidopsis* Genome Initiative sequence database (available through TAIR (The Arabidopsis Information Resource) at www.arabidopsis.org) and so where a mutant is identified in an ecotype other than Columbia it makes good sense to use Columbia as the second ecotype to produce a recombinant mapping population. Landsberg and Columbia have another great advantage when used together to provide polymorphisms for map-based cloning and that is that Cereon (www.arabidopsis.org/cereon) have a large database of polymorphisms between these two genotypes, which is available to researchers subject to agreement that a maximum of 20 polymorphisms used to map a given gene may be published.

It quickly became clear that the *icx2* leaf phenotype as described above was ambiguous in a Col-3 x *icx2* $F_2$ population. With this in mind, Columbia was added to characterisation experiments where the trait being studied might aid mapping. Col-3 x *icx2* F2 and L.*er* x *icx2* $F_2$ populations were also used in characterisation.

An alternative approach to help define the role of *ICX2* was also carried out. A screen for suppressor mutants of *icx2* was initiated to look for single mutations which could suppress the *icx2* phenotype, as these would be likely to cast light on *icx2* function, and control of *CHS* expression.

## 4.2. The *icx2* leaf phenotype

Understanding how a genotype is phenotypically represented is crucial when such a phenotype is to be relied upon for the production of a population used for map-based cloning. The concepts of penetrance and expressivity are important in characterising the representation of the genotype in the phenotype. Penetrance is defined as the proportion of individuals of a given genotype manifesting an associated phenotype, and expressivity measures the degree of severity with which a phenotype is expressed.

The variability of the *icx2* phenotype is illustrated in Figure 4.2, which shows *icx2* (4L13BC2) and wild type (L.*er*) plants, grown under white light of fluence 20 μmol $m^{-2}$ $s^{-1}$ (LWL), or 150 μmol $m^{-2}$ $s^{-1}$ (HWL), and photographed after 4 weeks. *CHS* expression would be expected to be greater in those plants grown in HWL, and the mutant phenotype more obvious. As the double backcrossed line, 4L13BC2, was used, all individuals can be said to be homozygous mutants. These photographs show that the *icx2* mutant has a problem of expressivity, as there is a large variation in the phenotypes displayed in *icx2* individuals. It is also evident from Figure 4.2 that *icx2* plants show high mortality rate. Further evidence of this is seen in Figure 4.3, which shows mortality among individuals transplanted in the course of leaf characterisation experiments. The only significant drop in the rate of survival is seen in *icx2* individuals transferred to HWL.

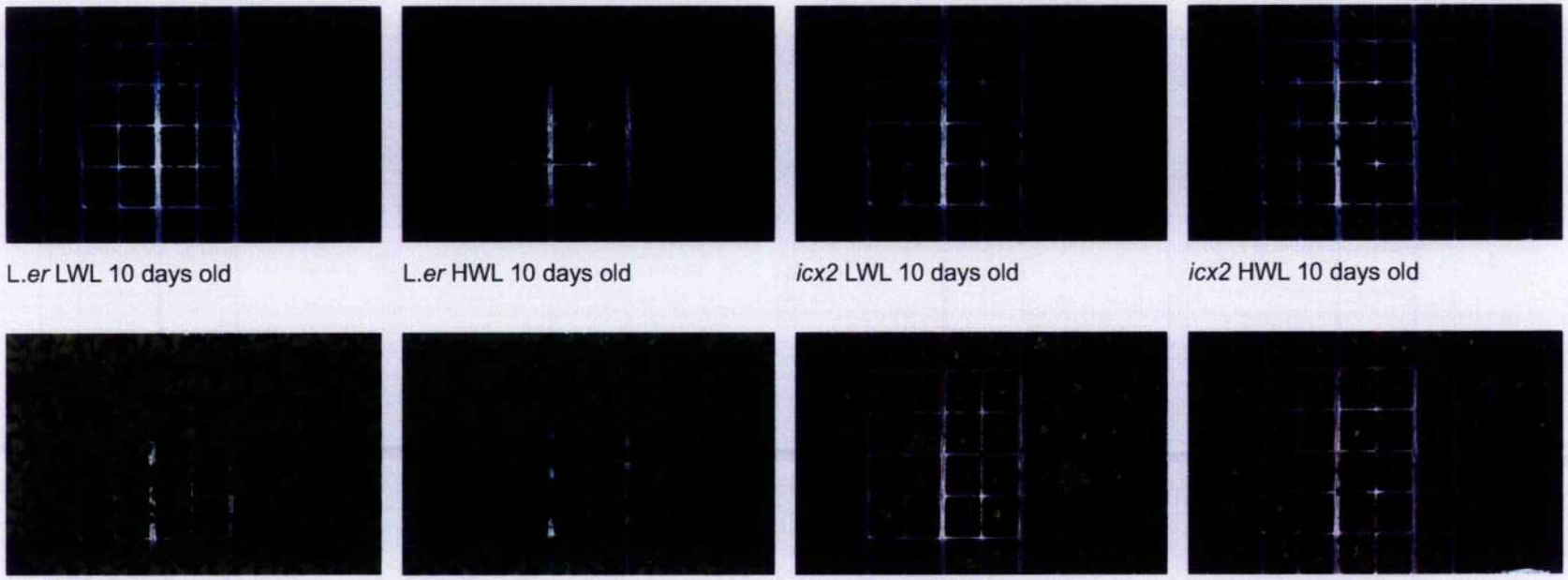


**Figure 4.2 The *icx2* mutant shows altered rosette diameter**

Wild type Landsberg *erecta* (L.*er*) *icx2* were grown in 60 well trays of compost for 1 week under low white light (20 µmol $m^{-2}$ $s^{-1}$, or LWL) before being either maintained in low white light or transferred to high white light (150 µmol $m^{-2}$ $s^{-1}$, HWL). High quality digital photographs were taken of each 60 well tray at 10 and 33 days old. Plants of 10 days old are of uniform size. *icx2* individuals however, show much reduced rosette diameter, but with higher variability when compared with wild type L.*er*.

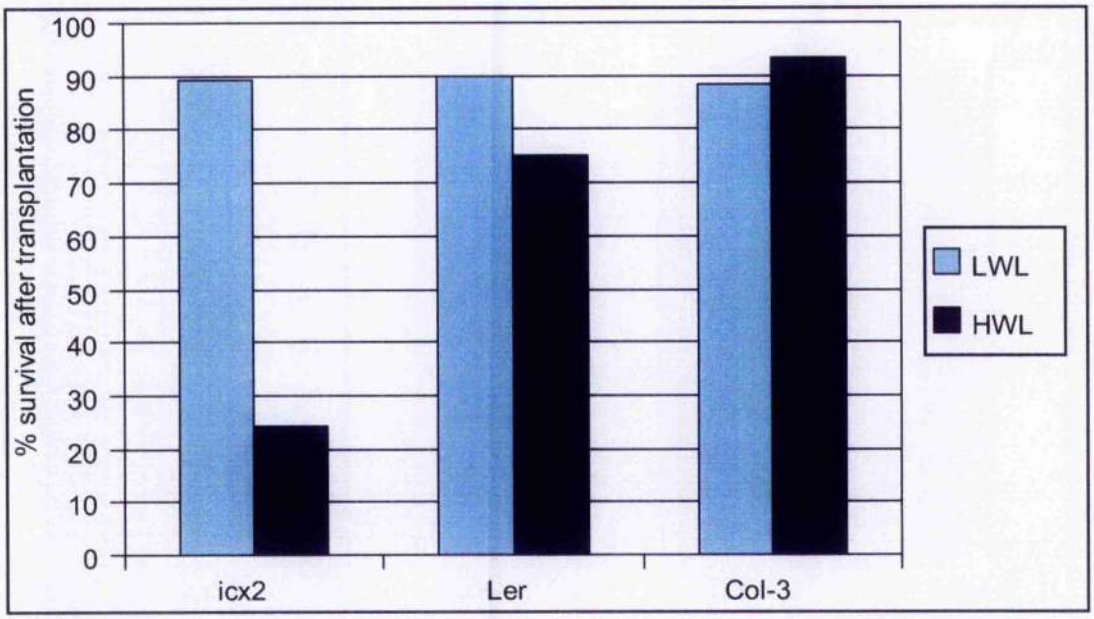


**Figure 4.3 The *icx2* mutant has a high rate of mortality in high white light**

Wild type Landsberg *erecta* (L.*er*), Columbia (Col-3), and *icx2* were grown in 60 well trays of compost for 1 week under low white light (20 µmol $m^{-2}$ $s^{-1}$, or LWL) before being either maintained in low white light or transferred to high white light (150 µmol $m^{-2}$ $s^{-1}$, HWL). High rates of mortality were seen in *icx2* individuals transferred to HWL. High rate of mortality was seen in *icx2* individuals transferred to HWL. Preliminary results based on one repeat (n=120).

An $F_2$ mapping population, numbering 140 was made, derived from $F_2$ of Col-3 x *icx2* crosses, and using the leaf phenotype as a basis for selection of 3 week old plants under HWL (150 µmol $m^{-2}$ $s^{-1}$). Confirmation of the phenotype, under the same conditions, in the $F_3$ generation led to the identification of only 64 individuals unequivocally suitable for use in mapping. It was decided that the efficiency of production of a mapping population might be improved if the *icx2* phenotype could be more reliably identified. This further justified the subsequent characterisation of the *icx2* mutant.

### 4.2.1. Rosette diameter in *icx2*

The *icx2* mutant exhibits reduced rosette growth, as seen in Figure 4.1. To characterise *icx2* rosette growth, individual pots of *icx2*, L.*er* and Col-3 were grown for 1 week under low white light (LWL = 20 µmol $m^{-2}$ $s^{-1}$) in order to allow (particularly *icx2*) plants to become established. After this time, 60 individual plants of each genotype were transplanted to compost (6 x 10 wells of a commercially available gravel tray insert) and further grown under either LWL, or high white light (HWL = 150 µmol $m^{-2}$ $s^{-1}$). High quality digital photographs were taken of each tray at specified time intervals from age 10 to 33 days post-germination. Each photograph included a scale bar, divided every centimetre, placed in the same plane as the surface level of the compost. Each photograph was digitally manipulated using Adobe Photoshop 6.0 to correct for parallax (using the grid of wells as reference) and scaled appropriately (with reference to the scale bar). Maximum rosette diameter was then measured by drawing circles with the marquee

tool, and reading off the diameter (to a resolution of 0.1 mm) from the panel labelled "info". Mean rosette diameter and standard deviation was calculated for each genotype in high and low white light and for each time-point. The results are shown in Figure 4.4.

As can be seen, all three groups are approximately the same size at the beginning of the experiment. In both HWL and LWL, however, *icx2* individuals quickly fall behind the rate of growth seen in both wild types and exhibit smaller rosettes than either wild type, but also show greater variation in size. This strongly suggests that rosette diameter is not a good enough phenotypic indicator of *icx2* to be used to generate a mapping population.

### 4.2.2. Timing of flowering in *icx2*

It had been noted that *icx2* flowers later than wild type plants grown alongside. When deciding if a mutant is early or late flowering, a distinction must be made between flowering which is developmentally altered and that which is simply chronologically altered and may be the result of slow growth. True late (or early) flowering mutants are altered in the developmental timing of flowering.

Developmentally and chronologically late flowering mutants are classically distinguished by counting the number of rosette leaves produced before bolting occurs. Landsberg *erecta* grown in constant light at 25 °C produce 6 – 8 rosette leaves before bolting (or 5 – 8 if seeds are vernalised, as in these experiments). All *icx2* and wild type plants grown in the conditions used in the rosette diameter study bolted at the 8 – 10 leaf stage.

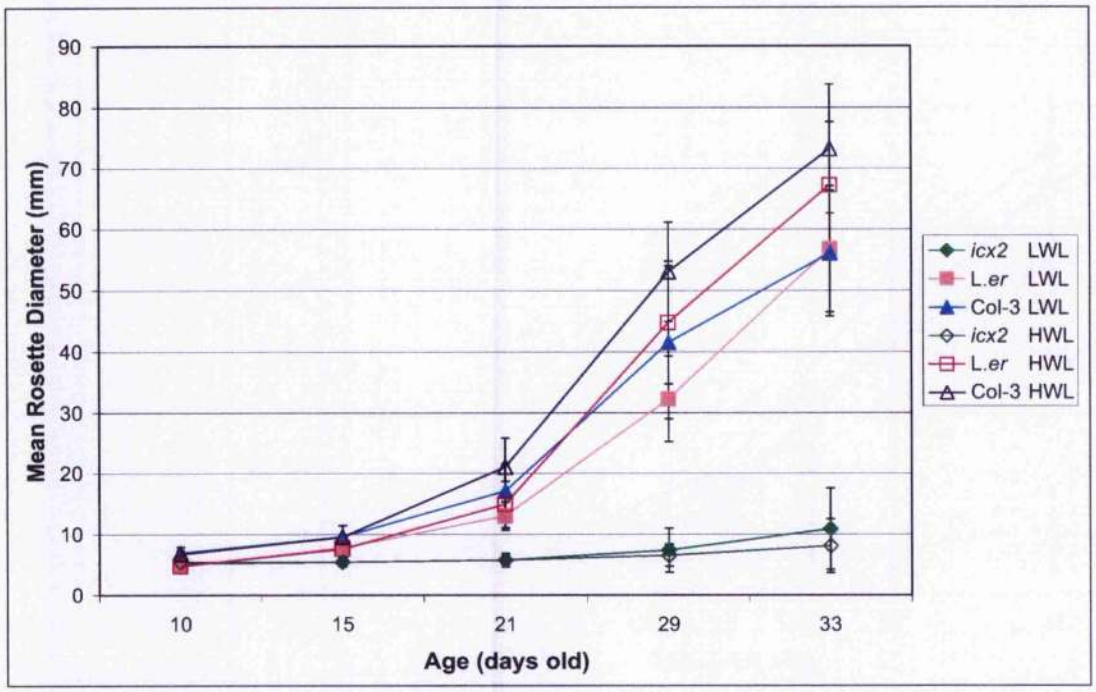


**Figure 4.4 The *icx2* mutant shows altered rosette diameter**

Wild type Landsberg *erecta* (L.*er*), Columbia (Col-3), and *icx2* were grown in 60 well trays of compost for 1 week under low white light (20 µmol $m^{-2}$ $s^{-1}$, or LWL) before being either maintained in low white light or transferred to high white light (150 µmol $m^{-2}$ $s^{-1}$, HWL). High quality digital photographs were taken of each 60 well tray at time intervals specified. Mean rosette diameter and standard deviation, calculated for each genotype in high and low white light at each time-point from measurements made as detailed in Materials and Methods 2.4.1.

The number of rosette leaves produced before bolting occurred was recorded for *icx2*, and both wild type ecotypes being characterised, L.*er* and Col-3. There was found to be no difference between *icx2* and wild type in number of rosette leaves produced before bolting. As can be seen in Figure 4.5, *icx2* is chronologically late in flowering. The fact that *icx2* bolts at the same developmental stage as wild type means that it is not a true late flowering mutant.

### 4.2.3. The effect of sucrose on *icx2*

Sucrose stimulates the expression of *CHS* in wild type *Arabidopsis*. This suggested that the *icx2* phenotype might be more easily identified in seedlings grown on medium containing sucrose and as such would add to *icx2* characterisation, and increase its accessibility to mapping.

#### 4.2.3.1. Anthocyanin accumulation in *icx2* in response to sucrose

The purple colour seen in the leaves of *icx2* individuals grown under light conditions expected to stimulate *CHS* expression correlates with an increased accumulation of anthocyanins in the epidermis (Dr. G. Fuglevand, unpublished data). This is commensurate with expectations, given the increases in *CHS* transcription described in section 4.1 and bearing in mind that CHS is the first committed step in the synthesis of flavonoids and DFR is the first enzyme in the branch of the pathway leading to anthocyanin biosynthesis (see Figure 1.2).

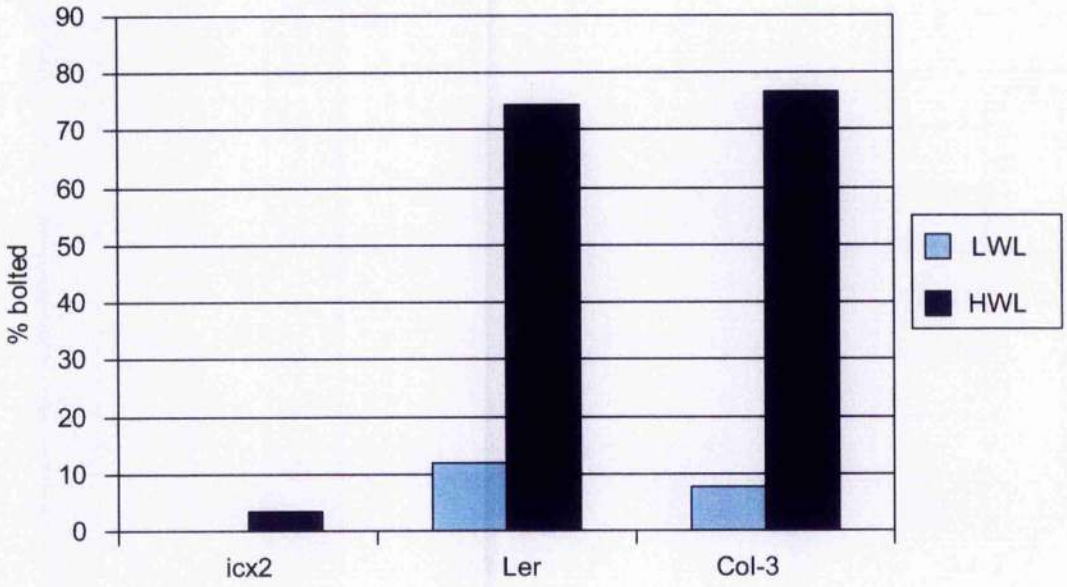


**Figure 4.5 The *icx2* mutant has a chronologically late flowering phenotype**

Wild type Landsberg *erecta* (L.*er*), Columbia (Col-3), and *icx2* were grown in 60 well trays of compost for 1 week under low white light (20 µmol $m^{-2}$ $s^{-1}$, or LWL) before being either maintained in low white light or transferred to high white light (150 µmol $m^{-2}$ $s^{-1}$, HWL). Percentage of plants having bolted at 40 days old is shown (n=60). No LWL grown *icx2* plants had bolted at 40 days old. Preliminary results based on one repeat.

*icx2*, L.*er* and Col-3 were grown on 0.8% agar containing 1/2 MS, and either 1.5% or 6% sucrose. Seedlings were harvested and anthocyanin concentration was spectrophotometrically determined from extracts as described in Materials and Methods. Figure 4.6 shows that more anthocyanins accumulated in *icx2* than in wildtype, when grown in the presence of sucrose. Interestingly, anthocyanin accumulation was approximately the same for *icx2* plants grown on 1.5% and 6% sucrose, but this difference in sucrose concentration produced a 3-4-fold increase in L.*er* and Col-3 anthocyanin accumulation. Wild type plants have around 7 times less anthocyanins than *icx2* when grown on 1.5% sucrose but only around 2 times less on 6% sucrose. This certainly corroborates the observable difference in phenotype under these two conditions.

## 4.3. The *icx2* root phenotype

### 4.3.1. The effect of sucrose on *icx2* root phenotype

*icx2* plants were initially grown on medium containing sucrose in an attempt to exaggerate the leaf phenotype, allowing further phenotypic characterisation and better classification of mapping population $F_2$ plants. It was immediately obvious however, that the most striking characteristic of *icx2* plants grown in this way was the very short primary root as seen in Figure 4.7. Figure 4.7a shows a photograph of L.*er*, Col-3 and *icx2* grown on 1.5% sucrose, where Figure 4.7b shows that the difference in root length between *icx2* and both wild type ecotypes is statistically significant. Figures 4.8 and 4.9 show the short primary root and root hair production in roots of *icx2* individuals.

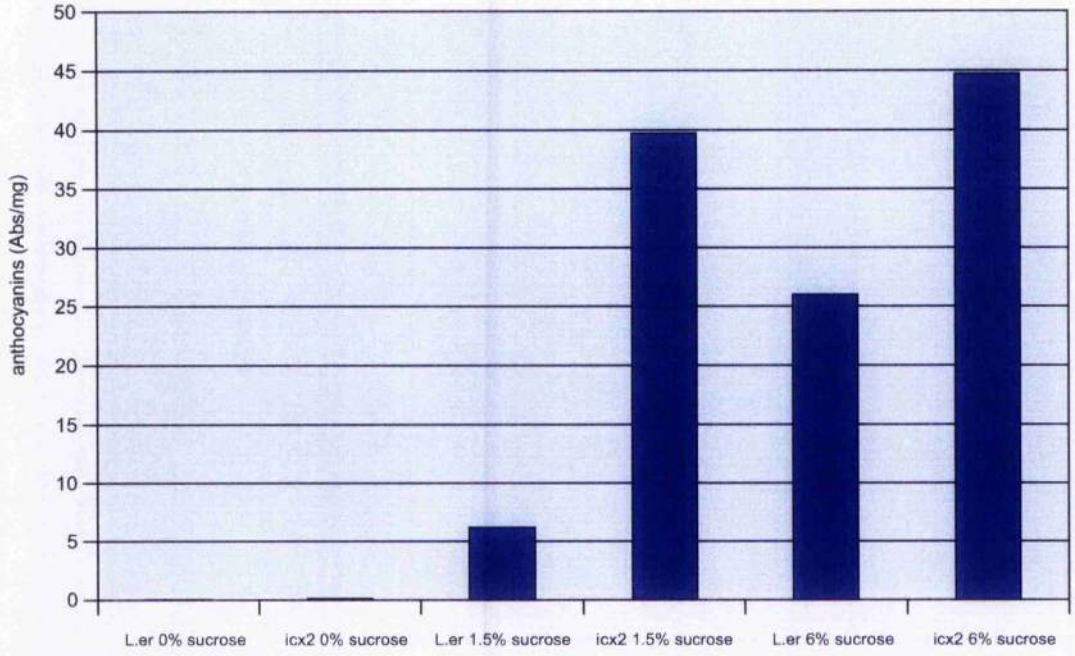


**Figure 4.6 *icx2* hyperaccumulates anthocyanins when grown on medium containing sucrose**

Wild type Landsberg *erecta* (L.*er*) and *icx2* seedlings were grown on solid plant growth medium, containing no, 1.5% or 6% sucrose for 10 days under low (20 μmol $m^{-2}$ $s^{-1}$, or LWL) white light. Anthocyanins were extracted and assayed according to Materials and Methods. These are preliminary data based on only one repeat, but agree with unpublished data collected by Dr. G. Fuglevand.

(a)

(b)

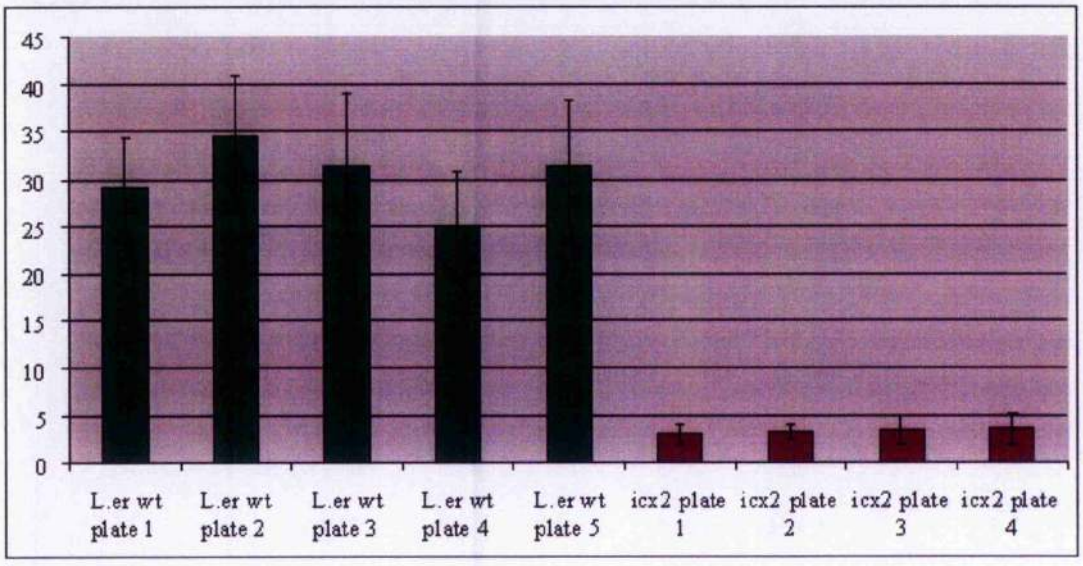


**Figure 4.7 *icx2* root phenotype**

(a) Wild type Landsberg *erecta* (L.*er*) (left), *icx2* (centre), and wild type Columbia (Col-3) (right) grown in 150 µmol $m^{-2}$ $s^{-1}$ white light for 10 days on solid plant growth medium, containing 1.5% sucrose. *icx2* individuals exhibit minimal primary root growth and dark purpling of the leaves. (b) Histogram showing the root length phenotype in the presence of 1.5% sucrose. Seedlings were grown on solid plant growth medium and measured at 10 days old. Results for several different plates are shown.

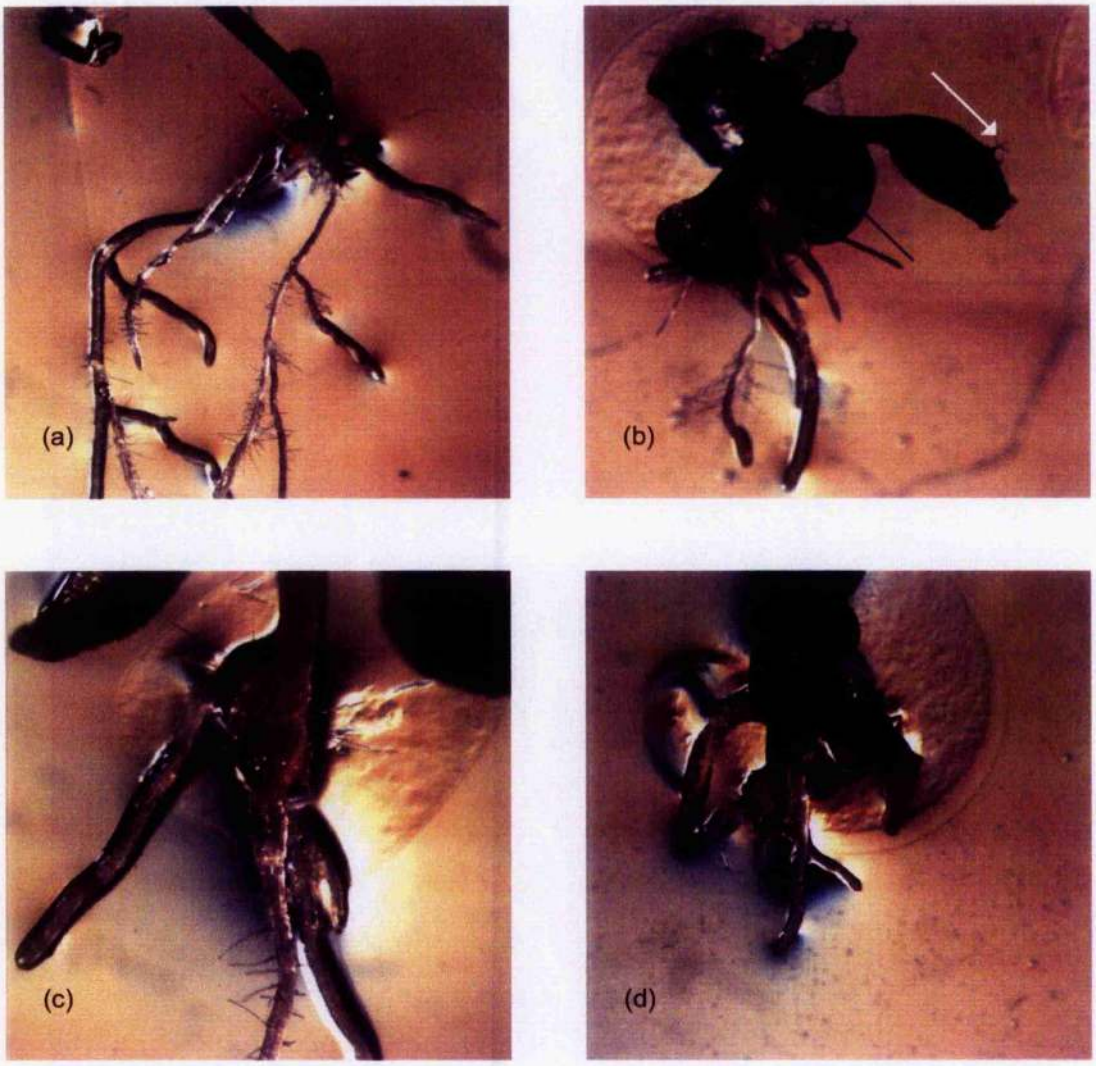


**Figure 4.8 *icx2* has altered root architecture**

*icx2* seedlings grown for 10 days on solid growth medium without sucrose (a), or on 1.5% sucrose (b)-(d). Note absence of primary root in seedlings (b)-(d), but presence in (a) (red arrow). Also note *icx2* exhibits wild type trichome development (white arrow), and purple leaf colouration (blue arrow) in (b).

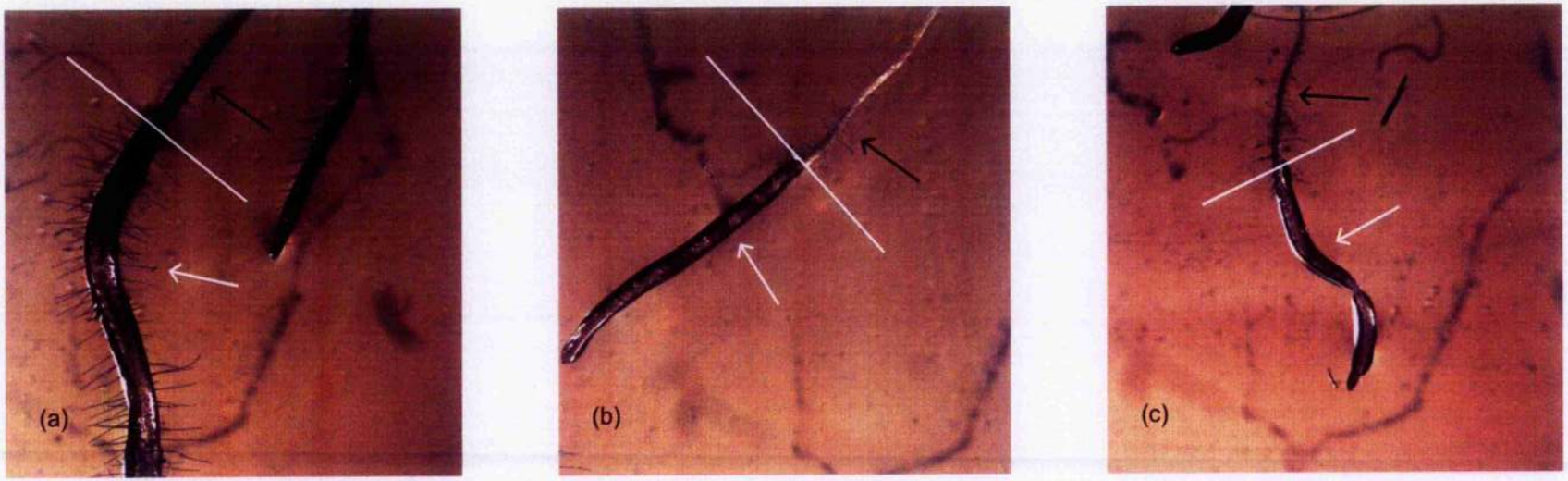


**Figure 4.9 *icx2* roots in contact with agar do not produce root hairs**

The distribution of root hairs on *icx2* roots. Air / agar root transitions denoted by white lines. (a) wild type Landsberg *erecta*, (b)-(c) *icx2*, all grown on medium containing 1.5% sucrose for 10 days. *icx2* individuals show lack of root hairs when in contact with agar (white arrows) but can produce them when not in contact with agar (black arrows).

Plants grown on 1.5% sucrose don't produce root hairs on the sections of root in contact with agar, but where a root has grown free of the surface of the plate, root hairs are formed.

Figure 4.10 shows that as well as there being different effects on anthocyanin accumulation between *icx2* and wild types, when grown on 1.5% or 6% sucrose, the same is also true of root length. All further characterisation of *icx2* roots, unless otherwise noted, was performed on 10 day old seedlings grown on solid medium (0.8% agar), containing 1/2 MS + B5 vitamins + 1.5% sucrose as described in Materials and Methods, as this produced the greatest difference between mutant and *icx2* x Col-3 $F_2$.

| | 1.5% Sucrose | 6% Sucrose |
|---|---|---|
| *icx2* purple leaf phenotype | 66.7% | 100% |
| *icx2* short root phenotype | 100% | 100% |
| L.er purple leaf phenotype | 8.7% | 32.1% |
| L.er short root phenotype | 0% | 0% |
| Col-3 purple leaf phenotype | 0% | 6.1% |
| Col-3 short root phenotype | 0% | 0% |
| icx2 x Col-3 $F_2$ purple leaf phenotype | 3.1% | 30.2% |
| icx2 x Col-3 $F_2$ short root phenotype | 10.8% | 32.6% |

**Figure 4.10 *icx2* root and leaf phenotype grown on 1.5% and 6% sucrose**

Wild type Landsberg *erecta* and *icx2* and $F_2$ crosses were grown under high white light 150 µmol $m^{-2}$ $s^{-1}$on medium containing 1.5% or 6% sucrose for 10 days and visually assessed for root and leaf phenotype. (n > 30).

### 4.3.2. Penetrance of the *icx2* root phenotype

In contrast to the leaf phenotypes, the root phenotype may be used to unequivocally distinguish *icx2* from L.*er* and Col-3 wild type. To characterize the penetrance of the mutant phenotype in a heterozygous background, L.*er* (control) and Col-3 (mapping $F_2$) were each crossed with *icx2*. In both cases, the relevant wild type was chosen to be the female parent, as this would make it easy to check that the crosses had worked via the appearance of individuals exhibiting the *icx2* phenotype in the $F_2$ generation. $F_2$ populations derived from *icx2* crossed to L.*er* or Col-3 would be expected to exhibit a 3:1 ratio of long to short rooted individuals if grown under the same conditions, assuming a single recessive mutation.

Figure 4.11 shows the distribution of root lengths of L.er, Col-3, *icx2* and $F_2$ from *icx2* x Col-3 and *icx2* x L.er, grown under HWL in medium containing 1.5% sucrose. This Figure shows that a 3:1 ratio of long to short rooted individuals is exactly what is obtained from the $F_2$ of an *icx2* x L.*er* cross ($0.5 < p < 0.1$ in $\chi^2$ test), but that this ratio is not seen in the $F_2$ of an *icx2* x Col-3 cross ($p < 0.005$ in $\chi^2$ test). A 3:1 ratio of long to short rooted individuals is seen if the cut-off point is moved in the *icx2* x Col-3 $F_2$ from 10 mm to 15 mm ($0.5 < p < 0.1$ in $\chi^2$ test), although this represents a 50% increase in those root lengths accepted. This may help explain the problems that were encountered in the production of a mapping population for the *icx2* mutant as the phenotype appears weaker in the mixed genetic background.

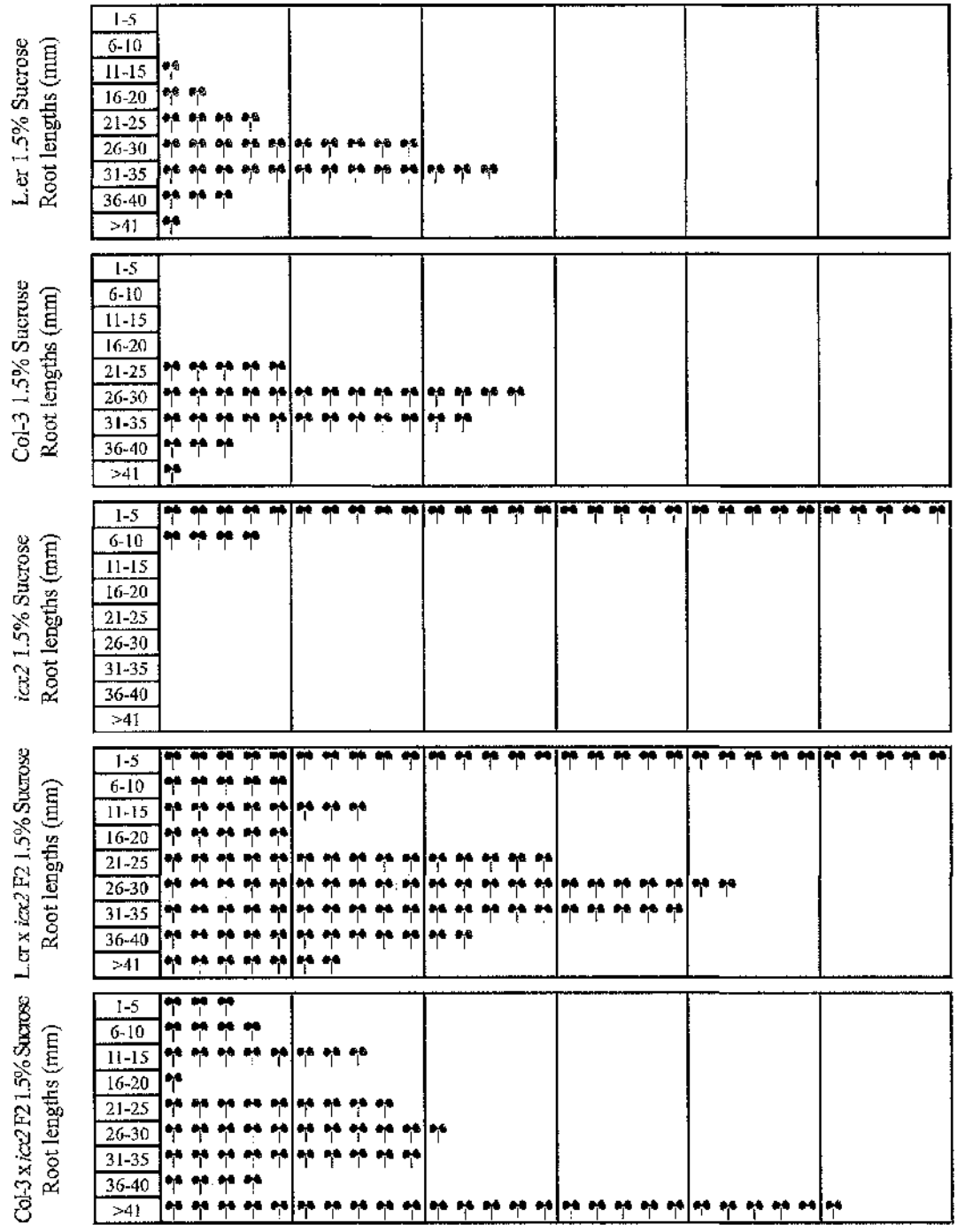


**Figure 4.11 Distribution of root lengths of *icx2*, L.er, Col-3 and $F_2$ progeny of *icx2* x wild type, grown on 1.5% sucrose**

Wild type Landsberg erecta (L.er), Columbia (Col-3), *icx2* and $F_2$ progeny of Col-3 x *icx2* and L.er x *icx2* were grown vertically on solid plant growth medium, containing 1.5% sucrose for 10 days under high white light (150 µmol $m^{-2}$ $s^{-1}$, or HWL). Root lengths of seedlings were measured to the nearest mm with a ruler divided every mm. Measurements were grouped in 5 mm bins, and numbers of seedlings per bin represented by symbols, each representing one seedling. coloured purple signifies those seedlings which would have been selected as *icx2* individuals. $\chi^2$ tests confirmed a 3:1 ratio of long to short rooted individuals in L.*er* x *icx2* $F_2$ ($0.5 < p < 0.1$ for rejection of null hypothesis "there is no 3:1 ratio") but did not confirm such a ratio in the Col-3 x *icx2* $F_2$ ($p < 0.005$) when root lengths < 10 mm were considered *icx2*-like. A 3:1 ratio was confirmed when this threshold was raised to 15 mm ($0.5 < p < 0.1$). This highlights the expressivity problem associated with the phenotype in a Col-3 x *icx2* background.

### 4.3.3. *icx2* root phenotype is not dependent on flavonoid accumulation

Anthocyanins have been shown to have an antagonistic effect on auxin signalling (Jacobs and Rubery, 1988: Brown et al 2001) and auxins are known to influence root morphology and stimulate root growth in *Arabidopsis*. It was conceivable therefore, that increased anthocyanin accumulation, decrease in root length and altered root architecture seen in *icx2* plants exposed to either 1.5 % sucrose and / or HWL may not be coincidental, but rather the aberrant root phenotype may be directly attributable to the observed rise in anthocyanin content. This was an attractive idea when the root length and anthocyanin accumulation in response to sucrose data are viewed together. Both imply that there is a threshold at which *icx2* is working and that might imply a common mechanism.

To test this hypothesis, *icx2* was grown alongside *tt4*, L.*er* and *icx2, tt4* double mutant seedlings under either high (HWL = 150 µmol $m^{-2}$) or low (LWL < 20 µmol $m^{-2}$) white light or darkness, on solid plant growth medium with and without 1.5% sucrose. *tt4* is a null mutant of the *CHS* gene (Koornneef, 1981). The *icx2, tt4* double mutant was therefore unable to produce CHS or any downstream secondary metabolites, including anthocyanins. Root lengths of 10 day old seedlings were measured as detailed in Materials and Methods. The results of this experiment are shown in Figure 4.12. It can be seen that whereas the *tt4* mutant behaves as wild type, *icx2* and *icx2, tt4* double mutant individuals exhibit the short root phenotype as typically expected from *icx2*.

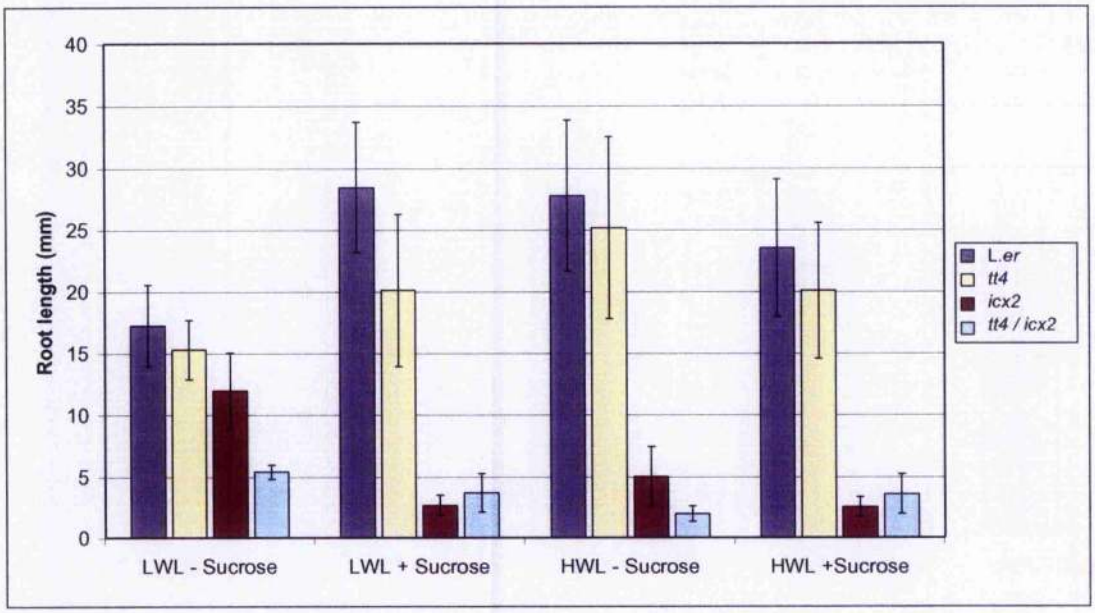


**Figure 4.12 *icx2* does not require CHS to mediate altered root phenotype**

Wild type Landsberg *erecta* (L.*er*), *icx2*, *tt4* (*CHS* mutant), and *tt4/icx2* double mutant seedlings were grown vertically on solid plant growth medium, containing no or 1.5% sucrose for 10 days under either low (20 µmol $m^{-2}$ $s^{-1}$, or LWL) or high (150 µmol $m^{-2}$ $s^{-1}$, or HWL) white light. Root lengths of seedlings were measured to the nearest mm with a ruler divided every mm. The typical *icx2* response is seen in *icx2* and the double mutant, but not in Landsberg or *tt4*, suggesting that CHS in not required for the *icx2* root phenotype.

Figure 4.12 demonstrates that ICX2 does not influence root length via the action of flavonoids or any downstream signal from *CHS*. This does not however, rule out a role of auxins or other plant signalling molecules, such as ABA, in the *icx2* short root phenotype.

In a second experiment, *icx2*, L.*er*, and *PAP1* seedlings were also grown under LWL and HWL and on solid plant growth medium with and without 1.5% sucrose. *PAP1* is an activation tagged line, over-expressing *AtMYB75* (Borevitz et al. 2000). *PAP1* individuals over-express *CHS*, and appear purple caused by increased anthocyanin accumulation via the action of MYB75.

This experiment showed, as reported in Figure 4.13, that *PAP1* root lengths did not differ significantly from those of wild type whereas *icx2* root lengths did, and so over-expression of *CHS* was not sufficient to produce short roots as seen in the *icx2* mutant.

### 4.4. *icx2* and hypocotyl growth

*icx2* was characterised for hypocotyl growth for two reasons. Firstly, if *icx2* were to be classified as a *cop / det / fus* (*constitutively photomorphogenic / de-etiolated / fusca*) mutant, it would be expected to have a partial light-grown phenotype when grown in darkness. Secondly, phototropic curvature of the hypocotyl might be expected to be altered in the mutant if it was altered in auxin transport or synthesis. Figure 4.14 shows *icx2* to exhibit wild type hypocotyl and petiole growth in the dark.

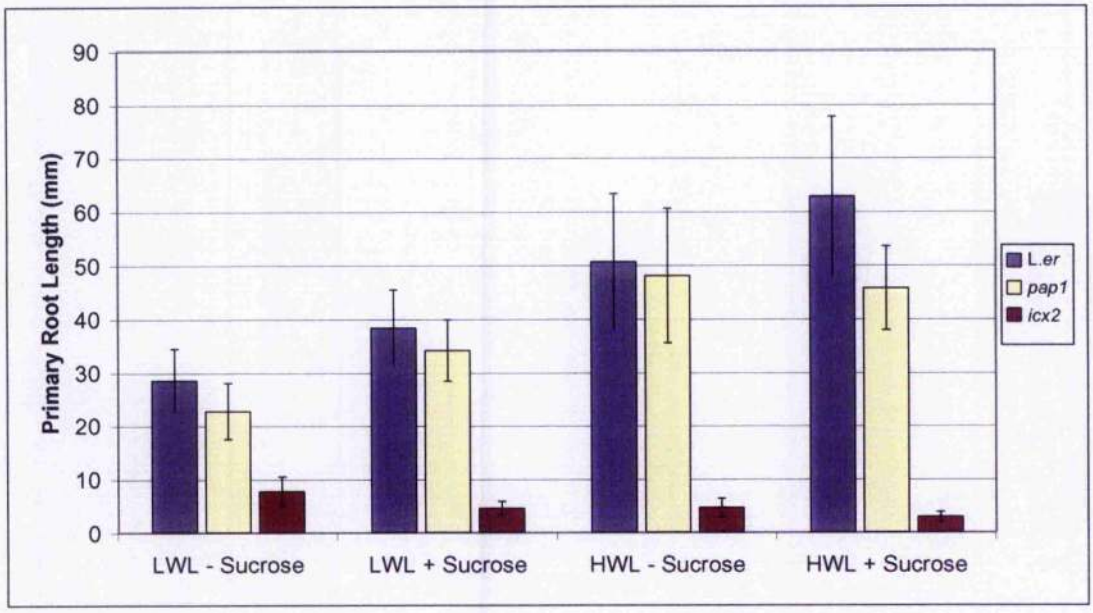


**Figure 4.13 *PAP1 CHS* over expression does not mimic *icx2* altered root phenotype**

Wild type Landsberg *erecta* (L.*er*), *icx2* and *PAP1* (*MYB75* over expressor, which results in *CHS* over expression) seedlings were grown vertically on solid plant growth medium, containing no or 1.5% sucrose for 10 days under either low (20 μmol $m^{-2}$ $s^{-1}$, or LWL) or high (150 μmol $m^{-2}$ $s^{-1}$, or HWL) white light. Root lengths of seedlings were measured to the nearest mm with a ruler divided every mm. The typical *icx2* response is seen in *icx2*, but not in Landsberg or *pap1*, suggesting that *CHS* over expression does not give rise to the *icx2* root phenotype.

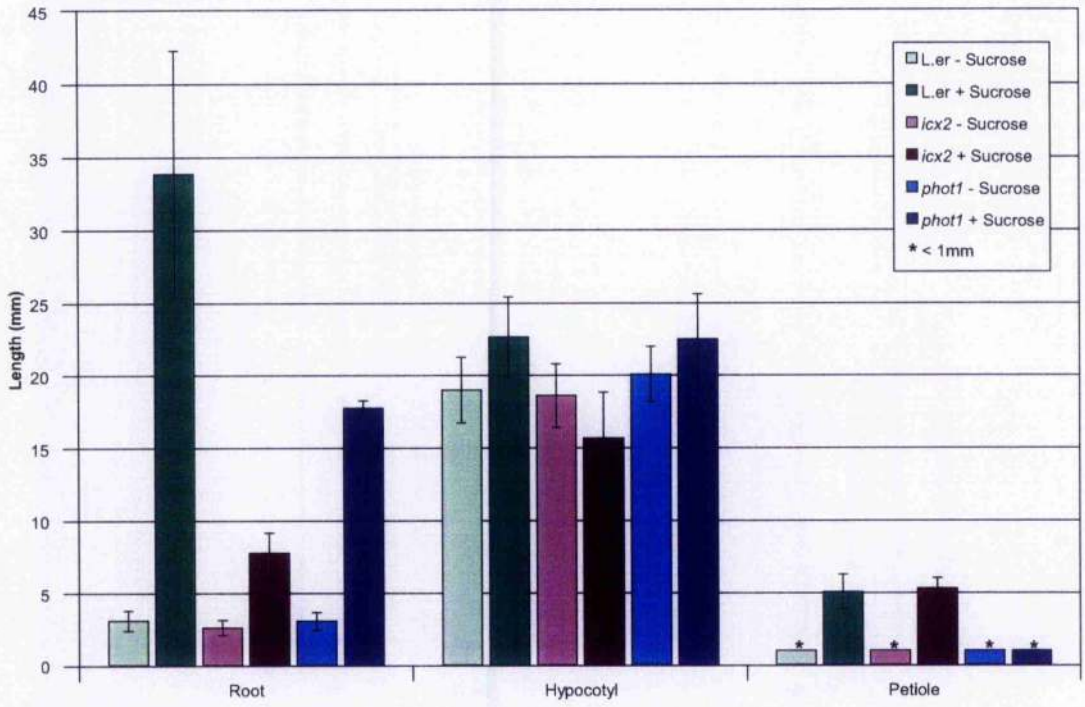


**Figure 4.14 Dark grown *icx2* exhibits wild type hypocotyl length**

*icx2*, L.er and *phot1* were grown on solid growth medium with or without sucrose in the dark for 10 days and root hypocotyl petiole lengths were measured.

It is interesting that the *icx2* root phenotype is less obvious in dark grown plants, but the short-root phenotype is clearly seen and so is not light-dependent. *phot1* individuals also exhibited shorter roots than wild type in the presence of sucrose.

*icx2* was shown not to be an extant *cop / det / fus* mutant by virtue of the fact that of all *cop / det / fus* mutants, only *COP9 (FUS7), COP3, DET1*, and two other associated proteins, *CIP7* (*COP1 interacting protein 7*), and a *COP1*-like protein were located on chromosome 4 (www.arabidopsis.org), but in every case these lay outside the region delimited as containing *icx2*, with other *cop / det / fus* mutants being located on other *Arabidopsis* chromosomes. In addition to this locational information, it was noted that despite reduced stature (which may look like a photomorphogenic trait), dark grown seedlings show unexpanded cotyledons, typical of skotomorphogenesis.

*icx2* was also tested against L.*er* for altered phototropism. Figure 4.15 shows that 3 day old, dark grown *icx2* seedlings retain the wild type ability to bend towards unidirectional blue light. It was also noted in dark-grown experiments that *icx2* did not seem to have altered gravitropic responses.

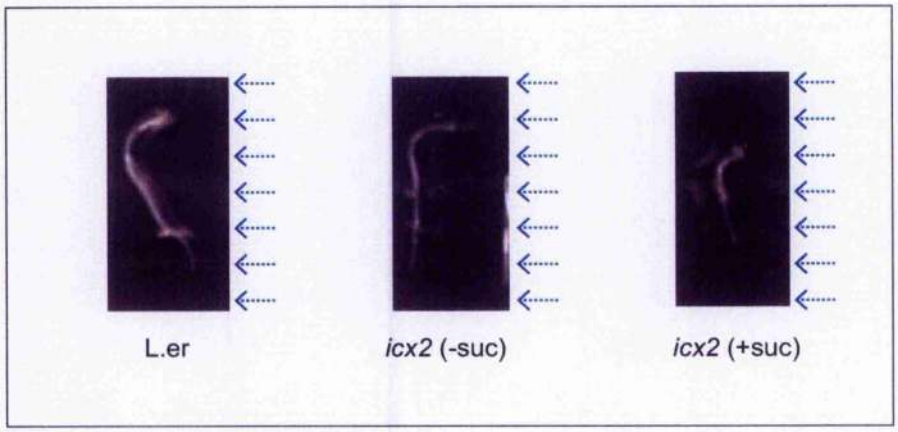


**Figure 4.15 *icx2* does not exhibit altered phototropism**

Wild type Landsberg *erecta* (L.*er*) (left), *icx2* -1.5% sucrose (centre), and *icx2* +1.5% sucrose (right) grown vertically on solid plant growth medium, containing no or 1.5% sucrose in darkness for three days following a 4 hour exposure to 150 μmol $m^{-2}$ $s^{-1}$ white light. Seedlings were then exposed to unidirectional blue light (from the right of each photograph as represented by the blue arrows) for 2 hours before being photographed. *icx2* individuals exhibit reduced hypocotyl growth in the presence of sucrose, but do show phototropism.

## 4.5. Mapping the *icx2* mutation

Map-based cloning of *icx2* had previously placed the mutation in a 12 cM (2990 kb) region on *Arabidopsis thaliana* chromosome 4 between markers AG (63.1 cM, 13530 kb) and PG11 (75.6 cM, 16520 kb), and close to mi422 (no recombinants found) (Dr. M.R. Shenton, personal communication, unpublished data). This region is shown in Figure 4.16. This attempt at mapping *icx2* had been made with a mapping population of 31 individuals but was abandoned, as the leaf phenotype proved unreliable as the basis for mutant screening. Figure 4.16 (b) shows primer sequences used to generate PCR-based markers used in the mapping of *icx2*.

An *icx2* x Col-3 $F_2$ generation was produced in preparation for the selection of a mapping population. As the leaf phenotype exhibited a problem of expressivity (section 4.2) and the root phenotype was compromised in the heterozygous background (Figure 4.11), individuals to be included in the mapping population were very carefully selected.

1106 individuals were selected on either the *icx2* leaf phenotype (140) or root phenotype (966). As it had not been categorically demonstrated that both the leaf and root phenotypes were caused by the same mutation and since a mapping population must be reliable, every individual selected was checked in the $F_3$ generation for the leaf phenotype and checked a second time where there was any ambiguity. Where any doubt existed over the genotype of any individual, it was discarded.

(a)

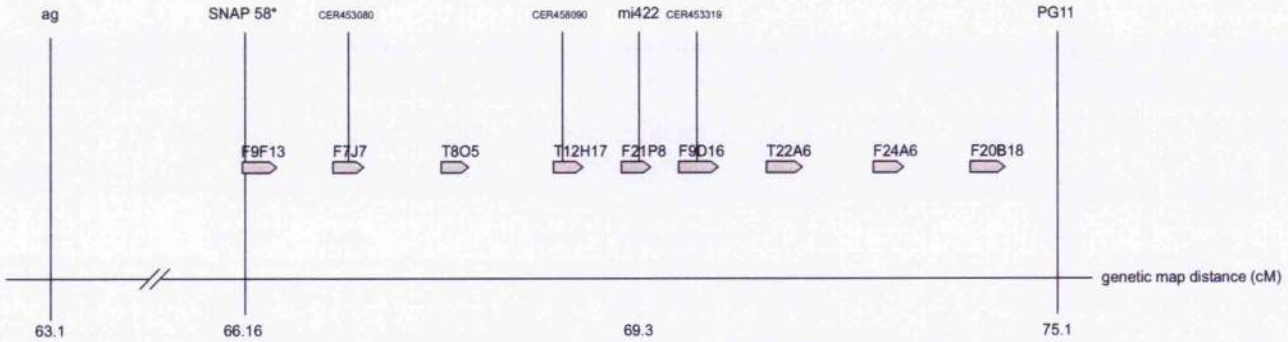


(b)

| BAC | Accession number | Marker | Position (bp) | INDEL size§ | Forward primer sequence (5'-3') | | | | | | | Reverse primer sequence (5'-3') | | | | | | |
|---|---|---|---|---|---|---|---|---|---|---|---|---|---|---|---|---|---|---|
| F7J7 | AL021960 | CER453080 | 28360 | -12/12 | ATT | CAA | TAT | ATA | TAT | ATA | TA | CAC | ATA | TAA | GAA | AAT | GTA | TG |
| T805 | AL021890 | CER461199 | 3487 | 12/-12 | CGG | CTT | GAG | CCA | TAA | TTC | CC | TCA | CAA | TCA | CAA | TCA | CAA | TC |
| T12H17 | AL021635 | CER458090 | 46303 | 13/-13 | TGT | TTT | AAA | GAA | TAA | ATG | AA | TAG | TAA | CCT | GGA | TGG | AAG | GA |
| F9D16 | AL035394 | CER453319 | 8865 | -11/11 | CCT | CCC | AAA | TTA | TTT | TTA | AA | TAT | TTA | TCA | AAA | GAA | GCT | TA |
| T22A6 | AL078637 | CER459388 | 77054 | 18/-18 | ACT | AAA | GAA | GAC | AGA | AAC | AG | GTG | TGT | GTT | TAT | GGT | AGA | AA |
| F24A6 | AL035396 | CER451125 | 50828 | -14/14 | ACG | GCG | ACG | GGA | AAA | TAG | AA | CCG | CAG | ATC | TCT | GTC | TCC | TC |
| F20B18 | AL049483 | CER450391 | 104131 | -14/14 | TTC | TTT | TGC | TCA | AAC | AAT | GT | TTT | GAC | TCC | ATA | ATA | TGT | GT |

§e.g. 4/-4 = 4bp insertion in Col/deletion in L.er
-4/4 = 4bp deletion in Col/insertion in L.er

*SNAP 58 primers (5'-3')

| | |
|---|---|
| Col forward | GGTACGGTGGCTACAGGGCGTCTC |
| Col/L.er reverse | TGAATACCCCTAAGCAACAACCCT |
| L.er forward | GGTACGGTGGCTACAGGGCGTGAT |

**Figure 4.16 *icx2* mapping**

(a) map location of *icx2* on cromosome 4, showing genetic positions of closest and flanking markers and BACs from which primers were designed. (b) primer sequences used to exploit polymorphisms between L.er and Col-3 as tools for mapping.

198 $F_2$ individuals died after transplantation, or produced no seed and 38 produced too few seeds to sow to assess the phenotype in the $F_3$ generation. 64 of 140 (45.7%) from the group selected based on leaf phenotype and 405 of 870 (46.6%) of the group selected on root phenotype were positively identified in the $F_3$ generation. Genomic DNA was extracted from these individuals, as detailed in Materials and Methods.

The use of genetic markers such as the *immutans* (*im*) mutation, which exhibits a variegated leaf phenotype and lies close to mi422 and PG11 was strongly considered, as this would facilitate selection of individuals with cross-overs in the region of interest (i.e. between *icx2* and *im*, in double mutant x wild type $F_2$ plants segregating both phenotypes). The problems with selection of the *icx2* phenotype led to this idea being disregarded, as the introduction of another mutant phenotype may have exacerbated these problems.

The Cereon database has a large collection of INDEL (insertion / deletion) polymorphisms between Landsberg and Columbia ecotypes. INDELs, appropriately positioned on chromosome 4, were selected and are displayed in Figure 4.16. These were in the size range 10 – 20 b.p., which could easily be resolved and distinguished in a DNA fragment of approximately 200 b.p. on a 4% agarose gel, or with real-time PCR. Appropriate surrounding genomic (BAC) sequence was obtained from TAIR (www.arabidopsis.org). With this information, primers were designed to produce PCR-based genetic markers as described in Materials and Methods, which would amplify fragments of different lengths from Landsberg and Columbia genomic DNA. In addition to these markers, CAPs (cleaved, amplified polymorphisms) and SNP (single nucleotide

polymorphisms) markers published at www.arabidopsis.org were investigated, but not used. SNAP 58 (Drenkard et al, (2000)), an SNP marker which used high fidelity PCR to distinguish Landsberg and Columbia sequences with respect to a single nucleotide was chosen as it lay on BAC F9F13 at 66.16 cM, between AG and mi422. Results gained using SNAP 58 (Figure 4.17) further delimited the region containing *icx2* to 8.94 cM, when samples Q47 and Q104 were shown to be carrying Columbia DNA at this marker. Markers designed using the Cereon database have defined the region of interest more finely. A double crossover in Q47 defined the region containing *icx2*. In order to get closer to *icx2*, numerous PCR-based markers were designed and tested. Three of these, CER453080, CER458090 and CER453319 gave informative results. Informative individuals from these experiments are also shown in Figure 4.17. The majority were not informative (e.g. 90.69% alleles tested at CER458090 were L.*er*).

These experiments suggested that CER453080 is a closer flanking marker than SNAP58. Results from CER458090 suggest that *icx2* lies between it and CER453080. Two individuals (marked with asterisks in Figure 4.17) do not fit with the rest of the mapping data. These may have double crossovers (it is still quite a large region), or may not be *icx2* individuals. Every effort has been made to ensure the reliability of the members of the *icx2* mapping population.

| | ag | SNAP 58 | CER453080 | CER458090 | mi 422 | CER453319 | PG II |
|---|---|---|---|---|---|---|---|
| Q 47 | | > | | | | | < |
| Q 104 | | > | | | | | |
| Q 87 | | | | | | | |
| I2MP178 | | | > | | | | |
| I2MP209 | | | > | | | | |
| I2MP210 | | | > | | | | |
| I2MP212 | | | > | | | | |
| I2MP231 | | | > | | | | |
| I2MP242 | | | > | | | | |
| I2MP243 | | | > | | | | |
| I2MP244 | | | > | | | | |
| I2MP246 | | | > | | | | |
| I2MP252 | | | > | | | | |
| I2MP394 | | | | < | | | |
| I2MP410 | | | | < | | | |
| I2MP859 | | > | | | | | |
| I2MP878 * | | | | | | | |
| I2MP891 * | | | | | | | |

| |
|---|
| Col-3 |
| L.*er* |
| Heterozygous |

**Figure 4.17 *icx2* mapping informative individuals**

PCR based markers ag, SNAP 58, CER453080, CER458090, mi422, CER453319 and PG II were used to further the mapping of *icx2*. Informative individuals Q 47 and Q 104, shown delimited the region in which *icx2* lies to between SNAP 58 and PG II. I2MP (*icx2* mapping population) 178 - 252 (as listed) and 859 suggested that CER453080 was a closer flanking marker than SNAP58. > and < denote direction of *icx2*.

* Data not consistent with other results presented.

### 4.6. Screen for suppressors of the *icx2* phenotype

The unambiguous "short-root" phenotype shown by *icx2* individuals grown on 1/2 MS medium containing 1.5% sucrose was so strong that it was considered a basis for a suppressor screen of the *icx2* mutation.

Mutants identified from an *icx2* $M_2$ population as having long roots may or may not also exhibit a lesion in the control of *CHS* gene expression (Figure 4.18). Analysis of these mutants should help elucidate the function of *ICX2* and any functional relationship between the pleiotropic phenotypes of the *icx2* mutant.

The mapping strategy for *icx2* suppressor mutants is likely to be complex, unless they have a visible phenotype of their own which is obvious in an *ICX2* (i.e. wild type) background. Where there is a visible phenotype, as has been seen in some *icx2* $M_2$ suppressors described below (i.e. leaf curling similar to auxin transport mutants), then this is a basis for map based cloning. If the suppressor mutant phenotype were not phenotypically divergent from wild type, then mapping it may be made easier if an *icx2* knockout can be found in a background other than Landsberg. Prior mapping of *icx2* would allow for the identification of an insertionally mutagenised line (or one found through TILLING), in an ecotype other than Landsberg, which may allow easy production of $F_2$ to be used in mapping. This strategy is dependent on the knockout mutation behaving in another ecotype as the *icx2* mutation does in Landsberg. This is not necessarily going to be the case, as suggested by Figure 4.11 and demonstrated by the problems of mapping *icx2* in a heterozygous Landsberg / Columbia background has demonstrated.

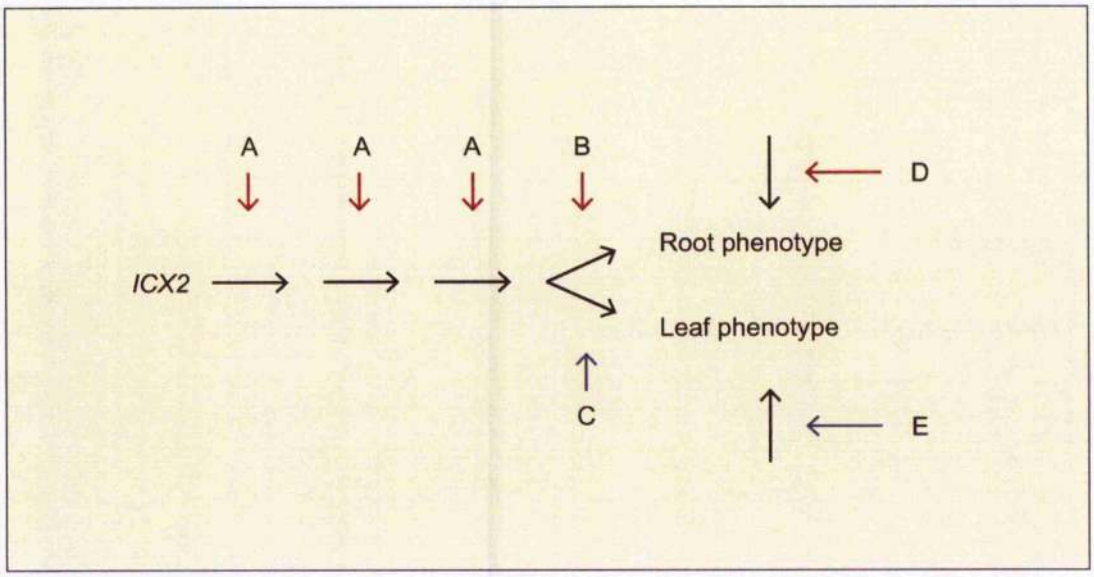


**Figure 4.18 Expected classes of *icx2* suppressor mutants**

Mutants may be discovered which correspond to lesions in genes affecting both the root and leaf phenotypes (A), and either root (B) or leaf (C) phenotypes individually. Class (D) and (E) mutants represent mutants which are epistatic to those of classes (B) and (C), respectively, but not involved in the *ICX2* pathway. The suppressor screen detailed in this chapter uses the root phenotype to select mutants, so can only find (A), (B) or (D) classes but cannot distinguish (B) from (D). The diagram shows multiple possible positions of class (A) mutants (red arrows). Class (B), (C), (D) or (E) mutants may also have multiple positions, just as there may be more or less points of action of class (A) mutations.

### 4.6.1. Assessment of *icx2* suppressor mutants

EMS mutagenesis was carried out according to the protocol of Leyser and Furner (see Materials and Methods). Batches of $M_2$ plants were prepared for screening by collecting seed from 20 $M_1$ plants per $M_2$ batch. Approximately 600 seedlings were screened per $M_2$ batch, corresponding to 30 $M_2$ seedlings per $M_1$ plant. As neither the number of gene products involved in the synergistic induction of *CHS*, nor the efficiency of mutation of these genes was known, the probability of generating relevant mutants cannot be calculated in this instance. The probability of isolating recessive and dominant mutants generated (i.e. present) was $P = 1-(0.75)^{10}$ or $<0.999$, and $P = 1-(0.25)^{10}$ or $<0.999$ respectively. 80 batches of *icx2* $M_2$ seeds were screened for suppressed *icx2* root length phenotype (a total of approximately 48000 seedlings).

Figure 4.19 shows the typical selection of long-root suppressor mutants. A total number of 22 suppressor mutants were found, 18 of which survived transplantation from agar to compost. Figure 4.20 shows the leaf phenotype for these 18 mutant lines. Suppressor mutants were selected on the basis of their root phenotype. It is interesting to note that these mutants included one which retained the *icx2* leaf phenotype and the others did not.

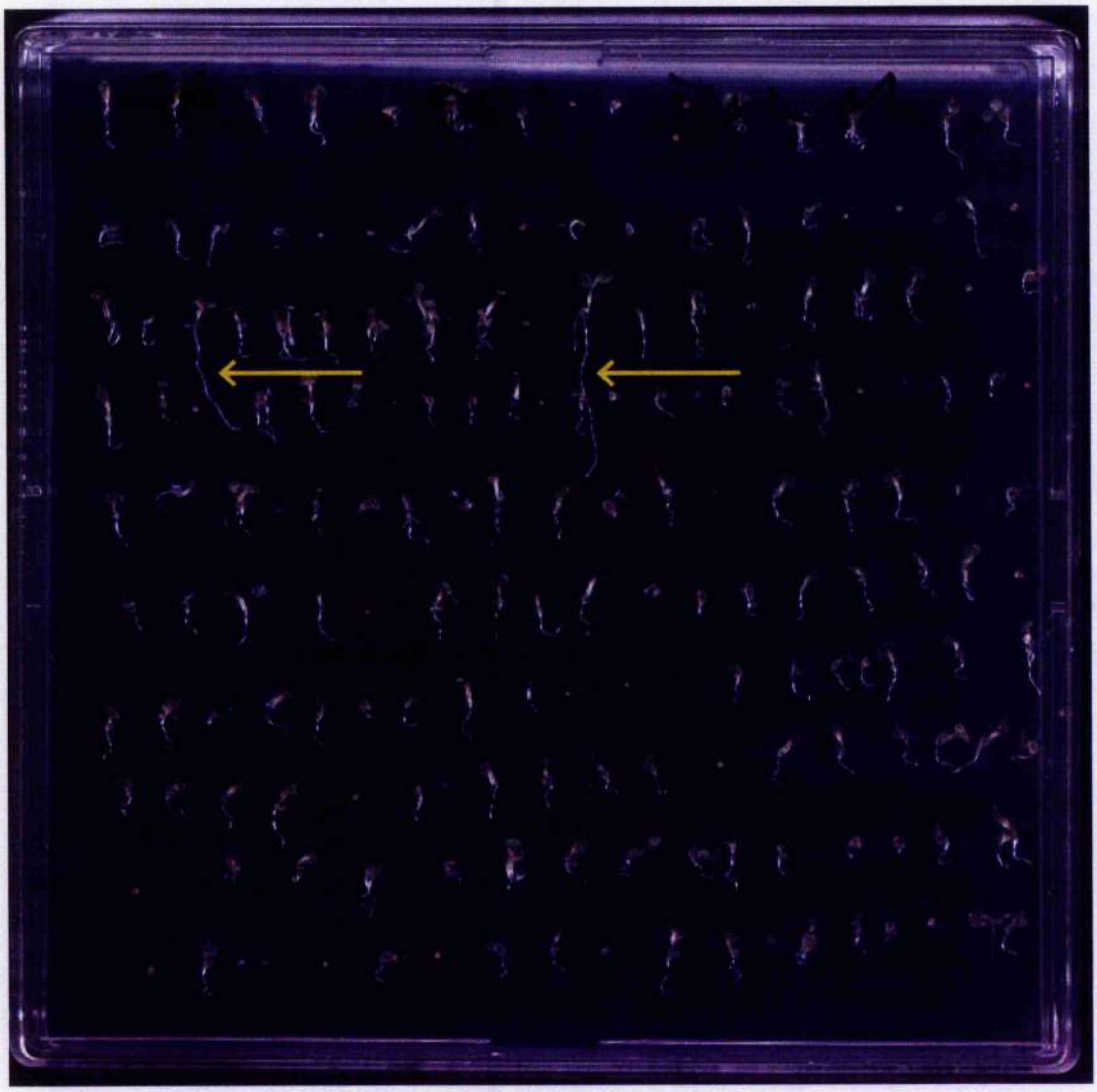

**Figure 4.19 Typical selection of *icx2* suppressor mutants**

*icx2* $M_2$ seedlings were grown for 10 days on 1.5% sucrose agar plates. Individuals exhibiting long roots (yellow arrows) were selected.

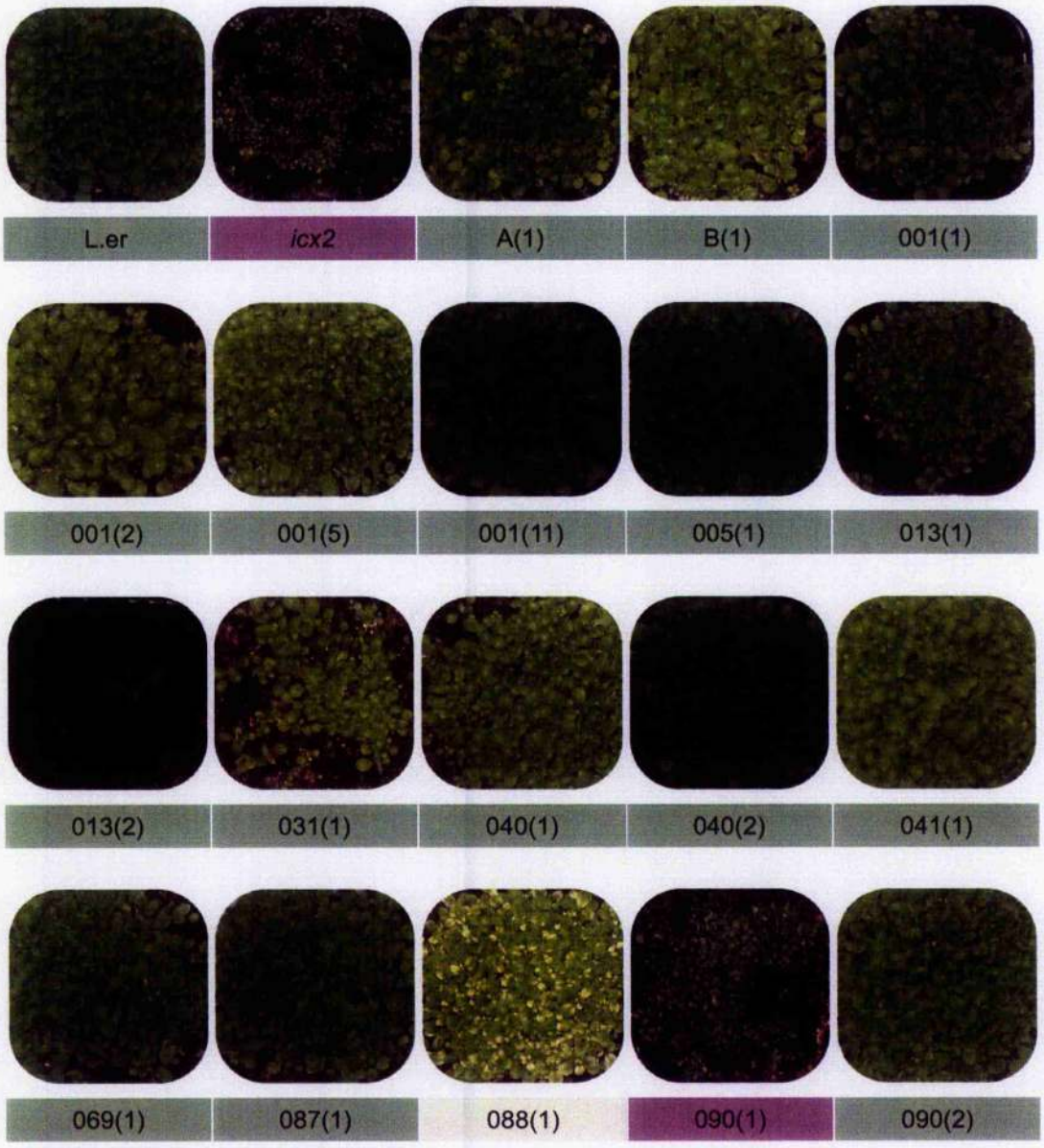


**Figure 4.20 *icx2* suppressor mutants**

L.*er*, *icx2* and 18 suppressor mutants, isolated as having wild type (long) root phenotype when grown on solid plant growth medium containing 1.5% sucrose, were grown on compost for 21 days under 150 μmol $m^{-2}$ $s^{-1}$ white light. After this time, they were photographed, and assessed for *icx2* leaf phenotype. Photographs of pots are reproduced above, with labels below each. Purple lables are used for those exhibiting *icx2* leaf phenotype. Dark green labels signify wild type phenotype, and light green is used for the variegated phenotype seen in 088(1).

## 4.7. Discussion and further work

### 4.7.1. *icx2* exhibits a complex conditional phenotype

Prior to the current study the *icx2* phenotype had been partially characterised, but most attention had been paid to the analysis of *CHS* and other flavonoid biosynthesis genes. *icx2* was described as having small stature and over accumulation of anthocyanins. These phenotypes were described as recessive. Experiments presented here extended this characterisation and confirmed (by assessing $F_1$ and $F_2$ plants in crosses) the recessive nature of the mutation. The current study found *icx2* to have a conditional phenotype which is complicated by being subject to incomplete penetrance and expressivity. A high degree of variability in rosette diameter was demonstrated in the *icx2* mutant. *icx2* was also shown to exhibit chronologically late flowering. In characterising the *icx2* phenotype, initially to facilitate map-based cloning, a further pleiotropic phenotype was discovered. *icx2* individuals grown on sucrose exhibited short roots. As discussed later in this section (4.7.4), *icx2* may be a regulatory mutant and other regulatory mutants (e.g. *hy5*) have similarly wide-ranging phenotypes. On the other hand, *icx2* may be a metabolic mutant or growth regulator (e.g. brassinosteroid) biosynthetic mutant. These too could have such a broad effect on phenotype.

The *icx2* mutation was shown in the current study to adversely influence not only root extension but also root hair production under certain environmental conditions. Flavonoid accumulation has been shown to have an antagonistic effect on auxin function and consequently an adverse effect on root growth (Brown et al. 2001). The role of flavonoid accumulation in *icx2* was assessed with reference to the root phenotype. Wild

type, *icx2*, *tt4* (*CHS* null mutant which does not accumulate flavonoids) and an *icx2tt4* double mutant were grown with or without sucrose on solid growth medium and their root lengths were measured after 10 days. This experiment showed that neither *CHS* nor flavonoid accumulation were required for the *icx2* short-root phenotype as it was conserved in the sucrose-grown double mutant, while *tt4* exhibited wild type roots. A similar experiment, using the anthocyanin hyper-accumulator *PAP1* showed that the presence of high levels of anthocyanins was not sufficient to give rise to the short-root phenotype.

### 4.7.2. Are the root and leaf phenotypes of *icx2* pleiotropic?

The genetic lesion giving rise to the *icx2* phenotype is not a result of the insertion of the transgene (*CHS:GUS*) in the NM4 line, as the original transgene has been crossed out of the line used here (4L13BC2). It is tempting to suggest a common mutation underlying the root and leaf phenotypes as both mutant phenotypes are evident under the same light and sucrose concentration conditions and a threshold of response is seen in each phenotype between 1.5% and 6% sucrose. It should be remembered, however, that both these phenotypes occur in different organs and are assessed at different stages of development.

Several results point to the root and leaf phenotypes of *icx2* resulting from a single mutation. If it could be shown that both the root and leaf phenotypes co-segregate, then the most likely explanation is that a single mutagenic event causally affects both phenotypes. The *icx2* leaf phenotype makes this difficult to assess in absolute terms but the percentages of mapping population individuals selected in the $F_3$ generation from $F_2$

plants selected on either leaf or root phenotype suggest very strongly that the mutation(s) responsible for each of the phenotypes are at the very least very closely linked. This observation, taken with the fact that EMS was used as the mutagen that produced *icx2*, further supports the single locus argument, as EMS produces point mutations, not large deletions etc., and as such would be unlikely to disrupt more than one gene with a single mutagenic event. Likewise, the isolation of suppressor mutants which suppress both the leaf and root phenotypes, strongly supports a single locus model. The possibility exists, though, that the *icx2* mutation lies in a regulatory sequence effecting two or more closely linked genes. Cloning and complementation of the *icx2* mutation would resolve this issue.

### 4.7.3. The *icx2* phenotype hampers its map-based cloning

The *icx2* mutant exhibits a conditional phenotype. *ICX2* negatively regulates *CHS* expression and anthocyanin production in mature leaves on exposure to inductive light conditions and sucrose. This leaf phenotype, which typifies *icx2*, is not reliably expressed but rather has incomplete penetrance and an associated problem of expressivity when found in a mixed L*er* / Col-3 background, as used for mapping. These problems have made the production of a reliable mapping population difficult.

Characterisation of the *icx2* phenotypes in the current chapter helped tackle the expressivity problem associated with them in an *icx2* x Col-3 $F_2$ mapping population. *icx2* individuals were selected from such a population based on their root phenotype and subsequently checked for the leaf phenotype in the $F_3$ generation. This led to the generation of a mapping population, which could be extended following the method

described. PCR-based primers were used which exploited INDEL (insertion / deletion) polymorphisms between L.*er* and Col-3 and helped delimit the region of chromosome four containing *icx2*.

### 4.7.4. What might *icx2* be?

*icx2* individuals may be thought of as having a super-light-grown phenotype, in that they exhibit short stature and hyper-accumulation of leaf anthocyanins, but these individuals exhibit normal skotomorphogenesis and mapping data also suggest that *icx2* is not a known *cop/det/fus* mutant.

ICX2 may, however be almost any class of protein, although, until recently it would be considered unlikely that it would be a transcription factor, as it functions as a negative regulator of gene expression. There is a transcription factor called *At*MYB4 (Hemm et al. 2001), which has the distinction of being the first described MYB which functions as a repressor. Another transcription factor, this time in maize (*intensifier 1*, (Franken et al. 1991) exhibits (like *icx2*) a negative regulatory effect on anthocyanin accumulation. It is easy to see how the pleiotropic function of *icx2* might be achieved were it a transcription factor with tissue specific negative (leaf) and positive (root) functions. It is far too early to speculate, but it may be said that ICX2 would appear to function in several important pathway, and as such may be any number of cellular components.

### 4.7.5. *icx2* suppressor screen

*icx2* characterisation had gone some way to help elucidate ICX2's function in the cell. Progress in mapping the mutation was beset with difficulties (as described in section 4.7.3) and only slow progress was being made. In the process of characterising *icx2*, a new pleiotropic short-root phenotype was described which immediately looked like a good candidate phenotype to make the basis of a suppressor screen. It was considered useful to conduct such a screen, as classes of mutants isolated could give insights into ICX2's complex cellular functions.

A suppressor screen for mutants in the *icx2* root phenotype was undertaken. This screen isolated a total number of 22 suppressor mutants, 18 of which survived transplantation from agar to compost. It is worth noting that the classes of *icx2* suppressor mutants found in the current study may cast light on the seemingly pleiotropic nature of the *icx2* mutation. They suggest that it is likely that both the leaf and root phenotypes shown in *icx2* individuals are caused by the same mutation. In addition, some mutants showed a similar leaf-curling phenotype to *mdr1* and *phot1/phot2* double mutant. *phot1/phot2* is glabrous, so it was possible to show that these suppressors were not contaminating *phot1/phot2* seed as they all had trichomes. All aspects of the root phenotype (short primary root, altered architecture and altered root hairs) along with the leaf curling seen in some *icx2* suppressor mutants suggest a link with auxin. Phototropism and gravitropism do not seem affected. The data gathered from the *tt4* experiment suggest that if auxin responses are altered in icx2, then it is not achieved via the antagonistic action of flavonoids.

### 4.7.6. Further work

*ICX2* should first be cloned. The work presented above provides a rough map location and the means to generate a larger, and more reliable mapping population. There may also be tagged mutant lines already generated which could allow the easy cloning of *ICX2*. The reported or postulated function of the *ICX2* gene, once cloned, may give insights into the mutant phenotype and the cellular role of ICX2. Discovery of the *ICX2* gene should help elucidate the genetic and molecular basis of the pleiotropy seen in the root and leaf phenotypes.

In the short term, RT-PCR studies with *icx2* to assess the expression of transcription factors involved in regulating *CHS* expression and anthocyanin biosynthesis (like HY5, MYB12, MYB75 and MYB90) may help to determine the role of *ICX2*. It would be interesting to see if *HY5* expression is affected, as *hy5* mutants have much reduced expression of *CHS* and display an aberrant "expanded" root phenotype (Oyama et al. 1997) which contrasts in both respects with the *icx2* phenotype. It would seem that ICX2 does have more than one function and as such, microarray analysis would help in discovering the extent of its influence, which may in turn help characterise its function.

Differences in expressivity of the *icx2* phenotypes seen between the mutation in a L.*er* background and a mixed L.*er* / Col-3 background highlight how plastic such responses can be and how such close ecotypes vary. This phenomenon might be exploited as the basis (with a deal of optimisation required) for QTL analysis of these phenotypes.

The root phenotype present in *icx2* individuals, as described in this chapter, deserves further characterisation. Simple experiments where the phenotype may be "chemically complemeted" may be possible. Some initial experiments in this area suggest (as might be expected) that the wild type phenotype cannot be restored by simple addition of auxin to the growth medium (results not shown). Other plant hormones with known roles in root development, such as ABA (abscisic acid) and cytokinin, may be tried.

## Chapter 5: Discussion.

### 5.1. Introduction

The results presented in both Chapters 3 and 4 relate to the isolation and characterization of *Arabidopsis* mutants altered primarily in the light induction of *CHS* gene expression. Chapter 3 describes the production of biological materials and development and optimization of methods for the selection of mutants altered in the UV-B / blue light synergistic induction of *CHS*. It then describes the screening process and initial characterization of putative mutants, finally leading to the identification of a novel mutant, which is likely to be a new *uvr8* (*ultra-violet resistance locus 8*) allele, although this awaits confirmation by sequencing the transcript produced in this mutant.

Chapter 4 deals with the characterization of *icx2* (*increased chalcone synthase expression 2*), a mutant previously identified in a forward genetic screen as being a high expressor of *CHS* under UV-B light (Dr. G. Fuglevand, unpublished). Prior to the work presented here, *icx2* had been partially characterized. *icx2* has been shown to have altered induction of *CHS* expression (and that of other flavonoid biosynthetic genes) under a range of light conditions, which results in the accumulation of leaf anthocyanins and an associated purple leaf colour. It is believed, then, that ICX2 is a negative regulator of *CHS* expression and anthocyanin accumulation. A previous attempt at mapping the mutant had been initiated and subsequently abandoned on account of its unreliable phenotype.

The current study attempted to increase the visibility of the *icx2* phenotype by growing the mutant on solid growth medium containing sucrose, as sucrose is known to

induce *CHS* expression and anthocyanin accumulation. This led to the discovery of an associated short-root phenotype, which was characterized with reference to the possible role of accumulated flavonoids in this phenotype. It had been asserted in the literature that flavonoids have an antagonistic effect on auxin function and root growth (Brown et al. 2001). The evidence points to the root phenotype being pleiotropic with the leaf phenotype, but the two traits cannot be said to be caused by the same mutation until that mutation is cloned and complementation performed. The short root phenotype provided the basis for further mapping of the *icx2* mutation and for a pilot suppressor screen of the mutant phenotype.

**5.2. The genetic approach**

The results of three forward genetic screens were important in the production of this thesis. The forward genetic approach was used for mutant isolation in Chapter 3 not least because it has been used successfully in the isolation of specific mutants, as in the screen that identified *icx2*. In addition, a suppressor screen was performed in Chapter 4.

The merits of the forward genetic approach are discussed in Chapters 1 and 3 and it remains only to repeat that it was strongly considered the best way to identify those classes of mutants desired in Chapter 3. It was employed because no genetic elements of UV-B or UV-B / blue synergistic photoreception or signal transduction leading to the expression of *CHS* had been identified previously. It was expected that looking for mutants altered specifically in UV-B or UV-B / blue light synergistic induction of *CHS*, in an $M_2$ population derived from a line containing a reporter gene driven by the *CHS* promoter would prove a successful approach, yielding important classes of mutants.

The *CHS:Luc* screen for mutants in UV-B / blue light synergistic induction of *CHS* (Chapter 3) and indeed, the *icx2* suppressor screen (Chapter 4) proved robust and successful in that both produced verifiable and informative mutants. In both these instances it should be noted that the success of the screens was helped by having clear expectations and by choosing screening conditions that maximise the difference between expected wild type and mutant responses.

Despite the justifiable enthusiasm with which work on the screens in Chapters 3 and 4 was begun and their eventual successes, the contents of both results chapters might also be considered a salutary lesson in the possible difficulties inherent in the genetic approach. These difficulties were predicted before this work was begun, but were considered acceptable risks.

The screen carried out in Chapter 3 produced a very high proportion of false positives whereas the *icx2* suppressor screen did not. This difference may be attributable, firstly, to the fact that the root length selection used in the *icx2* suppressor screen was essentially qualitative (either they were short or long, there were no ambiguous individuals), whereas the larger scale *CHS:Luc* synergism screen had been designed from the outset with a secondary screen included and so could afford to take more ambiguous (and so potentially interesting and subtle) putative mutants. Secondly, selection in the *CHS:Luc* synergism screen relied on reporting of a biochemical phenotype via luciferase luminescence, which itself required a photon counting camera, computer and software for visualisation whereas the *icx2* suppressor screen was based on a physical phenotype, which required no reporter. Moreover, mutants which caused altered luciferin uptake or diminished ATP available for luciferase activity would have generated false positives.

*icx2* had been isolated from an EMS mutagenised population (*CHS* expression was reported in this screen via a *CHS:GUS* reporter line (NM4 (non-mutant line 4)) which used the *Sinapis alba CHS* promoter fused to the coding sequence of the *GUS* gene). Luciferase, as used and discussed in Chapter 3, is a far more dynamic reporter than GUS and remains a good choice for the screen described as it allowed for a multi-stage screen to be developed.

### 5.2.1. Map-based cloning

Difficulties were encountered in the attempted mapping of *icx2*, as the leaf phenotype exhibited incomplete penetrance and poor expressivity in the L.*er* x Col-3 $F_2$ mapping population. The recognition of an associated short root phenotype exhibited by *icx2* individuals grown on sucrose was not subject to incomplete penetrance, so allowed this problem to be overcome in the mutant (L.*er* background). This phenotype was subject to the problem of expressivity as seen in the leaf phenotype but did seem better as a means of selection of a reliable mapping population as a higher proportion of individuals showing the *icx2* phenotype could be obtained using the root phenotype. All individuals selected for the mapping population were further verified by demonstrating the presence of the leaf phenotype in those mutants isolated by virtue of their short root. No matter whether mutants were selected from the L.*er* x Col-3 $F_2$ population based on their root or leaf phenotype, they all proved as likely to show the leaf phenotype in the $F_3$ generation (64 of 140 (45.7%) from the group selected based on leaf phenotype and 405 of 870 (46.6%) from the group selected based on root phenotype). This would suggest that there is no recombination happening between the mutations responsible for both phenotypes

(meaning that they are likely to be the same). Despite the problems encountered, progress was made in mapping *icx2*, a foundation for the production of a mapping population has been produced (469 individuals selected in $F_3$ of 1106 $F_2$ selected individuals) and PCR-based markers designed to facilitate mapping.

Problems in map-based cloning of *CHS:Luc* mutants were also anticipated (as described in section 3.1.3.3) and strategies developed for mapping mutants which may have been found and which lacked an easily assessed phenotype. Mapping would seem not to be required for the strongest mutant(s) to come through the screen as these are likely to be alleles of a known gene.

### 5.3. UVR8

The mutant screen described in Chapter 3 led to the isolation of at least one mutant which exhibits under-expression of *CHS* in UV-B and UV-B / blue light synergistic conditions, as assessed by luciferase luminescence and RT-PCR. It looks very likely from the allelism analysis that the *CHS:Luc 68* mutant(s) represent a single novel mutant allele of *uvr8*. Sequencing of the *uvr8* gene in these mutants is underway. It has also been shown in Chapter 3 that in *uvr8* the UV-B / blue light synergistic induction of *CHS* is abolished.

*uvr8* mutants have been found by two previous studies which unfortunately limit the impact of the results of this screen. Kliebenstein et al. (2002) identified *uvr8-1* as a UV-B hypersensitive mutant and found *UVR8* to have significant sequence similarity (35% identity and 50% similarity) to human *RCC1* (*regulator of chromatin condensation 1*). *uvr8-1* was shown to be unable to make *CHS* transcript or protein and has reduced flavonoid levels in response to UV-B. *PR-1* (*pathogenesis related - 1*) and *PR-5* protein

level is however increased, which correlates well with increased stress caused by UV-B damage. Kliebenstein et al. (2002) show that a 15-bp deletion in *uvr8-1* is responsible for its UV-B sensitivity. RCC1 has a regulatory role in nucleocytoplasmic transport and cell cycle progression in animals and fungi via its function as a nucleotide exchange factor for the small G-protein, Ran. Ran homologues are evident in the published *Arabidopsis* genome sequence, and so a similar function may be retained in plants. In *Saccharomyces cerevisiae,* RCC1 functions in pre-mRNA processing and transport (Aebi, 1990; Kadowaki et al., 1993), mating behavior (Clark and Sprague, 1989), initiation of mitosis (Matsumoto and Beach, 1991), and chromatin decondensation (Sazer and Nurse, 1994) and as might be expected, mutations in *RCC1* result in pleiotropic phenotypes or even lethality. Kliebenstein et al. (2002) suggest that the apparent lack of pleiotropic phenotypes seen in the *uvr8-1* mutant suggest that the function of UVR8 in plants may be specific to the UV-B response and further back up their argument by pointing out that nuclear localization sequences present in animal and fungal *RCC1* are missing from *UVR8*. Despite the lack of a nuclear localization sequence in *UVR8*, recent evidence shows that it is localized to the nucleus and has no Ran activity (Brown, Cloix, Jiang, Kaiserli, Herzyk, Kliebenstein and Jenkins, submitted).

A second study (Brown, 2005) used the biological materials developed for the screen described in Chapter 3. A similar approach was taken to that described in Chapter 3, the main difference being that Brown screened for mutants altered in UV-B induction of *CHS* in a one-step screen which isolated further alleles of *uvr8*. It is fascinating to consider that only *uvr8* mutants were reported from these screens.

Brown (2005) found that UVR8 acts specifically in UV-B to regulate *CHS* gene expression. In addition, it was found in Chapter 3 that the *uvr8* mutant has impared UV-B / blue light synergistic induction of *CHS* but wild type levels of blue light induction, which supports this claim. A microarray analysis (Brown 2005) of the *uvr8-2* allele has given further weight to the suggestion that UVR8 functions specifically in the UV-B response. Expression levels of flavonoid biosynthetic genes, ELIPS (early light induced proteins), which have photoprotective roles in *Arabidopsis* (Hutin et al. 2003), the DNA photolyase *PHR1* and several other genes concerned with UV protection were shown to be altered in expression in the mutant. Further research has shown that UVR8 has very little Ran GEF (guanine exchange factor) activity, indicating that it functions differently to RCC1. UVR8 associates with chromatin, similarly to RCC1 and the significance of chromatin binding seems to be that it facilitates the UV-B regulation of target genes, including *HY5* (Brown, Cloix, Jiang, Kaiserli, Herzyk, Kliebenstein and Jenkins, submitted). The study of further mutant alleles, such as that identified in the work described in Chapter 3 will help to characterize the structure / function relationship of UVR8.

### 5.4. *icx2* characterisation

A second approach to study the genetic basis of flavonoid gene regulation was to further characterise a previously isolated mutant, *icx2*, which was originally identified as a mutant over-expressing *CHS* transcript in the presence of UV-B. Previous characterisation (see 4.1.1) had shown *icx2* to over-express not only *CHS* but also other enzymes of the flavonoid biosynthetic pathway in response to a range of light qualities.

In addition, *icx2* individuals exhibited reduced stature and deep purple leaves. The purple leaf phenotype resulted from hyper-accumulation of anthocyanins.

The work presented in this thesis further characterised the pleiotropic phenotype of *icx2* and identified a new short-root phenotype which was seen in individuals grown on medium containing sucrose. The plant hormone auxin has an effect on root architecture and has its own function disrupted by flavonoids (Brown et al. 2001). In order to assess the role of flavonoid accumulation in the root phenotype, *icx2* was grown on sucrose and compared with *tt4* (a null mutant of the *CHS* gene, which does not produce flavonoids), *tt4icx2* double mutant and wild type, all similarly grown. The short-root phenotype was observed in *icx2* and the double mutant, but not in *tt4*. This showed the short-root phenotype to be independent of *CHS* over-expression or flavonoid accumulation. In addition, comparison of root length in *icx2* and another flavonoid hyper-accumulating mutant, *pap1*, showed that hyper-accumulation of flavonoids was not sufficient to produce the short-root phenotype. Other auxin-related responses, such as gravitropism and phototropism were not altered in *icx2*.

A screen for suppressor mutants of the *icx2* mutation was carried out. The suppressor screen selected long rooted *icx2* $M_2$ individuals grown on sucrose. Of those mutants selected, there were individuals which retained the leaf phenotype. In addition, some mutants did not. It could be suggested that the pleiotropic phenotypes of *icx2* are monogenic as mutants were found where both the root and leaf phenotypes were abolished. The full implications of the results of the screen are discussed in section 4.7.5, but it does suggest that *icx2* has functions other than those involved in *CHS* expression.

Map-based cloning of *icx2* had been attempted before, but had been abandoned because of an unreliable phenotype. Efforts were made in this study to characterise and overcome the problems with the phenotype. Problems associated with the penetrance and expressivity of the *icx2* phenotypes were addressed. This led to the extension of existing mapping resources and data and the foundation for future map-based cloning of *icx2*.

### 5.5. Conclusions

Ever since T.H. Morgan found the first white-eyed fruit fly, the forward genetic approach has proved a powerful one and has provided great successes. This approach was successfully implemented in Chapters 3 and 4 of this thesis, allowing both the identification of mutants in light regulation of *CHS* and suppressor mutants of *icx2*.

A genetic screen was designed and developed in Chapter 3 to find mutants specifically altered in UV-B / blue light induction of *CHS* expression. No mutants were found in this interaction, but a new allele of *uvr8* has probably been identified (pending sequence confirmation) which has specifically reduced *CHS* expression in UV-B and UV-B / blue synergistic conditions but not in blue light alone. This allele will be immediately sequenced in order to advance structure / function analysis of UVR8. The fact that *uvr8* has emerged as the only UV-B mutant from this and two other screens suggests that it is a key player in the UV-B induction of *CHS*. In addition to the identification of this mutant, the design of the screen allowed several classes of mutants to emerge. These have yet to be fully characterised and so may yet help elucidate light regulation of *CHS*.

Problems associated with the genetic approach were anticipated and encountered, but the successful identification of mutants in both screens demonstrated its effectiveness. Problems were also met in the attempted map-based cloning of *icx2*. These were all together more frustrating but have been overcome sufficiently to allow a mapping population to be built.

*icx2* has shown itself to be a strong negative regulator of light-induced *CHS* expression but it has also been shown in Chapter 4 to have a pleiotropic phenotype which suggests a wider sphere of influence. Characterisation of these phenotypes has shown that it certainly has relevance to leaf and root development.

**5.6. Further work**

As indicated in the discussions of Chapters 3 and 4, the work presented in this thesis could be extended in the further characterisation of mutants gained through both mutant screens, structure / function analysis of *uvr8* and further characterisation and mapping of *icx2*.

It is likely that this screen has identified a new uvr8 allele, so in the short term, the *uvr8* allele will be sequenced from the *CHS:Luc 068* mutant(s). New mutant screens could be performed (as discussed in Chapter 3) and characterisation of mutants arising from these screens along with uncharacterised mutants from the synergism screen assessed with respect to *CHS* induction in a range of conditions.

*ICX2* should be cloned using the methods for building a mapping population presented in Chapter 4. This will give an insight into its function and hopefully suggest the basis of the pleiotropic phenotypes seen in *icx2*. Clues as to the role of *icx2* are also

likely to come from characterisation of the suppressor mutants gained and from RT-PCR expression studies of transcription factors known to be involved in *CHS* expression in the *icx2* mutant. In addition, further studies on the *icx2* phenotype should be undertaken.

**References**


Ahmad, M. and A. R. Cashmore (1993). "Hy4 Gene of a-Thaliana Encodes a Protein with Characteristics of a Blue-Light Photoreceptor." Nature **366**(6451): 162-166.

Altschul, S.F., Gish, W., Miller, W., Myers, E.W. & Lipman, D.J. (1990) "Basic local alignment search tool." J. Mol. Biol. 215:403-410

Ambasht, N. K. and M. Agrawal (1997). "Influence of supplemental UV-B radiation on photosynthetic characteristics of rice plants." Photosynthetica **34**(3): 401-408.

Ambasht, N. K. and M. Agrawal (1998). "Physiological and biochemical responses of Sorghum vulgare plants to supplemental ultraviolet-B radiation." Canadian Journal of Botany-Revue Canadienne De Botanique **76**(7): 1290-1294.

Andersson, C. R. and S. A. Kay (1998). "COP1 and HY5 interact to mediate light-induced gene expression." Bioessays **20**(6): 445-448.

Ang, L. H., S. Chattopadhyay, et al. (1998). "Molecular interaction between COP1 and HY5 defines a regulatory switch for light control of Arabidopsis development." Molecular Cell **1**(2): 213-222.

Bagnall, D. J., R. W. King, et al. (1996). "Blue-light promotion of flowering is absent in hy4 mutants of Arabidopsis." Planta **200**(2): 278-280.

Boccalandro, H. E., C. A. Mazza, et al. (2001). "Ultraviolet B radiation enhances a phytochrome-B-mediated photomorphogenic response in Arabidopsis." Plant Physiology **126**(2): 780-788.

Borevitz, J. O., Y. J. Xia, et al. (2000). "Activation tagging identifies a conserved MYB regulator of phenylpropanoid biosynthesis." Plant Cell **12**(12): 2383-2393.

Briggs, W. R. and J. M. Christie (2002). "Phototropins 1 and 2: versatile plant blue-light receptors." Trends in Plant Science 7(5): 204-210.

Briggs, W. R. and M. A. Olney (2001). "Photoreceptors in plant photomorphogenesis to date. Five phytochromes, two cryptochromes, one phototropin, and one superchrome." Plant Physiology **125**(1): 85-88.

Brosche, N. and A. Strid (2003). "Molecular events following perception of ultraviolet-B radiation by plants." Physiologia Plantarum **117**(1): 1-10.

Brown, D. E., A. M. Rashotte, et al. (2001). The Absence of Flavonoids in the Chalcone Synthase Mutant *tt4* Leads to Elevated Auxin Transport and Impaired Gravitropic Bending. International Conference on Arabidopsis Research, Madison.

Brown, D. E., A. M. Rashotte, et al. (2001). "Flavonoids act as negative regulators of auxin transport in vivo in Arabidopsis." Plant Physiology **126**(2): 524-535.

Brown, R. A. (2005). A Genetic Approach to Understanding the Responses of *Arabidopsis thaliana* to Ultraviolet-B Light. Plant Molecular Science Group, Division of Biochemistry and Molecular Biology, Institute of Biomedical and Life Sciences. Glasgow, University of Glasgow.

Bub, A., B. Watzl, et al. (2003). "Fruit juice consumption modulates antioxidative status, immune status and DNA damage." Journal of Nutritional Biochemistry **14**(2): 90-98.

Burbulis, I. E. and B. Winkel-Shirley (1999). "Interactions among enzymes of the Arabidopsis flavonoid biosynthetic pathway." Proceedings of the National Academy of Sciences of the United States of America **96**(22): 12929-12934.

Caldwell, M. M., L. O. Bjorn, et al. (1998). "Effects of increased solar ultraviolet radiation on terrestrial ecosystems." Journal of Photochemistry and Photobiology B-Biology **46**(1-3): 40-52.

Casati, P. and V. Walbot (2003). "Gene expression profiling in response to ultraviolet radiation in maize genotypes with varying flavonoid content." Plant Physiology **132**(4): 1739-1754.

Chattopadhyay, S., L. H. Ang, et al. (1998). "Arabidopsis bZIP protein HY5 directly interacts with light- responsive promoters in mediating light control of gene expression." Plant Cell **10**(5): 673-683.

Christie, J. M. and G. I. Jenkins (1996). "Distinct UV-B and UV-A blue light signal transduction pathways induce chalcone synthase gene expression in Arabidopsis cells." Plant Cell **8**(9): 1555-1567.

Christie, J. M., P. Reymond, et al. (1998). "Arabidopsis NPH1: A flavoprotein with the properties of a photoreceptor for phototropism." Science **282**(5394): 1698-1701.

Christie, J. M., M. Salomon, et al. (1999). "LOV (light, oxygen, or voltage) domains of the blue-light photoreceptor phototropin (nph1): Binding sites for the chromophore flavin mononucleotide." Proceedings of the National Academy of Sciences of the United States of America **96**(15): 8779-8783.

Christie, J. M., T. E. Swartz, et al. (2002). "Phototropin LOV domains exhibit distinct roles in regulating photoreceptor function." Plant Journal **32**(2): 205-219.

Cluis, C. P., C. F. Mouchel, et al. (2004). "The Arabidopsis transcription factor HY5 integrates light and hormone signaling pathways." Plant Journal **38**(2): 332-347.

Colon-Carmona, A., D. L. Chen, et al. (2000). "Aux/IAA proteins are phosphorylated by phytochrome in vitro." Plant Physiology **124**(4): 1728-1738.

Crozier, A.; Ican, M. E. J; McDonald, M. S.; Black, C. Quantitative Analysis of the Flavonoid Content of Commercial Tomatoes, Onions, Lettuce and Celery. J. *Agric. Food Chem.* **1997,** 45, 590-595.

Dakora, F. D.: Philiphs D. A. Diverse Functions of Isoflavonoids in Legumes Transcend Anti-microbial Definitions of Phytoalexins, *Phsiol Mol Plant,* **1996,** 49, 1-20.

Franken, P., U. Niesbachklosgen, et al. (1991). "The Duplicated Chalcone Synthase Genes C2 and Whp (White Pollen) of Zea-Mays Are Independently Regulated - Evidence for Translational Control of Whp Expression by the Anthocyanin Intensifying Gene (in)." Embo Journal **10**(9): 2605-2612.

Franklin, K. A. and G. C. Whitelam (2004). "Light signals, phytochromes and cross-talk with other environmental cues." Journal of Experimental Botany **55**(395): 271-276.

Frederick, J. E. and D. Lubin (1988). "The budget of biologically active ultraviolet radiation in the earth atmosphere system." Journal of Geophysical Research-Atmospheres **93**: 3825 - 3832.

Frederick, J. E., H. E. Snell, et al. (1989). "Solar Ultraviolet-Radiation at the Earths Surface." Photochemistry and Photobiology **50**(4): 443-450.

Frohnmeyer, H., L. Loyall, et al. (1999). "Millisecond UV-B irradiation evokes prolonged elevation of cytosolic-free Ca2+ and stimulates gene expression in transgenic parsley cell cultures." Plant Journal **20**(1): 109-117.

Fuglevand, G., J. A. Jackson, et al. (1996). "UV-B, UV-A, and blue light signal transduction pathways interact synergistically to regulate chalcone synthase gene expression in Arabidopsis." Plant Cell **8**(12): 2347-2357.

Gao, Y., J. M. Li, et al. (2004). "An Arabidopsis promoter microarray and its initial usage in the identification of HY5 binding targets in vitro." Plant Molecular Biology **54**(5): 683-699.

Genoud, T. and J. P. Metraux (1999). "Crosstalk in plant cell signaling: structure and function of the genetic network." Trends in Plant Science **4**(12): 503-507.

Hardtke, C. S., K. Gohda, et al. (2000). "HY5 stability and activity in Arabidopsis is regulated by phosphorylation in its COP1 binding domain." Embo Journal **19**(18): 4997-5006.

Hartmann, U., W. J. Valentine, et al. (1998). "Identification of UV/blue light-response elements in the Arabidopsis thaliana chalcone synthase promoter using a homologous protoplast transient expression system." Plant Molecular Biology **36**(5): 741-754.

Hedin, P. A.; Jenkins, J. N.; parrot, W. I.; Evaluation Of Flavonoids In Gossypium-Arboreum (L) Cottons as Potential Source OF Resistance To Tobacco Budworm, *Journal of Chemical Ecology,* **1992,** 18, 105-114.

Heelis, P. F., S. T. Kim, et al. (1993). "The Photo Repair of Pyrimidine Dimers by DNA Photolyase and Model Systems." Journal of Photochemistry and Photobiology B-Biology **17**(3): 219-228.

Hemm, M. R., K. M. Herrmann, et al. (2001). "AtMYB4: a transcription factor general in the battle against UV." Trends in Plant Science **6**(4): 135-136.

Hertog, M. G. L.; Hollman, P. C. H.; Katan, M. B. Content of Potentially Anticarcinogenic Flavonoids of 28 Vegetables and 9 Fruits Commonly Consumed in The Netherlands, *J. Agric. Food Chem.*, **1992,** 40, 2379-2383.

Hertog, M. G. L.; Feskens, E. J. M.; Hollman, P. C. H.; Katan, M. B.; Krohout, D.; Dietry Antioxidant Flavonoids and Risk of Coronary Heart Disease: The Zutphen Elderly Study, *The Lancet.*, **1993,** 342, 1007-1011.

Hoch, W. A., E. L. Singsaas, et al. (2003). "Resorption protection. Anthocyanins facilitate nutrient recovery in autumn by shielding leaves from potentially damaging light levels." Plant Physiology **133**(3): 1296-1305.

Hoensch, H. and W. Kirch (2005). "Potential role of flavonoids in the prevention of intestinal neoplasia: a review of their mode of action and their clinical perspectives." International Journal of Gastrointenstinal Cancer **35**(3): 187-196.

Hoffman, P. D., A. Batschauer, et al. (1996). "PHH1, a novel gene from Arabidopsis thaliana that encodes a protein similar to plant blue-light photoreceptors and microbial photolyases." Molecular & General Genetics **253**(1-2): 259-265.

Hutin, C., L. Nussaume, et al. (2003). "Early light-induced proteins protect arabidopsis from photooxidative stress." Proceedings of the National Academy of Sciences of the United States of America **100**(8): 4921-4926.

Imaizumi, T., H. G. Tran, et al. (2003). "FKF1 is essential for photoperiodic-specific light signalling in Arabidopsis." Nature **426**(6964): 302-306.

Iwashina, T. (2000). "The structure and distribution of the flavonoids in plants." Journal of Plant Research **113**(1111): 287-299.

Jackson, D.; Martinez-Garcia, J. F.; Prescott, A. G.; Roberts, K.; Martin, C. Expression Patterns of *myb* Genes from *Antirrhinum* Flowers. *The Plant Cell*, **1991,** 3, 115-125.

Jackson, J. A., G. Fuglevand, et al. (1995). "Isolation of Arabidopsis Mutants Altered in the Light- Regulation of Chalcone Synthase Gene Expression Using a Transgenic Screening Approach." Plant Journal **8**(3): 369-380.

Jacobs M, Rubery PH (1988) Naturally occurring auxin transport regulators. Science **241**: 346-349

Jenkins, G. I., J. M. Christie, et al. (1995). "Plant responses to UV and blue light: Biochemical and genetic approaches." Plant Science **112**(2): 117-138.

Jenkins, G. I., J. C. Long, et al. (2001). "UV and blue light signalling: pathways regulating chalcone synthase gene expression in Arabidopsis." New Phytologist **151**(1): 121-131.

Jin, H. L., E. Cominelli, et al. (2000). "Transcriptional repression by AtMYB4 controls production of UV- protecting sunscreens in Arabidopsis." Embo Journal **19**(22): 6150-6161.

Jin, H. L. and C. Martin (1999). "Multifunctionality and diversity within the plant MYB-gene family." Plant Molecular Biology **41**(5): 577-585.

Jorda, L. and P. Vera (2000). "Local and systemic induction of two defense-related subtilisin- like protease promoters in transgenic Arabidopsis plants. Luciferin induction of PR gene expression." Plant Physiology **124**(3): 1049-1057.

Jorgensen, R. (1993). "The Origin of Land Plants - a Union of Alga and Fungus Advanced by Flavonoids." Biosystems **31**(2-3): 193-207.

Kagawa, T. (2003). "The phototropin family as photoreceptors for blue light-induced chloroplast relocation." Journal of Plant Research **116**(1): 77-82.

Kagawa, T., T. Sakai, et al. (2001). "Arabidopsis NPL1: A phototropin homolog controlling the chloroplast high-light avoidance response." Science **291**(5511): 2138-2141.

Kagawa, T. and M. Wada (2002). "Blue light-induced chloroplast relocation." Plant and Cell Physiology **43**(4): 367-371.

Kanadaswami, C., L. T. Lee, et al. (2005). "The antitumour activities of flavonoids." In Vivo **19(5)**: 895-909.

Kato, R.; Nakadate, T.; Yamamoto, S.; Sugimura, T. Inhibition of 12-O-tetradecanoylphorobol-13-acedate-induced Tumor Promotion and Orthine Decarboxylase Activity by Quercetin: Possible Involvement of Lipoxygenase Inhibition. *Carcinogenesis,* **1983,** 10, 1301-1305.

Kaul, S., H. L. Koo, et al. (2000). "Analysis of the genome sequence of the flowering plant Arabidopsis thaliana." Nature **408**(6814): 796-815.

Kim, B. C., D. J. Tennessen, et al. (1998). "UV-B-induced photomorphogenesis in Arabidopsis thaliana." Plant Journal **15**(5): 667-674.

Kim, S. T. and A. Sancar (1993). "Photochemistry, Photophysics, and Mechanism of Pyrimidine Dimer Repair by DNA Photolyase." Photochemistry and Photobiology **57**(5): 895-904.

Kleine, T., P. Lockhart, et al. (2003). "An Arabidopsis protein closely related to Synechocystis cryptochrome is targeted to organelles." Plant Journal **35**(1): 93-103.

Kliebenstein, D. J., J. E. Lim, et al. (2002). "The Arabidopsis RCC1 Homologue UVR8 Mediates UV-B Signal Transduction and Tolerance." Submitted to PNAS.

Kliebenstein, D. J., J. E. Lim, et al. (2002). "Arabidopsis UVR8 regulates ultraviolet-B signal transduction and tolerance and contains sequence similarity to human Regulator of Chromatin Condensation 1." Plant Physiology **130**(1): 234-243.

Konjevic, R., B. Steinitz, et al. (1989). "Dependence of the Phototropic Response of Arabidopsis-Thaliana on Fluence Rate and Wavelength." Proceedings of the National Academy of Sciences of the United States of America **86**(24): 9876-9880.

Koornneef, M. (1981). "The complex syndrome of *ttg* mutants." Arabidopsis Information Service **18**: 45-51.

Koornneef, M., E. Rolff, et al. (1980). "Genetic Control of Light-inhibited Hypocotyl Elongation in *Arabidopsis thaliana* (L.) Heynh." Z. Pflanzenphysiol. **100**: 147-160.

Kootstra, A. (1994). "Protection from Uv-B-Induced DNA-Damage by Flavonoids." Plant Molecular Biology **26**(2): 771-774.

Kubasek, W. L., B. W. Shirley, et al. (1992). "Regulation of Flavonoid Biosynthetic Genes in Germinating Arabidopsis Seedlings." Plant Cell **4**(10): 1229-1236.

Lampinen J, Koivisto L, Wahlsten M, Mantsala P, Karp M. (1992). "Expression of luciferase genes from different origins in Bacillus subtilis." Mol Gen Genet. 1992 Apr;232(3):498-504.

Li, J. Y., T. M. Oulee, et al. (1993). "Arabidopsis Flavonoid Mutants Are Hypersensitive to Uv-B Irradiation." Plant Cell **5**(2): 171-179.

Lin, C., M. Ahmad, et al. (1996). "*CRY2*: A second member of the *Arabidopsis* cryptochrome gene family." Plant Physiology **110**: 1047.

Lin, C. T. (2000). "Photoreceptors and regulation of flowering time." Plant Physiology **123**(1): 39-50.

Liscum, E. and W. R. Briggs (1995). "Mutations in the Nph1 Locus of Arabidopsis Disrupt the Perception of Phototropic Stimuli." Plant Cell **7**(4): 473-485.

Long, J. C. and G. I. Jenkins (1998). "Involvement of plasma membrane redox activity and calcium homeostasis in the UV-B and UV-A blue light induction of gene expression in Arabidopsis." Plant Cell **10**(12): 2077-2086.

Mackerness, S. A. H., C. F. John, et al. (2001). "Early signaling components in ultraviolet-B responses: distinct roles for different reactive oxygen species and nitric oxide." Febs Letters **489**(2-3): 237-242.

Mackerness, S. A. H., S. L. Surplus, et al. (1999). "Ultraviolet-B-induced stress and changes in gene expression in Arabidopsis thaliana: role of signalling pathways controlled by jasmonic acid, ethylene and reactive oxygen species." Plant Cell and Environment **22**(11): 1413-1423.

Maher, E.; Bate, N.; Ni, W.; Elkind, Y.; Dixon, R. A. Increased Disease Susceptibility of Transgenic Tobacco Plants with Suppressed Levels of Preformed Phenylpropanoid Products, *Proc. Natl. Acad. Sci. USA,* **1994,** 91, 7802-7806.

Maniatis, T.; Fritsch, E. F.; Sambrook, J. Molecular Cloning: A Laboratory manual. **(1982)** Cold Spring Harbor University Press, Cold Spring Harbor, NY.

Martin, C. and J. PazAres (1997). "MYB transcription factors in plants." Trends in Genetics **13**(2): 67-73.

Mehrtens, F., H. Kranz, et al. (2005). "The Arabidopsis Transcription Factor MYB12 Is a Flavonol-Specific Regulator of Phenylpropanoid Biosynthesis." Plant Physiology **138**: 1083-1096.

Michelet, B. and N. H. Chua (1996). "Improvement of arabidopsis mutant screens based on luciferase imaging in planta." Plant Molecular Biology Reporter **14**(4): 320-329.

Millar, A. J., I. A. Carre, et al. (1995). "Circadian Clock Mutants in Arabidopsis Identified by Luciferase Imaging." Science **267**(5201): 1161-1163.

Millar, A. J. and S. A. Kay (1996). "Integration of circadian and phototransduction pathways in the network controlling CAB gene transcription in Arabidopsis." Proceedings of the National Academy of Sciences of the United States of America **93**(26): 15491-15496.

Millar, A. J., S. R. Short, et al. (1992). "A Novel Circadian Phenotype Based on Firefly Luciferase Expression in Transgenic Plants." Plant Cell **4**(9): 1075-1087.

Millar, A. J., S. R. Short, et al. (1992). "Firefly Luciferase as a Reporter of Regulated Gene Expression in Higher Plants." Plant Molecular Biology Reporter **10**(4): 324-337.

Moyano, E.; Martinez-Garcia, J. F.; Martin, C. Apparent Redundancy in *myb* Gene Function Provides Gearing for the Control of Flavonoid Biosynthesis in *Antirrhinum* Flowers, *The Plant cell,* **1996,** 8, 1519-1532.

Murashige. T, and Skoog, F.; A Revised Medium for Rapid Growth and Bio Assays with Tobacco Tissue Cultures, *Phisiologica Plantarum,* **1962,** 15, 473-497.

Negre-Salvayre, A.; Salvayre, R. Quercetin Prevents the Cytotoxicity of Oxidised LDL on Lymphoid Cell Lines, *Free Radical Biology & Medicine*, **1992,** 12, 101-106.

Nozue, K., T. Kanegae, et al. (1998). "A phytochrome from the fern Adiantum with features of the putative photoreceptor NPH1." PNAS **95**(26): 15826-15830.

Okada, K., T. Wada, et al. (1998). "Regulatory systems of root patterning." Journal of Plant Research **111**(1102): 315-321.

Osterlund, M. T., C. S. Hardtke, et al. (2000). "Targeted destabilization of HY5 during light-regulated development of Arabidopsis." Nature **405**(6785): 462-466.

Ow, D.W. *et al.* (1986) Transient and stable expression of the firefly luciferase gene in plant cells and transgenic plants. *Science* 234, 856—9.

Oyama, T., Y. Shimura, et al. (1997). "The Arabidopsis HY5 gene encodes a bZIP protein that regulates stimulus-induced development of root and hypocotyl." Genes & Development **11**(22): 2983-2995.

Oyama, T., Y. Shimura, et al. (2002). "The IRE gene encodes a protein kinase homologue and modulates root hair growth in Arabidopsis." Plant Journal **30**(3): 289-299.

Rice-Evans, C. A.; Miller, N. J.; Paganga, G. Antioxidant Properties of Phenolic Compounds, *Trends in Plant Science*, **1997**, 2, 152-159.

Romero, I., A. Fuertes, et al. (1998). "More than 80R2R3-MYB regulatory genes in the genome of Arabidopsis thaliana." Plant Journal **14**(3): 273-284.

Rousseaux, M. C., C. L. Ballare, et al. (1999). "Ozone depletion and UVB radiation: Impact on plant DNA damage in southern South America." Proceedings of the National Academy of Sciences of the United States of America **96**(26): 15310-15315.

Rousseaux, M. C., R. Julkunen-Tiitto, et al. (2004). "Solar UV-B radiation affects leaf quality and insect herbivory in the southern beech tree Nothofagus antarctica." Oecologia **138**(4): 505-512.

Schepens, I., P. Duek, et al. (2004). "Phytochrome-mediated light signalling in Arabidopsis." Current Opinion in Plant Biology **7**(5): 564-569.

Schmitt, J., J. R. Stinchcombe, et al. (2003). "The adaptive evolution of plasticity: Phytochrome-mediated shade avoidance responses." Integrative and Comparative Biology **43**(3): 459-469.

Shinkle, J. R., A. Atkins, et al. (1999). UV-B-induced phototropism is mediated by a distinct photoreceptor. Plant Biology 1999, Baltimore, American Society of Plant Biologists.

Shiono, M., N. Matsugaki, et al. (2005). "Structure of the blue cornflower pigment." Nature **436**: 791.

Somers, D. E., R. A. Sharrock, et al. (1991). "The Hy3 Long Hypocotyl Mutant of Arabidopsis Is Deficient in Phytochrome-B." Plant Cell **3**(12): 1263-1274.

Stafford, H. A. (1991). "Flavonoid Evolution - an Enzymatic Approach." Plant Physiology **96**(3): 680-685.

Suesslin, C. and H. Frohnmeyer (2003). "An Arabidopsis mutant defective in UV-B light-mediated responses." Plant Journal **33**(3): 591-601.

Surplus, S. L., B. R. Jordan, et al. (1998). "Ultraviolet-B-induced responses in Arabidopsis thaliana: role of salicylic acid and reactive oxygen species in the regulation of transcripts encoding photosynthetic and acidic pathogenesis- related proteins." Plant Cell and Environment **21**(7): 685-694.

Tamaoki, M., T. Matsuyama, et al. (2004). "A method for diagnosis of plant environmental stresses by gene expression profiling using a cDNA macroarray." Environmental Pollution **131**(1): 137-145.

Ulm, R., A. Baumann, et al. (2004). "Genome-wide analysis of gene expression reveals function of the bZIP transcription factor HY5 in the UV-B response of Arabidopsis." Proceedings of the National Academy of Sciences of the United States of America **101**(5): 1397-1402.

van der Meer, I. M.; Stam, M. E.; van Tunen, A. J.; Mol, J. N. M.; Stuitje, A. R. Antisense Inhibition of Flavonoid Biosynthesis in Petunia Anthers Results in Male Sterility. *The Plant Cell,* **1992,** 4, 253-262.

van Leeuwen, W., T. Ruttink, et al. (2001). "Characterization of position-induced spatial and temporal regulation of transgene promoter activity in plants." Journal of Experimental Botany **52**(358): 949-959.

Verhoeyen, M. E., A. Bovy, et al. (2002). "Increasing antioxidant levels in tomatoes through modification of the flavonoid biosynthetic pathway." Journal of Experimental Botany **53**(377): 2099-2106.

Wade, H. K. (1999). Regulation of Chalcone Synthase Gene Expression in wild-type and Mutant Arabidopsis. Ph. D. Thesis. Glasgow, University of Glasgow.

Wade, H. K., T. N. Bibikova, et al. (2001). "Interactions within a network of phytochrome, cryptochrome and UV-B phototransduction pathways regulate chalcone synthase gene expression in Arabidopsis leaf tissue." Plant Journal **25**(6): 675-685.

Wade, H. K., A. K. Sohal, et al. (2003). "Arabidopsis ICX1 is a negative regulator of several pathways regulating flavonoid biosynthesis genes." Plant Physiology **131**(2): 707-715.

Wang, H. Y., L. G. Ma, et al. (2001). "Direct interaction of Arabidopsis cryptochromes with COP1 in light control development." Science **294**(5540): 154-158.

Winkel-Shirley, B. (1999). "Evidence for enzyme complexes in the phenylpropanoid and flavonoid pathways." Physiologia Plantarum **107**(1): 142-149.

Winkel-Shirley, B. (2001). "Flavonoid biosynthesis. A colorful model for genetics, biochemistry, cell biology, and biotechnology." Plant Physiology **126**(2): 485-493.

Wattenberg LW. 1985, "Chemoprevention of cancer." Cancer Res. 1985 Jan;45(1):1-8.

Yamasaki, H.; Sakihama, Y.; Ikehara, N. Flavonoid-peroxidase Reaction as a Mechanism for H2O2 Scavenging in Vascular Plants. *Plant Physiol Suppl.* **1997**, 114, 436-436.

Yang, H. Q., R. H. Tang, et al. (2001). "The signaling mechanism of Arabidopsis CRY1 involves direct interaction with COP1." Plant Cell **13**(12): 2573-2587.

Ylstra, B.; Touraev, A.; Moreno, R.M.B.; Stoger, E.; van Tunen, A. J.; Vicente, O.; Mol, J. N. M.; Herberle-Bors, E. Flavonols Stimulate Development, Germination, and Tube Growth of Tobacco Pollen. *Plant Physiol.* **1992**, 100, 902-907.

Ylstra, B., M. Muskens, et al. (1996). "Flavonols are not essential for fertilization in Arabidopsis thaliana." Plant Molecular Biology **32**(6): 1155-1158.